GEUS

Report File no

14970

Gravity models in the Disko-Nuussuaq area of Central West Greenland

Chalmers, J.A.

GEUS

Copenhagen

02/09-1998

DANMARKS OG GRØNLANDS GEOLOGISKE UNDERSØGELSE RAPPORT 1998/21

Gravity models in the Disko-Nuussuaq area of central West Greenland

James A. Chalmers

ISBN 87-7871-053-7

GEOLOGICAL SURVEY OF DENMARK AND GREENLAND
MINISTRY OF ENVIRONMENT AND ENERGY

DANMARKS OG GRØNLANDS GEOLOGISKE UNDERSØGELSE RAPPORT 1998/21

Gravity models in the Disko-Nuussuaq area of central West Greenland

James A. Chalmers

ISBN 87-7871-053-7

GEOLOGICAL SURVEY OF DENMARK AND GREENLAND
MINISTRY OF ENVIRONMENT AND ENERGY

G E U S

Contents

Introduction

The background for the report is the series of petroleum activities in the Disko–Nuussuaq area that started with the discovery by the Geological Survey of Greenland (GGU) in 1992 of bitumen in basalts on the Nuussuaq peninsula (Christiansen *et al.* 1993). Additional work by GGU (since 1995, the Geological Survey of Denmark and Greenland, GEUS) both at outcrop and by drilling (Christiansen *et al.* 1994; Christiansen *et al.* 1995; Christiansen *et al.* 1996; Christiansen *et al.* 1997) and exploration work carried out by grønArctic Energy Inc. under the terms of their various licences (Christiansen *et al.* 1996) has found oil and bitumen at and near the surface in many areas of northern Disko, western Nuussuaq, several smaller islands and skerries and on the south coast of Svartenhuk. grønArctic's work included the drilling of 3 slim-core wells in 1995 and a deep conventional exploration well in 1996 (Fig. 1). The discovery of widespread oil shows has challenged the existing opinion that the whole of the West Greenland area is gas-prone and in particular has promoted the Nuussuaq Basin from being merely a model for what might be found offshore to being an exploration province in its own right.

A single short 15-fold seismic line acquired by GGU in 1994 on the south coast of Nuussuaq (Christiansen *et al.* 1995) showed that the sediments in at least one part of the basin are much thicker (5-8 km) than the previously known 2–3 km thickness exposed onshore. However, little else was known of the sub-surface structure of the basin. There were no data that could be used to understand the structure of the basin as a whole and that could point to where hydrocarbons may have been generated and where future exploration could best be carried out.

In order to provide such information, in the summer of 1995 GGU acquired 711 km of multichannel seismic and gravity data in Disko Bugt, Vaigat and Uummannaq Fjord, north of Nuussuaq. The data were acquired using the Danish Navy ship 'Thetis' under charter to Nunaoil and acquisition was financed by funds provided by the Government of Greenland, Minerals Office and the Danish State through the Mineral Resources Administration for Greenland. Originally it was planned to acquire seismic data farther north, both east and west of Ubekendt Ejland and east of Svartenhuk Halvø, but 'Thetis' captain did not wish to sail in these poorly charted waters. The multichannel seismic lines are shown on Fig. 1.

The present report deals only with modelling of the gravity data acquired on the cruise supplemented by older data from the archive held by the Danish National Survey and Cadastre (KMS after its initials in Danish). Interpretation of the multichannel seismic data and integration of them with the gravity interpretations, single-channel seismic data acquired by GGU in 1972 (the Brandal data) (Denham 1974) and 1979 (the Dana data) (Brett & Zarudzki 1979) and a new evaluation of the fault pattern onshore will be the subject of a separate (refereed) paper. However, to include every gravity profile in such a paper would be too cumbersome, so this report has been produced as a record of the details of the gravity modelling.

Summary of the geology

Cretaceous–Paleocene sediments overlain by volcanic rocks crop out between 69º and 72ºN, onshore central West Greenland. The sediments were laid down in a basin, the Nuussuaq Basin, whose present outcrop is bounded to the east by extensional faults (Rozenkrantz & Pulvertaft 1969).

The exposed Cretacous sediments are of Albian to Maastrichtian age. Sandstones and coals were deposited in a fluvial and wave-dominated delta, which fanned out to the west and northwest (Pedersen & Pulvertaft 1992). In the north-west of the present-day exposures, dark, marine mudstones indicate a deeper-water environment.

Tectonic activity occured during the Maastrichtian and early Paleocene (Rosenkrantz & Pulvertaft 1969; Pulvertaft 1989; Dam & Sønderholm in press). Uplift was followed by the incision of valleys in the underlying sediments and the valleys were filled by both turbiditic and fluvial sandstones and mudstones of Late Maastrictian to middle Paleocene age, while on a fault-controlled slope to the west more than 2.5 km of turbidite sands alternating with marine mudstones were deposited (Dam & Sønderholm in press).

Basalts were erupted in the mid-Palaeocene, and the volcanic pile built up to be sub-aerial in the west from which hyaloclastite breccias, with cross-beds up to 700 m thick, prograded eastwards (Clarke & Pedersen 1976), initially into the sea and later into a succession of lakes dammed by the basalt pile (Pedersen *et al.* 1996; G. K. Pedersen, personal communication 1998). Organic-rich mudstones were deposited in the lakes.

The basalts can be traced on seismic lines to at least 100 km west of the present coast-line where they are overlain by at least 2-3 km of sediments (Whittaker 1995, 1996). It is possible that the present-day outcrop was also buried by post-basaltic sediments and has been lifted to its present location in the Neogene.

Gravity data

Gravity data were recorded during the 1995 'Thetis' cruise using a La Coste and Romberg gravity meter. The data were processed to yield free-air data. Additional data from the KMS database has been compiled from data acquired by the Geological Survey of Canada offshore, KMS onshore and GGU both on and offshore. All the onshore data were terrain corrected and converted to Bouguer anomalies. These were amalgamated with free-air data offshore to form a single data set. These data were contoured and the resulting map is shown in Fig. 2.

The corrections applied to the data imply that all the data have been adjusted to the same, sea-level datum and that the effects of rocks above sea-level should have been removed. Consequently, all modelling shows *only* the effect from rocks that lie *below* sea-level.

Gravity modelling techniques

The standard technique of gravity interpretation starts by subtracting a 'regional field' from the measured data so that only upper crustal structures are modelled (Nettleton, 1976). This regional field consists of low spatial frequencies which are thought to arise only from deep crustal and upper mantle structures. Inspection of the gravity map in Fig. 2 shows that Bouguer anomaly values are very low (around -60 to -70 mgals) over areas of basement outcrop such as those east of Disko Bugt. Attempts at identifying a regional field by interpolating between the observed values over areas of known basement were ambiguous and inconclusive, so an alternative modelling technique was adopted.

A reference model was defined consisting of 30 km of continental crust of density 2.8 Mg/m^3 resting on mantle of density 3.3 Mg/m^3 (Fig. 3). The GRAVMAG software (Pedley *et al.* 1993) allowed the definition of a 'background' density, and this was taken to be mantle density of 3.3 Mg/m^3. The 'crustal' prism was defined to be from -10 000 km to +10 000 km in both the plane of the model and at right angles to it. This 'reference model' generated a reference anomaly of -628 mgal which was added to all the measured values. All subsequent modelling was therefore with respect to the reference model.

In order to distinguish the gravity profiles from the seismic profiles, the following nomenclature has been adopted. The gravity model profile along seismic line GGU/95-x has been named gravity profile GGUx (e.g. the gravity profile along seismic line GGU/95-05 is GGU5). Location along the seismic lines is given by Shot Point (S.P.). Location along the gravity profiles is given in kilometres (Km) in such a way that Km 0 is at the same location as S.P. 0. Along profiles GGU2, GGU3, GGU4 and GGU5, 1 Km corresponds to 40 S.P. on seismic lines GGU/95-02, -03, -04 and -05 respectively. Along profiles GGU6 and GGU8, 1 Km corresponds to 53 1/3 S.P. on lines GGU/95-06 and -08.

Where possible the gravity profiles coinciding with the seismic lines were extended for several tens of km into where basement is exposed, either onshore or at the sea-bed as in the area south of Disko. This procedure was possible at both ends of profiles GGU2, GGU3, GGU4 and GGU5, but only towards the south-east on GGU6 and towards the east on GGU8. Water depths were entered into the models either from the seismic lines themselves or from a bathymetric map. Where basement is known to be exposed, the only spatial variable in the model is the depth to the base of the crust, which was adjusted until a satisfactory agreement between modelled and observed fields was obtained.

On profiles GGU2, GGU3, GGU4 and GGU5 basement is exposed at two separated locations, so depths to the base of the crust were interpolated through the intervening area where sediments are interpreted on the seismic lines. The depth-converted interpretations of 'acoustic basement' from the seismic lines were used as starting points for modelling total sediment thickness, and in many places the gravity model showed these to be depth to actual basement. However, in other places, lack of reflectivity in the deeper sedimentary section means that actual basement is deeper than 'acoustic basement', so, where necessary, additional thicknesses of sediment were modelled until a satisfactory agreement between modelled and observed fields was obtained. In places, it was found necessary to make adjustments to the interpolated base of the crust profile in the basin areas.

The technique described above relies on having at least two areas of exposed basement between which the 'regional field', in practise the modelled depth to the base of the crust, can be interpolated simply and uniformly. This condition is met where areas of basement are exposed onshore south and east of Disko Bugt, in eastern Nuussuaq, in central Disko (the Disko gneiss ridge) and the area where basement crops out at the sea-bed south of Disko (Fig. 1). The condition is *not* met along Vaigat, in western Nuussuaq and areas north of Nuussuaq and west of the Disko gneiss ridge. Without additional constraint in these areas, it is necessary to *extrapolate* in some way the regional gravity field (depth to base of the crust) from where it is constrained.

Constraint is not available from seismic lines GGU/95-06, -08, and -19. Because of the high density of icebergs and consequent danger to towed equipment, the length of seismic streamer that could be deployed on these lines was limited to 1200 metres (Christiansen *et al.* 1996). During processing of the seismic data, it was found that the sea-bed multiples were very strong and that the differential move-out along the short streamer between the sedimentary and multiple reflections was insufficient to attenuate the multiples. Thus on lines GGU/95-06, -08, and -19 only reflections that originate from shallower two-way times (TWT) than the first sea-bed multiple can be interpreted. The sediments along most of lines GGU/95-06, -08, and -19 are thicker than this.

Fortunately a single, short 15-fold seismic line (GGU/NU94-01) was acquired onshore in 1994 along part of the south coast of Nuussuaq (Christiansen *et al.* 1995). Line GGU/NU94-01 is roughly parallel to, and about 8 km north of, line GGU/95-06, approx. S.P.s 5500 to 6200. A final stacked section of line GGU/NU94-01 is shown in Fig. 4. The data quality is fairly good and reflections can be seen down to about 3.5 seconds TWT. In general, the section shows a sedimentary succession with apparent dip 6º–16º towards the south-east, which agrees with the structural information at outcrop where marginal marine Cretaceous sediments are exposed. Reflections down to about 2.5 secs TWT clearly come from sediments plus possibly some thin, cross-cutting sills (Christiansen *et al.* 1995). What lies below 2.5 secs TWT is not clear on the seismic evidence alone. It is possible that the event at about 3.3 secs TWT is a peg-leg multiple. If so, then the band of reflections at about 2.5 secs TWT may indicate basement at a depth of between 4.5 and 6 km. If the event at about 3.3 secs is real, basement could be between 7 and 8 km depth. This deepest unit may not be sedimentary, however. Several of the prograding hyaloclastite flows within the Vaigat Formation exposed on Nuussuaq consist of silica enriched basalts (Pedersen *et al.* 1993), as does the volcano at Ilugissoq, 12 km to the north of seismic line GGU/NU94-01 (L.M. Larsen, personal communication 1997). Storage of magma in a sill complex intruded into upper-crustal basement or deeply-buried sediments is the most likely explanation for such contamination, and it is possible that the reflections from below about 2.5 secs TWT could come from such a sill complex.

The uncertainty concerning depth to basement on seismic line GGU/NU94-01 means that there is a corresponding uncertainty in the calibration of sediment thicknesses and base of the crust depths on the gravity profiles along Vaigat, in western Nuussuaq and areas north of Nuussuaq and west of the Disko gneiss ridge. Because of this, two alternative models have been calculated for the profiles whose results depend on the interpretation on seismic line GGU/95-06, one for each alternative depth-to-basement interpreted from line GGU/NU94-01. Models based on the assumption that basement lies between 4.5 and 6 km depth on GGU/NU94-01 are labelled with suffix 'a' (e.g. GGU6a), while those based on the assumption that basement lies between 7 and 8 km depth on GGU/NU94-01 are labelled with suffix 'b' (e.g. GGU6b).

Seven 'artificial' gravity profiles, called Disko-1 to Disko-7 (with a and b suffixes, where appropriate), were constructed from gravity observations that lie approximately along a straight line. The location of these profiles is shown on Fig. 2. Profiles Disko-1, Disko-2, Disko-3, Disko-4 and Disko-7 were constructed in such a way that they passed over two areas of basement outcrop, in order to be able to 'calibrate' the base of the crust (regional) profiles. Profiles Disko-5 and Disko-6 run from an area of basement outcrop through seismic line GGU/NU94-01 to provide calibration. Profile Disko-5 was extrapolated northwards to tie with profile GGU8, which in turn has been extended eastwards from the seismic line to pass over outcropping basement. However, there is no unambiguous calibration of the profiles west of the Disko gneiss ridge, over western Nuussuaq and north of Nuussuaq. Profiles in these areas must therefore be treated circumspectly and it was felt that it would not be justified to extend the modelling as far north as seismic line GGU/95-19 (Fig. 1).

Additional constraints on the gravity models are obtained from known outcrop limits of sediments, basement and basalts. A further constraint is the requirement that the modelled profiles should tie at their intersections.

Densities used for the various units are shown in Table 1 and the choices discussed in Appendix 1.

TABLE 1

Densities used in the gravity modelling.

Water	1.0 Mg/m^3
Sediment	2.55
Continental Basement	2.8
Igneous rocks of all kinds	3.0
Mantle	3.3
Background density	3.3

Description of model profiles

The modelled profiles are shown in Figs 5 to 17. Sediment and basalt interpreted from the seismic sections are shown in different tones from those interpreted only from the gravity models.

Disko island east of the Disko gneiss ridge and Disko Bugt south and east of Disko island

GGU5 (Figs 5a and 5b): Gravity profile GGU5, which is seismic line GGU/95-05 extended onto areas of basement outcrop onshore both to the north and south, gives good control on depths to the base of the crust and therefore the regional field. Gravity modelling was started using a depth to the base of the crust that fitted the observed field where basement is exposed and a smooth interpolation between these areas, together with the envelope of the deepest sedimentary reflections visible on the seismic line ('acoustic basement'). In order to fit the observed field over the sedimentary basin, it was found necessary along most of the line to model additional sediments below the 'acoustic basement'.

Basement is interpreted to crop out south of Km 5.6 (S.P. 230) where a fault throws basement down some 800 metres to the north. The sediments thin northwards to only about 100 metres thick south of a second fault at Km 15 (S.P. 600) across which they thicken to about 500 metres. From there to Km 79 (S.P. 3160) only the shallower part of these sediments is interpreted from the seismic data. It was found necessary to model an additional layer of sediment at the base of which the top basement dips steadily northwards to nearly 1900 metres depth at Km 77 (S.P. 3080). Between there and Km 84.25 (S.P. 3330), basement is modelled to rise abruptly by about 1 km then fall again almost as abruptly, possibly indicating some kind of faulting. From Km 84.25 (S.P. 3330) to a large fault at Km 130 (S.P. 5200), the sediments are about 2 km thick. Some of the sediments are reflective and are interpreted on the seismic data. Other parts are non-reflective and top 'acoustic basement' was interpreted at the top of these sections. However the gravity modelling indicates that many of these areas must also consist of sediments.

The part of line GGU5 north of Km 130 is discussed later in the section on Vaigat and Nuussuaq.

The base of the crust along profile GGU5 was calculated to be between about 32 and 36 km depth, between 2 and 6 km deeper than required for isostatic equilibrium.

GGU3a and GGU3b (Figs 6a and 6b): Profile GGU3 is seismic line GGU/95-03 extended eastwards onto onshore basement outcrop and westwards over where basement, and farther west basalt, is interpreted on seismic and magnetic data to crop out at sea-bed. The basement outcrop is the southern extension of the gneiss ridge exposed on Disko (the Disko gneiss ridge).

To the east of the Disko gneiss ridge, the gravity model shows that the thickness of sediment interpreted on the seismic data may well be the entire thickness of sediment. The basement surface is irregular at a depth of about 1 km below sea-level, probably because of faulting. The seismic data also shows what probably are many sills intruded into the sediments, but it has not been necessary to model them on the gravity data.

Basalts are interpreted to crop out on line GGU/95-03 west of Km 108.75 (S.P. 4350), based on interpolation from nearby Brandal magnetic profiles. However the part of profile GGU3 west of about Km 109 is discussed below in the section about the area west of the Disko gneiss ridge.

The base of the crust on profile GGU3 is calculated to be at between 33 and 36 km depth under Disko Bugt east of the Disko gneiss ridge (from Km -40 to about Km 70), 3 to 6 km deeper than would be required for isostatic equilibrium. West of the Disko gneiss ridge depth to the base of the crust is modelled to decrease to 26 km (see below).

GGU2 (Figs 7a and 7b): Profile GGU2 is seismic line GGU/95-02 extended eastwards onto onshore basement outcrop and westwards to where basement is interpreted on seismic and magnetic data to crop out at sea-bed, similarly to profile GGU3. Only a thin (about 100-150 metres thick) veneer of sediment was interpreted from the seismic data, and there are few if any faults. Gravity modelling suggests that basement reaches a maximum depth of about 1000 metres along this line. Apart from a small outlier on the flank of a trough at around Km 12, the western limit of sediments may be at a small fault at approximately Km 17 (S.P. 680). The eastern limit of sediments is east of the seismic coverage and appears from gravity modelling alone to be a faulted contact at Km 69.5, about 5 km west of the coast.

Depths to the base of the crust under profile GGU2 are between 31.5 and 34 km, 1.5 to 4 km greater than required for isostatic equilibrium.

GGU4 (Figs 8a and 8b): Profile GGU4 is seismic line GGU/95-04 extended south-eastwards onto known basement outcrop and north-westwards to the north coast of Disko across the Disko gneiss ridge. In this section, only the part of the line south-east of the Disko gneiss ridge is discussed.

The gravity modelling shows that there is a significantly thicker sedimentary succession along the offshore part of GGU4 (Km 0 to Km 60) than was apparent from seismic interpretation alone. There is a significant change in depth to basement between Km 40.75 (S.P. 1630) and Km 48.5 (S.P. 1940), which may indicate faulting with a total throw of around 300 to 400 metres down to the south-east. The sediments appear to extend along line GGU/95-04 to approximately the limit of seismic coverage at Km 61.25 (S.P. 2450). The gravity modelling shows that the top of the basement dips northwards here at only about 4° which indicates that, south of their present limits, the sediments have been eroded away.

The interpretation of GGU4 over Disko is controlled by the known outcrop of sediment and basement at the Disko gneiss ridge. Since basalt along this profile is everywhere exposed *above* sea-level, the basalts exposed on Disko do not appear in the model along GGU4. It is assumed that their gravity effect has been compensated in calculation of the Bouguer and terrain corrections for the onshore data. However, the terrain on Disko is alpine and in places capped with ice. All the measurements were made on exposed rock (on nunataks within the ice-caps), but no attempt was made during terrain corrections to compensate for the unknown thickness of ice (R. Forsbeg, personal communication 1998). Consequently the calculations done to produce the Bouguer anomalies are simplified and there may be considerable uncertainty in the gravity anomalies and therefore in the modelling in central Disko.

The model on GGU4 shows basement under central Disko dipping north-westwards from the north-western end of line GGU/95-04 at Km 0. Basement depths are greatest, nearly 3 km, at about Km 38, north-west of which the basement rises again to the Disko gneiss ridge at Km -64 (minus 64). Top basement is shown dipping at about 19º on the eastern flank of the Disko gneiss ridge, but this is a minimum figure since the profile cuts the ridge at an acute angle (Figs 1 and 2). It is therefore possible that margin of the Disko gneiss ridge is faulted where profile GGU4 crosses it.

The base of the crust under Disko Bugt on profile GGU4 is interpreted to be at least 2.5 deeper than isostatic equilibrium would require along the entire line, increasing to about 6.5 km under the Disko gneiss ridge at about Km -70. The assumptions about the modelled depths to the base of the crust along profile GGU4 north-west of about Km -70 are discussed below.

Disko-1, Disko-2, Disko-3 and Disko-4 (Figs 9a and 9b, 10a and 10b, 11a and 11b, and 12a and 12b): Two gravity profiles have been constructed running east -west across eastern Disko and Disko Bugt (profiles Disko-1 and Disko-2) and another two across eastern Disko, eastern Vaigat and eastern Nuussuaq (profiles Disko-3 and Disko-4). All of these profiles extend west of the Disko gneiss ridge and those parts of the profiles are discussed below. In this section only those parts of the profiles east of the Disko gneiss ridge are discussed.

Disko-1 shows little relief on basement at a depth of between 2 and 3 km under eastern Disko. The eastern termination of sediments is probably at a fault at about Km 165 but the steepest part of the westwards termination against the Disko gneiss ridge, between Km 58 and Km 67, dips at only 16º.

On Disko-2, there is evidence for block faulting at about Km 125 and the eastern termination of the sediments at Km 152 is also probably at a fault. On this profile, the basement dips steeply eastwards from the gneiss ridge at Km 63 suggesting that the eastern margin of the Ridge is a faul. There is low relief on the basement between Km 64 and Km 122, similar to that on Disko-1.

Disko-3, which runs NE–SW, shows the most marked evidence for block-faulting and for the thickest sediments in eastern Disko and Disko Bugt, over 7 km, in a downfaulted block east of the Disko Gneiss ridge. As discussed above, the terrain on Disko is alpine and in places capped with ice, so the oversimplified calculations done to produce the terrain corrections of the Bouguer anomalies mean that there may be considerable uncertainty in the accuracy of the gravity anomalies and therefore in the modelling in central Disko. The details of the model shown on this profile are therefore uncertain. Other fault blocks are shown on this profile in the area near and north of Vaigat. Between Km 109 and Km 129, Disko-3 runs over Saqqaqdal on Nuussuaq where many dolerite sheets are exposed. Top basement is modelled as very shallow (less than 2 km depth) between Km 109 and Km 122, but it is possible that basement lies deeper than this in this area and that the excess mass consists of denser igneous intrusions.

Disko-4 also runs from east Disko across Vaigat, but gravity modelling on Disko-4 is influenced by modelling on profiles GGU6a and GGU6b and is discussed later.

On all of the profiles east of the Disko gneiss ridge, depths to the base of the crust are greater than required by isostatic equilibrium and all of them show that the crust is up to 38 km thick under the gneiss ridge where isostatic equilibrium requires only 30 km thick crust.

Northern Disko island, Vaigat, Western Nuussuaq and north of Nuussuaq

*Eastern Vaiga*t: On seismic lines GGU/95-05 and GGU/95-06 at the south-eastern end of Vaigat, what appears to be a small graben containing over 1500 metres thickness of parallel bedded and reflective sediment can be seen. The seismic response from these sediments is significantly different from that from the sediments farther south under Disko Bugt, but similar to that farther west in Vaigat and north of Nuussuaq. This graben lies between Km 130 (S.P. 5200) and Km 141.75 (S.P. 5670) on profile GGU5 (Figs 5a and 5b) and between Km 11.25 (S.P. 600) and Km 21.5 (S.P. 1150) on profile GGU6 (Figs 13a, 13b, 13c and 13d). Gravity interpretation of profile GGU5 (Figs 5a and 5b) shows that the sediment thickness visible on the seismic data in the graben is, in fact, the total thickness of sediment. However the fault at Km 130 appears to throw basement down only a few hundred metres and separates two areas of sediment of similar thickness but of very different facies. The facies to the south of the fault is entirely non-reflective and was interpreted as basement on the seismic data alone. However the gravity modelling that this facies be interpreted as sediment in this area. The fault at Km 141.75 (S.P. 5670) on profile GGU5 bounds the basin north of it basement crops out at the sea-bed.

GGU6a and *GGU6b* (Figs 13a, 13b, 13c and 13d): Gravity models GGU6a and GGU6b have been constructed along Vaigat based on water depths, minimum sediment thickness and evidence of the presence of basalt provided by line GGU/95-06. The extension to the south-east is controlled by basement outcrop, and control midway along profiles GGU6a and GGU6b is provided by seismic line GGU/NU94-01, which is roughly parallel to and about 8 km north of line GGU/95-06 between approx. S.P. 5500 (Km 103) to S.P. 6200 (Km 116).

Seismic line GGU/95-06 shows sediments to its south-eastern end at S.P. 209 (Km 3.9). Gravity models GGU6a and GGU6b are the same at their south-eastern ends. Both show that the sediments terminate south-eastwards against a fault with a throw of about 1.5 km at Km 1.4, about 2.5 km beyond the end of the seismic coverage on line GGU/95-06. Both models show depths to the base of the crust of 34 to 35 km under the exposed basement at the south-east end of the profile. Both models also show that, south-east of Km 27 (S.P. 1440), the total thickness of sediment is visible on the seismic line.

Some control on the models is obtained where profiles Disko-3 and Disko-4 cross profile GGU6 at Km 48 (S.P. 2580) and Km 64.5 (S.P. 3450). Both Disko-3 and Disko-4 are constrained where they cross the basement outcrops of the Disko gneiss ridge and north-east Nuussuaq.

Northwest of Km 64.5 on GGU6, the only control deeper than the first sea-bed multiple on GGU/95-06 is provided by seismic line GGU/NU94-01 between Km 103 and Km 116 (S.P.s 5500 to 6200), where, as described above, basement on profile GGU6a has been assumed to lie between 4.5 and 6 km depth and basement on profile GGU6b has been assumed to lie between 7 and 8 km depth. These different assumptions are the cause of the differences between the profiles labelled with a and b suffixes.

Profile GGU6a shows the base of the crust at more than 33 km depth south-east of Km 88, from where it shallows to about 31 km depth at Km 106 under line GGU/NU94-01 and 26 km depth at Km 190, north-west of which it remained at 26 km depth. Profile GGU6b shows depths to the base of the crust greater than 33 km south-east of Km 82.5 from where they shallow to around 30.5 km at Km 102 under GGU/NU94-01 north-west of which there is again a gradual shallowing to about 26 km depth at about Km 195. Farther to the north-west the base of the crust remains at 26 km depth.

The modelled depths to the base of the crust and the interpretation of faults at shallow depth on the seismic data constrain the modelled depth to basement. On both GGU6a and GGU6b, depth to basement is modelled to increase steadily to the north-west from about 2 km at Km 30 to nearly 3 km at Km 48, at the tie with Disko-4. To be consistent with the fault interpreted at Km 115 on that profile, a fault throwing basement down to about 5 km depth has been interpreted on GGU6a and GGU6b at Km 49, north-west of which basement depths shallow again to between 2.3 km at Km 53.5 and 1.8 km at Km 67. A fault at Km 67 throws basement down to 3.7 km depth. Depths to top basement first shallow to 2.8 km at Km 74, north-west of which profiles GGU6a and GGU6b differ. Depths to top basement at Km 103 reach 4.4 km on GGU6a and 4.6 Km on GGU6b.

Seismic line GGU/95-06 shows a major fault which reaches the sea-bed at S.P. 5270, corresponding to Km 99 on profiles GGU6a and GGU6b. On seismic line GGU/NU94-01 (Fig. 4) what may be a large fault can be interpreted below 2.5 secs TWT on the eastern part of the section. The extrapolation of this fault reaches the surface at Nuuk Killeq on the south coast of Nuussuaq where a change of about 400 m in altitude of the base of the Tertiary hyaloclastite breccias is known (Pedersen *et al.* 1993). This fault is modelled on both profiles, where it throws basement down to the north-west, from 4.4 km to about 6 km depth at Km 105.5 on GGU6a and from 4.4 km to over 8 km depth on GGU6b.

A major regional fault with throw down to the west can be traced on Disko where it is known as the Kungannguaq fault and on Nuussuaq where it is known as the Qunnilik fault.

It crosses seismic line GGU/95-06 at S.P. 6100 (Km 114 on profiles GGU6a and GGU6b). Profiles GGU6a and GGU6b both show a major fault block between the Kunganngguaq-Qunnilik fault and the Itilli fault at Km 143 (S.P. 7620). Depth to basement on the crest of the Kunganngguaq-Qunnilik fault's foot-wall block is modelled at Km 119 at a depth of 2.8 km on GGU6a and at a depth of 2.5 km on GGU6b. Basement is thrown down across this fault to 8 km depth on GGU6a and 10 km on GGU6b. Both models show basement shallowing north-westwards to just over 2 km depth on the crest of the footwall of the Itilli fault at Km 146-147.

Both models show basement thrown down to about 11 km depth to the north-west of the Itilli fault, from which point basement depths shallow towards the north-west, reaching 5 km depth on GGU6a and 8 km depth on GGU6b at Km 190, the end of the measured profile.

There is, of course, major interaction between the modelled basement depths and basalt thicknesses. Basalts at sea-bed outcrop can be seen on seismic line GGU/95-06 north-west of S.P. 6340 (Km 119). Reflections from sediments below the base of the basalts can be seen between S.P.s 7120 (Km 133.5) and 7720 (Km 145) where the Itilli fault is crossed, which constrains the modelled thickness of basalt in this section of profile. This observation is consistent with the thickness of basalt penetrated by various onshore commercial drill-holes within this fault-block (GANE#1 and GANK#1, Christiansen *et al.* 1996; GRO#3, Christiansen *et al.* 1997), which reached base basalt between 22 and 386 metres below sea-level.

South-east of the Itilli fault, maximum modelled depth to base basalt is about 1.5 km, but both profiles GGU6a and GGU6b show much thicker basalts to the north-west of the Itilli fault, a maximum depth to base basalts between 9 and 10 km around Km 160 on both profiles. Farther north-west the basalts are thinner. It is unlikely that such thicknesses of basalt would exist without substantial intrusions in the crust. Therefore a more likely geological model would be obtained if some of the excess mass were transferred into the crust. The result would be that the basalt was modelled to be thinner, depth to top basement would be shallower and basement density would be higher. Because there is no independent control over depths to base basalt, depths to basement or depths to the base of the crust north-west of the Itilli fault, details of the models in this area are very uncertain and may be incorrect. In particular, all the igneous material is modelled in the shallowest unit and no attempt was made to model intrusions in the crust or sediments. However, all attempts failed to model the major increase in basalt thickness as occurring across the Itilli fault. The gravity data consistently indicate that the maximum excess mass of igneous material lies about 10 km north-west of the Itilli fault.

Other profiles: A number of other profiles have been constructed in the northern Disko, Vaigat and western Nuussuaq area, passing through what are thought to be major structural elements. Where there are differences between the 'a' and 'b' profiles, it has been found that it is possible to construct models along these profiles that fit either assumption about depth to basement on line GGU/NU94-01 and hence on GGU6a or GGU6b. Modelled *depths* to basement are different on the alternative models, but the *locations* of the major changes in basement depth are similar, indicating that the locations of major faults, horsts and grabens are fairly reliable.

Profile Disko-4 (Figs 12a and 12b) runs from west of and across the Disko gneiss ridge, across eastern Disko, Vaigat, the sedimentary basin of eastern Nuussuaq and onto the basement in eastern Nuussuaq. GGU6 is intersected by Disko-4 at about Km 48. It has been found difficult to make a consistent tie between profiles GGU6 and Disko-4 at both the base of the crust and top basement levels simultaneously. The best tie has been obtained by modelling the base of the crust at less than 30 km depth at Km 130. This produces the rather abrupt shallowing of the base of the crust shown on Fig. 12b which looks artificial. Alternative interpretations that produce more geologically likely models can be envisioned, such as a magma chamber within the crust. Without additional constraints the choice is somewhat arbitrary. Consequently, actual modelled depths to basement and base of the crust on this profile should be treated sceptically. Nonetheless, the overall modelled structure at top basement level is probably reasonably accurate.

There is some kind of fault-block between Km 116 and the Saqqaqdal fault at Km 133 and there is a fairly smooth, probably unfaulted, slope on the east flank of the Disko gneiss ridge. This unfaulted slope may be significant, because the borehole Falconbridge FP93-3-1 was drilled at 70º 04´ 56.3"N, 53º 35´ 45.5"W near the its top (Fig. 1). FP93-3-1 intersected basement at a height of 160 metres above sea-level below 55 metres of probably brackish water Apto-Albian sediment (H. Nøhr-Hansen, personal communication 1998). It is unlikely that such sediment has been preserved without ever having been buried deeper, so it may be an erosional remnant whose presence indicates that the Disko gneiss ridge has been uplifted at some time after deposition of the sediment, probably in the Late Maastrichtian and/or Early Paleocene.

Profile Disko-5 (Figs 14a, 14b, 14c and 14d) runs south to north along the Disko gneiss ridge, across Vaigat, intersects seismic lines GGU/95-06 and GGU/NU94-01 and continues northwards across Nuussuaq to terminate on seismic line GGU/95-08 (Fig. 1). Modelling control is obtained along the gneiss ridge, where the profile intersects several other gravity profiles, and at the intersections with profiles GGU6a, GGU6b and GGU/NU94-01. Control of the northern limit of the gneiss ridge is given by the borehole Falconbridge FP93-3-1 at 70º 04´ 56.3"N, 53º 35´ 45.5"W which, as discussed earlier, intersected basement at a height of 160 metres above sea-level (Fig. 1).

Gravity modelling along this profile has proved to be a serious problem, and eventually 4 models have been produced. The models are labelled Disko-5a and Disko-5b according to which assumption is made about depth to basement on seismic line GGU/NU94-01. However, two different models have been produced for each assumption because of uncertainties in how to interpret the section between Km 130 and Km 140, and the 'alternative' models are labelled *Disko-5a alternative* and *Disko-5b alternative* are shown in Figs 14e, 14f, 14g and 14h.

From the northern end of the Disko gneiss ridge at about Km 97, basement drops abruptly to 5.4 km depth (Disko-5a) or 5.7 km depth (Disko-5b), rises again to about 1.4 or 1.5 km depth near the north coast of Disko before dropping again to 5.5 km (Disko-5a, Km 130) or 8 km (Disko-5b, Km 130), depending on which interpretation is used on line GGU/NU94-01.

It is necessary to interpret excess mass between Km 130 and Km 140 either as some form of pluton intruded into the basement or at the basement–sediment interface (Disko-5a and Disko-5b) or as a narrow ridge of basement that rises steeply immediately north of seismic line GGU/NU94-01 to less than 1 km depth at Km 132-133 then descends again to 5 km depth at Km 138 (Disko-5a alternative) or 7 km depth at Km 144 (Disko-5b alternative). The 'alternative' models pose serious problems in drawing a structure map. The very shallow basement at Km 132-133 would imply the existence of a fault parallel to seismic line GGU/NU94-01, and if it is assumed that such a fault has a hade of about 30°, the fault plane should be at 5 km depth at Km 130 and 8 km depth at Km 128. However, there is no indication of the implied fault on seismic line GGU/NU94-01. The alternative interpretation of a pluton in the basement is supported by the observation that the Nuuk Killeq volcanic member, exposed within the Tertiary volcanic series in this area, consists of silica-rich contaminated basalt lavas and hyaloclastites (Pedersen *et al.* 1993). The contamination implies that this material resided in a mid- or upper-crustal magma chamber for some time before being erupted (L. M. Larsen, personal communication 1997). There is an eruption centre at Ilugissoq (L. M Larsen, personal communication 1995), near Km 142 on Disko-5, which could have been derived from a magma chamber within the basement or at the basement–sediment interface, and seismic line GGU/NU94-01 shows several cross-cutting reflections, possibly from sills (Christiansen *et al.* 1995) which be or could have come from such a source.

Disko-5a shows basement dipping steadily northwards to over 10 km depth at Km 178 from where it rises to 5.5 km depth at Km 185, the tie with GGU8. Disko-5b shows a more irregular basement between 7 km and 10 km depth between Km 140 and Km 154 before it rises to 5 km depth at Km 185, the tie with GGU8.

Profile Disko-6 (Figs 15a, 15b, 15c and 15d) crosses the exposed basement on eastern Nuussuaq east of Km 67 and the sedimentary basin in central Nuussuaq from Km 67 to Km 103, where depth to top basement is modelled at about 5 km on Disko-6a and as rising from 5 km depth at Km 70 to 2 km depth at Km 102. Seismic line GGU/NU94-01 provides control from Km 103 to Km 117, west of which models Disko-6a and Disko-6b have been modified from models GGU6a and GGU6b. The models between Km 103 and Km 117 are taken from GGU/NU94-01, west of which the Kungannguaq-Qunnilik fault is crossed. Depth to basement is modelled at 3.5 km (Disko-6a, Km 117) or 2.8 km (Disko-6a, Km 120) on the crest of the foot-wall block of the Kungannguaq-Qunnilik fault. Basement is thrown down across this fault to 8.6 km (Disko-6a, Km 120) or 9.1 km depth (Disko-6b, Km 122). Disko-6b shows basement shallowing westwards to the crest of the footwall of the Itilli fault, to 1.3 km depth at Km 152. However Disko-6a shows an intermediate fault at Km 140 to 143 between the Kungannguaq-Qunnilik fault at Km 120 and the Itilli fault at Km 156–158. On Disko-6a, basement shallows westwards from 8.6 km at Km 120 to 1.1 km depth at Km 141. It is then thrown down across the intermediate fault to 6.5 km at Km 143 and then rises again to the west to 4.7 km at Km 158 on the crest of the footwall block of the Itilli fault.

The area onshore north-western Disko west of the Kungannguaq-Qunnilik fault and just to the south of Disko-6 contains many volcanic necks and many areas where the volcanic rocks contain sandstone and bituminous shale xenoliths. Native iron produced by reactions between magma and Cretaceous bituminous shales and sandstones rich in sulphur compounds (Clarke & Pedersen 1976) is also common. The amount of sedimentary contamination in the basalts implies that they have passed through fairly thick sediments and the number of volcanic necks and intrusions may imply upper crustal magma chambers. It is possible therefore that both the basement and the sediments west of the Kungannguaq-Qunnilik fault contain many intrusions and should therefore be denser than is assumed here. If so, the modelled shallow top basement (around Km 130 to Km 140 on Disko-6a and Km 130 to Km 150 on Disko-6b) may not be real. Basement and sediments should have a higher average density, top basement should be deeper and there should be thicker sediment in this area than modelled here.

The depth to top basement on Disko-4 north-west of Km 58 (Figs 12a and 12b) is modelled to tie with Disko-6, so on this line, too, top basement may be deeper than shown and there may be thicker sediments than shown in Figs 12a and 12b.

Disko-6a and Disko-6b show similar models for the basalts west of the Itilli fault, as do GGU6a and GGU6b from which they are modified. Disko-6a and Disko-6b both show that the Itilli fault throws top basement down to about 11 km depth, at Km 158 on Disko-6a and Km 155 on Disko-6b, north-west of which it rises again to 8.8 km at Km 180 on Disko-6a and 8.3 km at Km 180 on Disko-6b.

Both Disko-6a and Disko-6b show similar models for the basalts to the west of the Itilli fault, and both models resemble those along GGU6. Thick basalts are modelled some distance to the west of the Itilli fault. Maximum depth to base basalt is shown on Disko-6a as 8.7 km at Km 164, 6-7 km west of the Itilli fault and on Disko-6b as 8.4 km at km 169, 14 km west of the Itilli fault. As was discussed above for GGU6a and GGU6b, it is unlikely that such thicknesses of basalt would exist without substantial intrusions in the crust. Therefore a more likely geological model would be obtained if some of the excess mass were transferred into the crust. The result would be that the shallow basalt was modelled to be thinner and depth to top basement would be shallower.

Profile Disko-7 (Figs 16a and 16b) crosses the Disko gneiss ridge from Km 24 to Km 70, GGU/95-06 (S.P. 4800, Km 90) at Km 95, the sediment basin in central Nuussuaq from Km 101 to Km 126 and the exposed basement on eastern Nuussuaq north-east of Km 126. The basement topography between the Disko gneiss ridge and the south coast of Nuussuaq (Km 70 to Km 101) on this profile is similar to that interpreted on the Disko-5 profile (Figs 14a, 14b, 14c and 14d). The Disko gneiss ridge ends to the north as a steep, presumably faulted, drop from the end of the Ridge to 5.7 km depth at Km 72, north-east of which is a fault-block whose crest is at a depth of 0.7 km at Km 85 under the north coast of Disko. Basement depths then increase across this fault to 4 km at Km 87 and dip gently north-eastwards to nearly 5 km at Km 96, where they are controlled by the tie with GGU6. Depths to top basement decrease farther north-west to about 2 km at Km 123 on the footwall of a fault that forms the south-western limit of a narrow graben about 7–8 km wide. The north-eastern boundary of the graben is the Ikorfat fault at Km 130. On Disko-7, the base of the graben is modelled at about 3 km depth.

The Ikorfat fault has been known for a long time (e.g. Rosenkrantz & Pulvertaft, 1969), but the fault at Km 123 has only recently been recognised at outcrop (T.C.R. Pulvertaft, personal communication 1997).

Basement is exposed between Km 130 and Km 145 on Disko-7, north-east of which sediments are exposed south of the north coast of Nuussuaq at Km 149. The exposed sediments dip north and north-eastwards at 9°–16° and the profile Disko-7 shows them as the southern part of a half graben about 2.5 km deep whose north-eastern bounding fault is at Km 170.

North of Nuussuaq: As discussed above, lack of control on the regional gravity field means that modelling along the gravity profiles through western Vaigat and western Nuussuaq is ambiguous. That remark applies with even greater force to gravity modelling in the area north of Nuussuaq. No independent control is available along or west of any of the seismic lines. In theory control is available over the exposed basement east of 52º 20´W (Fig. 1), but this area consists of islands and peninsulas of extremely rugged topography. The map in Fig. 2 shows the gravity field in the area from the north coast of Nuussuaq to 71º 10´N and between 52ºW and 50º 40´W to consist of a complex pattern of closed highs and lows, each some 10–20 km across. Inspection of the original reduced Bouguer data points shows a strong correlation with topography, so it is suspected that the complex gravity topography shown in this region may be due to incompletely reduced terrain corrections.

Because of these considerations, the results of any gravity modelling in the area north of Nuussuaq should be treated with considerable reserve. Only one profile has been modelled, along seismic line GGU/95-08 and its eastward extension. Profile GGU8 is shown in Figs 17a and 17b. The model was made consistent with the major faults visible on the seismic data, and reflections visible from below top basalt between Km 66.5 (S.P. 3550) and Km 78 (S.P. 4150) were assumed to be from base basalts/top sediments. Some control on modelling is available from the tie at about Km 60 with the northern end of profile Disko-5 (Figs 14b and 14d) which suggests a depth of 27 km to the base of the crust. However, these depths are themselves the result of extrapolating the gravity models along the ambiguous profile Disko-5, which had to be adjusted at its northern end to tie with GGU8, so sediment thickness and depth to the base of the crust can be varied relative to one another to produce an almost unlimited variety of models along this profile. Model GGU8 is, however, consistent with the other geological and geophysical evidence in the area. In particular, depth to the base of the crust under the basement at the eastern end of the profile is controlled and depth to the base of the crust at the western end of the profile is *assumed* to be the same as modelled at the north-western end of GGU6a and GGU6b. Modelling the regional field was then a matter of modelling the base of the crust between these to areas in a geologically meaningful way that resembled the models calculated on GGU6a and GGU6b.

Seismic line GGU/95-08 shows major faults that with downthrow to the west. Between the faults up to 2 km of eastwards-dipping sediments can be seen. Basalt can be seen at seabed west of S.P. 3550 (Km 66.5) on line GGU/95-08 and from S.P. 3550 (Km 66.5) to S.P.

4150 (Km 78) reflections can be seen from below top basalts that have been interpreted to come from the base of the basalts and the underlying sediments.

The modelling reveals depths to basement comparable to those found on profiles GGU6a and GGU6b. GGU8 indicates basement depths around 11 km west of the fault at Km 89 where the base of the crust is assumed to be at a depth of 26 km. The Itilli fault is at Km 68 to Km 71, the Ikorfat fault is at Km 46 and the Kuk fault at Km 7.

West of the Disko gneiss ridge

There is no seismic control of the area west of the Disko gneiss ridge and the outcrop is entirely of basalt (Fig. 1). However, some control over gravity modelling is obtained from the known basalt stratigraphy in the area (A.K. Pedersen, pers. comm. 1997), together with evidence from contaminated basalts (e.g. metallic iron and sediment xenoliths) that the erupted magma had passed through organic-rich, terrigenous, siliciclastic sediments. It has also been assumed that the depth to the base of the crust of 26 km calculated at the western end of GGU6 is reached as near as possible to the west of the Ridge. Gravity models based on these constraints are shown at the western ends of profiles Disko-1 (Fig. 9b), Disko-2 (Fig. 10b), Disko-3 (Fig. 11b), Disko-4 (Fig. 12b), GGU3 (Fig. 6b) and GGU4 (Fig. 8b). The models were made with the same crustal density, 2.8 Mg/m^3, as elsewhere in the region. However, as discussed above about profile Disko-6, it is possible that there are large numbers of Tertiary intrusions both in the sediments and in the basement this area, which would have the effect of raising their average density. Since basalt thickness is fairly well controlled, it is possible that depths to top basement should be deeper, and sediment thicknesses greater, than those calculated. However, there is no systematic way to take these effects into account, so depths to top basement shown should be regarded as *minima*.

At outcrop, the Disko gneiss ridge is bounded to the north-west by the extension of the Kungannguaq-Qunnilik fault that crosses GGU6 at Km 114 and Disko-6 at Km 120. However, this fault seems to die out before it reaches GGU4. Farther south, where Disko-4, Disko-7, Disko-2 and Disko-1 cross the Ridge, the top basement dips westward at 10° or less, indicating that there is no single large fault here. Farther south again, profiles GGU3 and Disko-3 indicate that the south-western margin of the Disko Gneiss ridge consists of a large fault.

Maps

Depths to top basement

Maps showing depths to basement as interpreted from the gravity profiles are shown in Figs 18 and 19. Fig. 18 is drawn from the 'a' profiles and Fig. 19 is drawn from the 'b' profiles. The maps are identical except where the 'a' and 'b' profiles differ – in north-western Disko, western Vaigat and western Nuussuaq. To the south and east, and in a north–south trending ridge on Disko, top basement is either above sea-level onshore or exposed at the sea-bed. These areas are marked. Where top basement is covered by sediments is referred to as the sedimentary basin.

Care has been taken during the drawing of Figs 18 and 19 to show the faults with realistic heaves. It was assumed that the faults all had hades of 30°, and the heaves were drawn accordingly. A 30° hade is consistent with the gravity models and with measured hades on the Saqqaqdal fault (Sa) (25°–33°) and the Kungannguaq-Qunnilik fault (K-Q) (25°) (Pedersen *et al.* 1993). Several of the faults shown on Figs 18 and 19 are known at onshore outcrop. In these cases, the contoured depth to top basement was used to calculate the heave from the outcrop of the fault, first to top basement on the footwall block and then to top basement on the hanging wall block.

Eastern Disko and Disko Bugt: The maps show that depths to basement under eastern Disko and Disko Bugt are not large, typically less than 3 km. Depths to basement greater than 3 km are shown only south-west of Arve Prinsens Ejland and (possibly as great as over 7 km) under central Disko.

The sedimentary basin is bounded to the east by faults, whose outcrop pattern is probably much more complex than shown on Figs 18 and 19. This is particularly true of the fault pattern from GGU3 in the south to Disko-2 in the north. The pattern drawn here is influenced partly by interpretation of the Brandal seismic lines, partly by aeromagnetic data (Thorning in press) and partly by the trend of shear zones onshore (Garde 1994). A fault on GGU5 at Km 74 (fault A) that throws down to the south complicates the picture even further.

The sediments in Disko Bugt thin to zero thickness towards the south, possibly because erosion has removed formerly more extensive sediments. On the west is the Disko gneiss ridge, whose eastern margin may in part be faulted (fault B).

Fault C runs NW–SE across Disko. It is drawn by joining the faults interpreted on Disko-2 at Km 125 and Disko-3 at Km 78-80. Fault C strikes at 120° which is very similar to the strike of shear zones exposed onshore north of Ilulissat (Jakobshavn). Depth to basement on the hanging wall of this fault is modelled as more than 7 km on line Disko-3, but, as discussed above, the terrain in this part of Disko is alpine and capped with ice, so the somewhat simplified calculations done to produce the Bouguer anomalies mean that there may be considerable uncertainty in the accuracy of the gravity anomalies and therefore in the modelling. The details of the modelling in this area are therefore very uncertain. The interpretation shown here implies the existence of a shallow basement ridge that strikes NW–SE under north-eastern Disko.

Basement is interpreted on seismic and magnetic data to crop out at the sea-bed south of Disko (Fig. 1). Part of the eastern limit of this outcrop is interpreted on Brandal seismic data to be a NW–SE trending fault (fault D). Fault E, east of and parallel to fault D, is interpreted on multi-channel seismic lines. While the strike of these two faults may be important in the general pattern of faults in the basin, neither has a throw great enough to be interpreted on the gravity profiles alone.

West of the Disko gneiss ridge: Fault F is interpreted on profiles Disko-3 at Km 23–26 and GGU3 at Km 108–112. The fault obtained by joining these locations strikes nearly N–S, but is not interpreted on the next profile to the north, Disko-1. Profiles Disko-1, Disko-2, Disko-4 and Disko-7 to the west of the Disko gneiss ridge all show top basement dipping to the west at about 6°–10°. It is difficult to reconcile the contours drawn through these lines with those drawn through GGU3 and Disko-3 without either a fault or an area of artificially steep contours, so fault F has been continued NW from profile Disko-3 and is shown on Figs 18 and 19 striking 115°–120° under Kangerluk.

As was discussed above, it is possible that there are large numbers of Tertiary intrusions in the basement west of the Disko gneiss ridge, which would have the effect of raising its average density. Since basalt thickness is fairly well controlled from outcrop stratigraphy, it is possible that the depths to top basement west of the Disko gneiss ridge on profiles Disko-1, Disko-2, Disko-7, Disko-4, GGU4 and Disko-6 should be deeper than those shown here, which would have the effect of making them more similar to those modelled on GGU3 and Disko-3 to the south and GGU6a and GGU6b to the north. If so, it is possible that more of the western limit of the Disko gneiss ridge than shown here is formed by faulting, and that fault F might continue northwards from Disko-3 and even join up with the Kungannguaq-Qunnilik fault (K-Q), which is known at outcrop. In this case, the fault striking 115°–120° in Kangerluk is an artifact of the uncertainty in gravity modelling and has more to do with the intensity of igneous intrusions in the basement than with structure at top basement.

The area where basement may be modelled too shallow because of igneous intrusions is shown on Figs 18 and 19 by tone.

Northern Disko island, Vaigat, western Nuussuaq and north of Nuussuaq

Fault G is interpreted to strike about 120° along eastern Vaigat. The fault is seen on profile GGU5 at Km 141.75 and is also indicated on Brandal seismic lines.

The major fault that separates the outcrop of basement from the outcrop of Cretaceous and Tertiary sediments in south-eastern Nuussuaq (Pulvertaft, 1989) is here termed the Saqqaqdal fault (Sa). It is shown on the top basement maps as being terminated to the south by fault G, because no fault that could be an extension of the Saqqaqdal fault into Vaigat is visible on seismic line GGU/95-06.

Fault H is seen on seismic line GGU/95-06 (profiles GGU6a and GGU6b) and is modelled on profile Disko-3. A discrepancy in the outcrop stratigraphy at Kingittoq on southern Nuussuaq (T.C.R. Pulvertaft, personal communication 1997) can best be resolved by a down to the west fault, and Disko-4 has been modelled accordingly. Fault H can be continued northwards to join the Ikorfat fault (Ik) where the latter is lost at outcrop, and the Saqqaqdal fault (Sa) has to be continued westwards from the limit of its outcrop to intersect with faults H and Ik to resolve what otherwise would be a space problem. Between faults H and Ik, basement is shown dipping northwards and eastwards from less than 1 km depth near the south coast of Nuussuaq to more than 4 km depth. The shallower depths are difficult to reconcile with the known outcrop stratigraphy in southern Saqqaqdal. However, there are many sill intrusions at outcrop in this area, so it is possible that there are also many intrusions in the basement, which would imply that the densities used for modelling this area are too low and that basement should therefore be deeper than shown on Figs 18 and 19.

The Ikorfat fault (Ik) (Rozenkrantz & Pulvertaft 1969) is known at outcrop and can also be seen on seismic line GGU/95-08 (Profile GGU8, Km 46). Fault J, which throws down to the northeast, is known at outcrop and strikes between 120° and 135°. Fault J is modelled with a nearly vertical hade because a hade of 30° would cause space problems where it joined the Ikorfat fault. However, fault J appears to be antithetic to the Ikorfat fault, so it is reasonable that an original hade of around 30° on this fault would be rotated nearer to the vertical as movement continued in the Ikorfat fault and its hanging wall block rotated.

Along the north coast of Nuussuaq, the eastern limit of sediments onshore is at the Kuuk fault (Ku), which can be continued offshore and is modelled on profile GGU8 at Km 7, which is east of the limit of seismic coverage on line GGU/95-08. The Kuuk fault is then shown as turning to strike 135° because of the outcropping basement on Appat and Salleq islands and the model on profile Disko-7. Figs 18 and 19 show the Kuuk fault merging with another fault exposed onshore to its west and two other faults between the Kuuk and Ikorfat faults onshore can be continued offshore to where faults can be seen on seismic line GGU/95-08 and modelled on profile GGU8. However, the fault pattern shown on Figs 18 and 19 between the Kuuk and Ikorfat faults is not the only one that can be drawn from the data available.

Fault L is known at outcrop, where it strikes 130° (M. Sønderholm & G. Dam, personal communication 1997). It throws down to the north-east.

On both Disko-7 and Disko-5, the northern limit of the Disko gneiss ridge is modelled as a fault, fault M, north of which is a rotated fault block and another fault, fault N, under the north-east coast of the island. The orientation of these faults is not entirely clear from the data, and their relationship to other faults in the area is also complex. This is discussed again below.

The Kunganguaq fault on Disko can now be joined across Vaigat with the Qunnilik fault on Nuussuaq. In this report the resulting single fault is termed the Kunganguaq-Qunnilik fault (K-Q). It crosses seismic line GGU/95-06 at S.P. 6100 (Km 114 on profiles GGU6a and GGU6b), and the location of the fault is controlled by its trace at outcrop. The Kunganguaq-Qunnilik fault has been extended north-west from its known outcrop limit to merge with the Itilli fault (It) as the simplest solution of how to contour the area to the south-east of the Itilli fault.

Fault P is mapped to the east of and roughly parallel to the K-Q fault. Fault P is visible on seismic line GGU/95-06 at S.P. 5270 (Km 99 on profiles GGU6a and GGU6b). At Nuuk Killeq on the south coast of Nuussuaq, a change of about 400 m in altitude of the base of the Tertiary hyaloclastite breccias (Pedersen *et al.* 1993) may be the eroded scarp of the same fault, and it can possibly be seen on seismic line GGU/NU94-01 (Fig. 4) below 2.5 secs TWT on the eastern part of the section. This interpretation is used to control the modelling of profile Disko-6 (a and b) where fault P is interpreted at Km 103. A fault is visible on seismic line GGU/95-08 at S.P.2230 (Km 46 on GGU8) which must continue southwards because the large depths to top basement modelled on the whole of Disko-5b and Disko-5a north of about Km 150 indicate the presence of a steep slope to the east of profile Disko-5 that is most easily interpreted as fault P. This steep slope is required everywhere on Fig 19 (the 'b' map) between profiles Disko-6b and GGU8. On Fig. 18 (the 'a' map) it is possible to interpret a gap of about 20 km in fault P from just north of profile Disko-6a, but it is also possible to draw a continuous fault as shown.

As discussed above, it was found that the most reasonable interpretation of profiles Disko-5a and Disko-5b between Km 130 and Km 140 is to postulate the existence of some form of igneous intrusion in the basement. The location of such a postulated intrusion is shown on Figs 18 and 19. It could be that the intrusion of such a body was controlled by the existence of fault K.

Two alternative interpretations of profile Disko-5 have been produced; 'Disko-5a alternative' (Figs 14e and 14f) and 'Disko-5b alternative' (Figs 14g and 14h). Maps based on the alternative interpretations are shown in Figs 20 and 21. The 'alternative' intepretations of Disko-5a and Disko-5b have no large igneous intrusion in the basement, but instead interpret a ridge of very shallow basement and a fault, fault R striking at about 130°, close to and parallel to seismic line GGU/NU94-01 (Figs 14e and 14f). However, as explained above, evidence of such a fault should be visible on line GGU/NU94-01, but it is not, which is why the 'alternative' interpretations shown on figs 20 and 21 are thought unlikely.

Alternative patterns are shown on Figs 18 and 19 for the interaction of fault P with faults M and N. Either alternative could be drawn on either the 'a' or 'b' models and the choice as to which version is shown on which map is arbitrary. One version is shown on Fig. 18 and the other on Fig. 19 for convenience. On Fig. 18, fault P is shown as being terminated to the south by fault N and both faults M and N continue north-westwards to terminate against fault K-Q. If this is the case, the crest of the footwall block of fault N strikes at 120°. Fault M is drawn parallel to fault N, which direction is consistent with the locations of fault M on profiles Disko-5a and Disko-7, but they are so close together that the strike of fault M is poorly constrained by them. The alternative pattern is shown in Fig. 19, where fault N is shown as being terminated to the west by fault P, which continues southwards to terminate against fault M. In this case, the strikes of faults M and N are poorly constrained. The faults do not cross profile Disko-4 or seismic line GGU/95-06 west of S.P. 3600 (profile GGU6 at Km 67.5) where there is a fault that may be a transfer fault to faults M and N. Because many other faults in the area strike 120°–130°, this direction has been used as a guide to how to draw faults M and N on Fig. 19.

Fault T is intepreted only on profile Disko-6a and not on Disko-6b. It has been drawn along the same strike as the many small faults that are exposed on north-west Disko, and has been extended to join the Itilli fault (It). Because fault T is not interpreted on profile GGU6, it was necessary to change the strike of the fault north of profile Disko-6a to north-north-west.

The location of the Itilli fault (It) is controlled by its onshore outcrop on Nuussuaq and Hareø and where it crosses profiles GGU8, GGU6 and Disko-6.

Fault V is interpreted west of the Itilli fault only on profile GGU8. Its strike is not known but has been drawn parallel to the Itilli fault.

Crustal thickness

Maps of the intepreted depths to the base of the crust are shown in Figs 22 and 23. The depths shown on Fig. 22 correspond to the 'a' models and those on Fig. 23 correspond to the 'b' models. The two maps differ only in the north-west where the 'a' models show the base of the crust to be deeper than the 'b' models. It should be remembered that these modelled depths are based on the *assumption* that continental crust is in isostatic equilibrium when its base is at a depth of 30 km. Any alteration to this assuption will necessitate a corresponding alteration in the depths shown in Figs 22 and 23, which perhaps should more accurately be labelled 'deviation from isostatic equilibrium of depths to the base of the crust'.

Acknowledgements

I wish to thank Mr. K. Olshefsky of Falconbridge Ltd. and Mr. Erik Andersen of Platinova A/S for permission to publish the infomation from Falconbridge borehole FP93-3-1. Chris Pulvertaft and Torben Bistrup are thanked for many useful and critical discussions and for their comments on the text.

References

Brett, C.P. & Zarudzki, E.F.K. 1979: Project Westmar. A shallow marine geophysical survey on the West Greenland continental shelf. Rapport Grønlands Geologiske Undersøgelse **87**, 29 pp.

Christiansen, F.G., Marcussen, C. & Pulvertaft, T.C.R. 1993: Petroleum-geological activities in. 1992: preparation and support for licensing rounds offshore West Greenland. Rapport Grønlands Geologiske Undersøgelse **159**, 38-42.

Christiansen, F.G., Dam, G. & Pedersen, A.K. 1994: Discovery of live oil at Marraat, Nuussuaq: field work, drilling and logging. Rapport Grønlands Geologiske Undersøgelse **160**, 57–63.

Christiansen, F.G., Marcussen, C. & Chalmers, J.A. 1995: Geophysical and petroleum geological activities in the Nuussuaq – Svartenhuk Halvø area 1994: promising results for an onshore exploration potential. Rapport Grønlands Geologiske Undersøgelse **165**, 32–41.

Christiansen, F.G., Bate, K.J., Dam, G., Marcussen, C. & Pulvertaft, T.C.R. 1996: Continued geophysical and petroleum geological activities in West Greenland in 1995 and the start of onshore exploration. Bulletin Grønlands Geologiske Undersøgelse **172**, 15–21.

Christiansen, F.G., Boesen, A., Dalhoff, F., Pedersen, A.K., Pedersen, G.K., Riisager, P. & Zinck-Jørgensen, K. 1997: Petroleum geological activities onshore West Greenland in 1996, and drilling of a deep exploration well. Geology of Greenland Survey Bulletin **176**, 17–23.

Clarke, D.B. & Pedersen, A.K. 1976: Tertiary volcanic province of West Greenland. In: Escher, A. & Watt, W.S. (eds): Geology of Greenland, 364-385. Copenhagen: Geological Survey of Greenland.

Dam, G. & Sønderholm, M. in press: Sedimentological evolution of a fault-controlled Early Paleocene incised-valley system, Nuussuaq Basin, West Greenland. In: Shanley, K. W. & McCabe, P.J. (eds): Relative role of eustasy, climate, and tectonism in continental rocks. Society of Economic Paleontologists and Mineralogists Special Publication **59**.

Denham, L.R. 1974: Offshore geology of northern West Greenland (69° to 74°N). Rapport Grønlands Geologiske Undersøgelse **63**, 24 pp.

Garde, A. A. 1994: Precambrian geology between Qarajaq Isfjord and Jakobshavn Isfjord, West Greenland, 1:250 000 map. Copenhagen: Geological Survey of Greenland.

Nettleton, L. L. 1976: Gravity and magnetics in oil prospecting, 464 pp. New York: McGraw-Hill.

Pedersen, A.K., Larsen, L.M. & Dueholm, K.S. 1993: Geological section along the south coast of Nuussuaq, central West Greenland. 1:20 000 coloured sheet. Copenhagen: Geological Survey of Greenland.

Pedersen, A.K., Larsen, L.M., Pedersen, G.K. & Dueholm, K.S. 1996: Filling and plugging of a marine basin by volcanic rocks: the Tunoqqu Member of the Lower Tertiary Vaigat Formation on Nuussuaq, central West Greenland. Bulletin Grønlands Geologiske Undersøgelse **171**, 5–28.

Pedersen, G.K. & Pulvertaft, T.C.R. 1992: The nonmarine Cretaceous of the West Greenland Basin, onshore West Greenland. Cretaceous Research **13**, 263–272.

Pedley, R.C., Busby, J.P. & Dabek, Z.K. 1993: GRAVMAG v1.5 USER MANUAL Interactive 2.5D gravity & magnetic modelling, 77 pp. Technical Report WK/93/26/R Regional Geophysics Series, British Geological Survey.

Pulvertaft, T.C.R. 1989: The geology of Sarqaqdalen, West Greenland, with special reference to the Cretaceous boundary fault system. Open File Series Grønlands Geologiske Undersøgelse **89/5**, 35 pp.

Rosenkrantz, A. & Pulvertaft, T.C.R. 1969: Cretaceous–Tertiary stratigraphy and tectonics in northern West Greenland. Memoir of the American Association of Petroleum Geologists **12**, 883–898.

Thorning, L. in press: Project Aeromag 1997. Results from a regional aeromagnetic survey in central West Greenland. Danmarks og Grønlands Geologiske Undersøgelse Rapport **1998/17**.

Whittaker, R.C. 1995: A preliminary assessment of the structure, basin development and petroleum potential offshore central West Greenland. Open File Series Grønlands Geologiske Undersøgelse **95/9**, 33 pp.

Whittaker, R.C. 1996: A preliminary seismic interpretation of an area with extensive Tertiary basalts offshore central West Greenland. Bulletin Grønlands Geologiske Undersøgelse **172**, 28-31.

Appendix 1 – Note on densities used in gravity modelling in the Disko–Nuussuaq area

by
T. C. R. Pulvertaft

Before gravity modelling in the Disko–Nuussuaq area can be carried out, values must be assumed for the densities of four units: 1) the upper mantle, 2) continental crust, 3) the sedimentary section, and 4) basalts, predominantly subaerial flows.

The upper mantle

No one actually knows the density of the upper mantle under the continents, largely because nobody has access to it but also because samples of upper mantle rock that can be obtained from nodules are probably samples of depleted mantle that has lost some of its original material through partial melting and tapping of the magma that brought the nodules to the surface. The value for the density of the upper mantle used in the present study is **3.3 Mg/m^3**, which is the value mentioned by for example Harris (1972) and also that used for the mantle underlying the continental crust below the Faroe Islands (unpublished data; K.R. Richardson, J.R. Smallwood, R.S. White, D. Snyder & P.K.H. Maguire, personal communication 1998),. Higher values have however been quoted in the literature, e.g. 3.375 Mg/m^3 (fig. 3.4 in Wilson, 1989).

Continental crust

In the modelling an average value for the density of the continental crust has been used, without any considerations about the Conrad discontinuity and what lies below it. Even if the depth to the Conrad discontinuity was known, the density of the lower crust and hence the average density of the entire crust would still be uncertain, since the composition of the lower continental crust is even more uncertain than the composition of the upper mantle.

In the present study an average density of **2.8 Mg/m^3** has been used for the continental crust. This value was proposed by Holmes (1965) on the basis of much less information than is available today. A density of 2.8 Mg/m^3 also indicated by Nettleton (1976) and is the average of values quoted by Østergaard (1975). Henderson (1969) recorded densities between 2.66 and 2.77 Mg/m^3 for sialic rocks collected from the basement in the Uummannaq area. In a more recent work Shaw *et al.* (1986) discussed the composition of the continental crust including that of the lower crust, and proposed an average chemical composition for the entire crust (op. cit. table 4, p. 280). This has been converted to a CIPW norm, and the density of the resulting hypothetical rock calculated using mineral densities from Deer *et al.* (1962). This procedure gave the result 2.83 Mg/m^3.

It should be noted that if the higher values of 3.375 and 2.83 for the upper mantle and continental crust respectively were to used in the gravity modelling, the model would be virtually unaffected, since it is the difference in densities between the layers that influences the model.

The sedimentary section

There are two sources of uncertainty regarding the average density of the sedimentary section in the Disko–Nuussuaq area: 1) the likelihood of lateral variation, i.e. that the variation from a sandstone-dominated section in the south-east to a mudstone-dominated section in the north-west seen at the level of surface outcrop is also found at depth; 2) the lack of information on lithology, in particular porosity, in the deep parts of the basin; this problem is acute now that we know from seismic line GGU/NU94-1 that the sedimentary section is at least 6 km thick.

The relatively high value of **2.55 Mg/m^3** has been chosen for the average density of the sedimentary section. The reasons for this choice are as follows:

Data on grain density and porosity are available from the cores of the three slim core wells GANE#1, GANK#1 and GANT#1 drilled by grønArctic Inc. in 1995. In the GANE#1 and GANK#1 wells the sediments underlying the hyaloclastite breccias resemble those of the Kangilia Formation (Dam 1996a, b), while the GANT#1 well penetrated 645 m of Campanian slope mudstones interbedded with thin turbiditic sandstones below the erosional unconformity that marks the base of the Kangilia Formation (Dam 1996c).

From the GANE#1 well the grain density and porosity of 192 samples from 219 m of core were measured (Andersen 1996). The average bulk density of these samples, assuming water saturation, is 2.55 Mg/m^3. From the GANK#1 core 44 samples from 131 m of core were measured (Andersen & Jensen 1997). The average bulk density of these samples is 2.49 Mg/m^3. From the GANT#1 well only 8 sandstone layers selected at random from the Campanian part of the section have been studied (N. Springer, personal communication 1997). The average bulk density of these samples is 2.56 Mg/m^3. Both the lower part of the GANT#1 core and the Campanian sediments exposed on the north coast of Nuussuaq are however dominated by mudstones. A discussion of mudstone (shale) densities has been given by Fertl (1977) whose fig. 4 shows examples of mudstones (shales) that have reached a density of 2.55 Mg/m^3 at depths as little as 2.5 km.

Some indication of how density increases with depth in the Nuussuaq basin can be obtained from the average velocities in seismic line GGU/NU94-1 (Christiansen *et al.*, 1995). There is a fairly rapid increase in the average velocity from 3400 m/s to 4150 m/s in the Atane Formation down to a distinct unconformity at approximately 1 sec. TWT. Below this the average velocity increases slowly from 4150 m/s to 4800 m/s at 4 sec. TWT. These average velocities suggest that most of the sediments in line GGU/NU94-1 are strongly compacted and therefore have a relatively high density. The deeper trend of average velocities corresponds to an interval velocity of 5000 m/s, which corresponds to a density of 2.55 Mg/m^3 for water-saturated sediments according to the plot of Nafe & Drake (1963).

The figures quoted in the foregoing paragraphs indicate that an average density of 2.55 Mg/m^3 is a realistic estimate for the sedimentary section in the north-west part of the area studied. However, the figure may well be too high for the relatively thin sedimentary section underlying Disko Bugt. The exposed Cretaceous section in eastern Disko is dominated by poorly consolidated subarkosic sandstones, and the overlying basalts have never been as thick here as in the western part of the area. The difficulties with using a lower density in this area are that 1) one would have to choose an arbitrary sandstone:mudstone ratio in the exposed section and/or an equally arbitrary basin depth to define the boundary between areas with higher and lower average bulk densities of the total sedimentary section, and 2) the modelling across this boundary would almost certainly result in a pseudo-fault in the basement surface at this boundary. For this reason the figure 2.55 Mg/m^3 is used for the entire basin, even though this may give slightly exaggerated depths to basement in the south-eastern part of the area.

It should be noted that an average bulk density of 2.55 Mg/m^3 for the sedimentary section gives an average porosity of 6.25%, assuming average grain density 2.66 Mg/m^3 (the average for the three grønArctic wells) and water saturation. However, porosities of up to 20.89 and 22.89 have been recorded from sandstone layers in the GANE#1 and GANK#1 cores respectively, and a porosity of 13.73 was measured in one sample from the Campanian part of the GANT#1 core. Thus the low average porosity does not rule out the presence of zones with good reservoir properties.

Basalts

Although there is less scope for variation in basalts than in siliciclastic sediments, the uncertainties governing the choice of bulk density for the West Greenland basalt section are almost as great as those regarding the sediments. Just as is the case with the sedimentary section in the Nuussuaq basin, there is lateral variation in the proportions of the components of the basalt section – hyaloclastic breccia, picrite basalt, contaminated basalt and plagioclase-porphyritic basalt. Massive basalt, free of vesicles, amygdales and scoriaceous zones, has a density of 2.95 to 3.2 Mg/m^3 (picrite basalt), but basalt flows are not massive throughout. On the contrary, gas bubbles or vesicles are ubiquitous in basaltic flows, mainly in the upper parts of the flows.The widespread occurrence of oil in basalts in the Marraat area is a striking reminder of the importance of porosity in basalts!

Density data are available for the basalt section penetrated by the 1920 m deep Iceland Research Drilling Project hole in eastern Iceland. This section is dominated by low-magnesia basalts and ferrobasalts; olivine tholeiites occur at some stratigraphic levels (Robinson *et al.* 1982). According to Christensen & Wilkens (1982), most porosity in the basalts here is less than 5%, but porosity up to 23% has been registered. The density of the flows increases with depth due to pressure closure of crack porosity and a higher degree of pore filling in vesicular zones. The spread of density values is 2.4 to 3.07 Mg/m^3. Schoenharting & Pálmason (1982) present a table of values for average densities of core samples from the same drill hole. In the uppermost 500 m of the hole the average density is 2.7 Mg/m^3, while samples from below 1440 m have an average density of 2.93 Mg/m^3. However, in modelling studies involving basalt sections notably lower values for the total section have been used, for example 2.82 Mg/m^3 for the deeper part of the basalt section under the Faroe Islands (unpublished data; K.R. Richardson, J.R. Smallwood, R.S. White, D. Snyder & P.K.H. Maguire, personal communication 1998), and 2.8 Mg/m^3 for the Erland Tertiary volcanic complex north of the Shetland Islands (Gatliff *et al.* 1984).

In the present study the high value of **3.0 Mg/m^3** has been used for the density of the basalt section. This is because in the area where lines with both seismic and gravity data cross basalts (lines GGU/95-06 and -08), the greater part of the basalt section consists of picritic basalts which have a distinctly higher density than the basalts drilled in eastern Iceland. Noe-Nygaard (1942) has recorded density values for two picrite samples from Svartenhuk Halvø; measured values were 3.15 and 3.08 Mg/m^3, while calculated values are higher – 3.31 and 3.29 Mg/m^3 respectively. If it is assumed that the average grain density of the picrite basalts is 3.15 Mg/m^3, the average porosity is 7% and the pore space is water-filled, the bulk density would be 3.0 Mg/m^3. However, there are other factors that work in different directions. Increasing the bulk density is the fact that vesicles and cracks in the picritic basalts are usually partially or totally filled by calcite and zeolite minerals. Reducing the bulk density is the fact that the contaminated and plagioclase-porphyritic tholeiitic flows in the section have a lower grain density than the picrites, and there is less late mineralisation in vesicles in the contaminated and plagioclase-porphyritic tholeiites than in the picrites.

At present there are insufficient data on bulk densities of the West Greenland basalts to allow a proper estimate of the average density of the total basalt section along the seismic and gravity lines to be made.

References

Andersen, G. 1996: Conventional core analysis on GANE#1 and GANE#1A cores, Eqalulik, Nuussuaq, West Greenland. Danmarks og Grønlands Geologiske Undersøgelse Rapport **1996/117**, 35 pp.

Andersen, G. & Jensen, M.K. 1997: Conventional core analysis on GANK#1 cores, Eqalulik, Nuussuaq, West Greenland. Danmarks og Grønlands Geologiske Undersøgelse Rapport **1997/84**, 21 pp.

Christensen, N. I. & Wilkens, R.H. 1982: Seismic properties, density, and composition of the Icelandic crust near Reydarfjördur. Journal of Geophysical Research **87**(B8), 6389–6395.

Christiansen, F.G., Marcussen, C. & Chalmers, J.A. 1995: Geophysical and petroleum geological activities in the Nuussuaq – Svartenhuk Halvø area 1994: promising results for an onshore exploration potential. Grønlands Geologiske Undersøgelse Rappport **165**, 32–41.

Dam, G. 1996a: Sedimentology of the GANE#1 and GANE#1A cores drilled by grønArctic Energy Inc., Eqalulik, Nuussuaq, West Greenland. Danmarks og Grønlands Geologiske Undersøgelse Rapport **1996/82**, 18 pp.

Dam, G. 1996b: Sedimentology of the GANK#1 and GANK#1A cores drilled by grønArctic Energy Inc., Kuussuaq, Nuussuaq, West Greenland. Danmarks og Grønlands Geologiske Undersøgelse Rapport **1996/83**, 14 pp.

Dam, G. 1996c: Sedimentology of the GANT#1 core drilled by grønArctic Energy Inc., Tunorsuaq, West Greenland. Danmarks og Grønlands Geologiske Undersøgelse Rapport **1996/96**, 18 pp.

Deer, W.A., Howie, R.A. & Zussman, J. 1962: Rock-forming minerals **1–5**. London: Longmans.

Fertl, W.H. 1977: Shale density studies and their application. In: Hobson, G.D. (ed.): Developments in petroleum geology – 1, 293–327. London: Applied Science Publishers Ltd.

Gatliff, R.W., Hitchen, K., Ritchie, J.D. & Smythe, D.K. 1984: Internal structure of the Erland Tertiary complex, north of Shetland, revealed by seismic reflection. Journal of the Geological Society (London) **141**, 555–562.

Harris, P. 1972: The composition of the Earth. In: Gass, I.G., Smith, P.J. & Wilson, R.C.L. (eds): Understanding the Earth, 53–69. Sussex: Artemis Press.

Henderson, G. 1969: The use of structural contour maps in the study of gneiss-metasediment relations in the Umanak area, West Greenland. Special Paper of the Geological Association of Canada **5**, 129–142.

Holmes, A. 1965: Principles of physical geology, 1288 pp. London: Nelson.

Nafe, J.E. & Drake, C.L. 1963: Physical properties of marine sediments. In: Hill, M.N. (ed.): The Sea, **3**, 794–815. New York: Interscience.

Nettleton, L.L. 1976: Gravity and magnetics in oil prospecting, 464 pp. New York: McGraw-Hill.

Noe-Nygaard, A. 1942: On the geology and petrography of the West Greenland basalt province. Part III. The plateaubasalts of Svartenhuk peninsula. Meddelelser om Grønland **137**(3), 78 pp.

Robinson, P.T., Mehegan, J., Gibson, I.L. & Schmincke, H.-U. 1982: Lithology and structure of the volcanic sequence in eastern Iceland. Journal of Geophysical Research **87**(B8), 6429–6436.

Schoenharting, G. & Pálmason, G. 1982: A gravity survey in the Reydarfjördur area, with interpretation. Journal of Geophysical Research **87**(B8), 6419–6422.

Shaw, D.M., Cramer, J.J., Higgins, M.D. & Truscott, M.G. 1986: Composition of the Canadian Precambrian shield and the continental crust of the Earth. Geological Society Special Publication (London) **24**, 275–282.

Wilson, M. 1989: Igneous petrogenesis, 466 pp. London: Unwin Hyman.

Østergaard, T.V. 1975: Den nye geologi, 88 pp. Copenhagen: P. Haase.

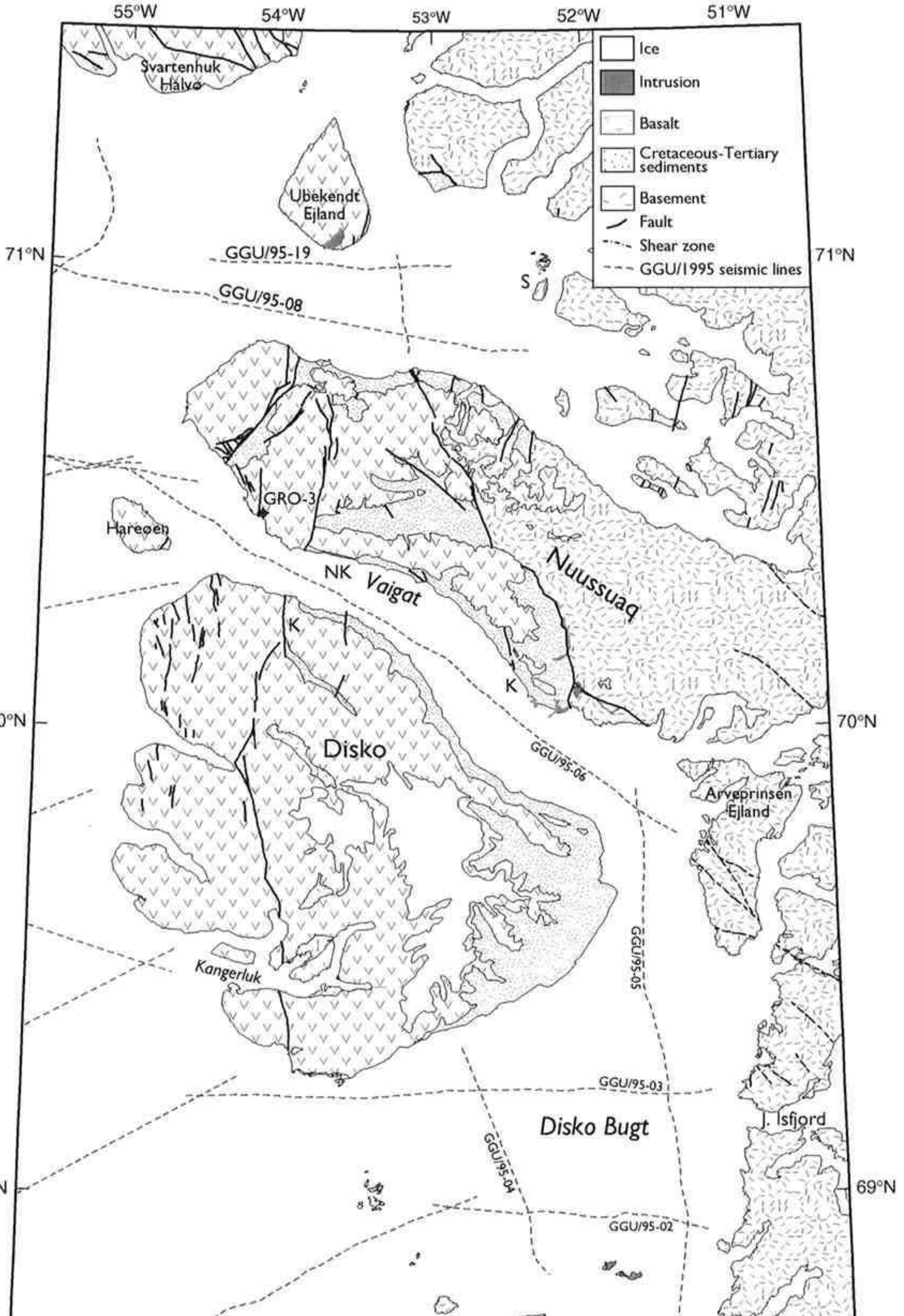

Fig. 1: Geology map of the Disko–Nuussuaq area showing place names and the seismic lines used in the interpretation. NK: Nuuk Killeq, K: Kingittoq, S: Salleq, J. Isfjord: Jakobshavn Isfjord, I: Ilulissat.

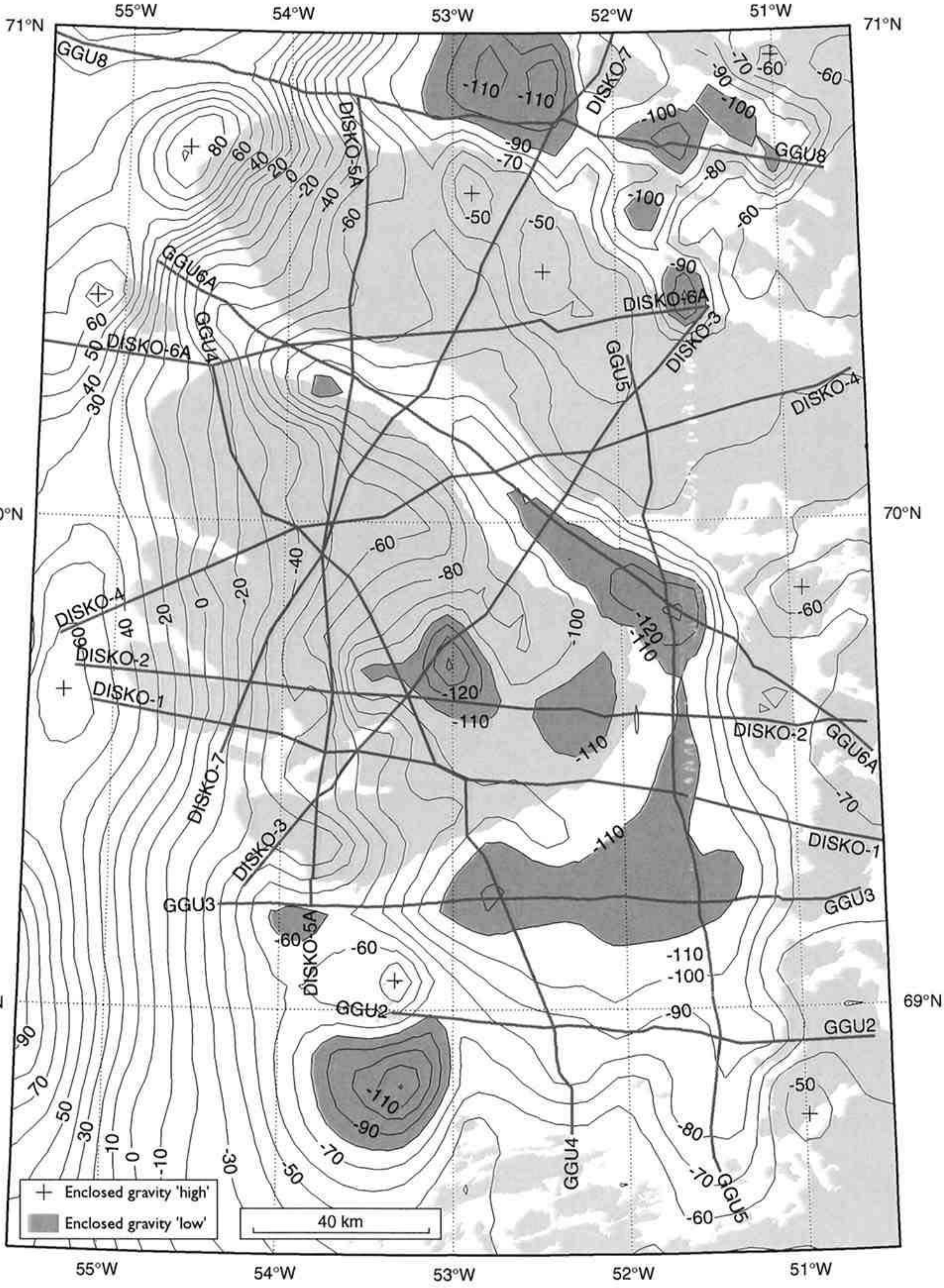

Fig. 2: Map showing Bouguer gravity onshore, free air gravity offshore. The profiles along which the gravity forward models were calculated are also shown.

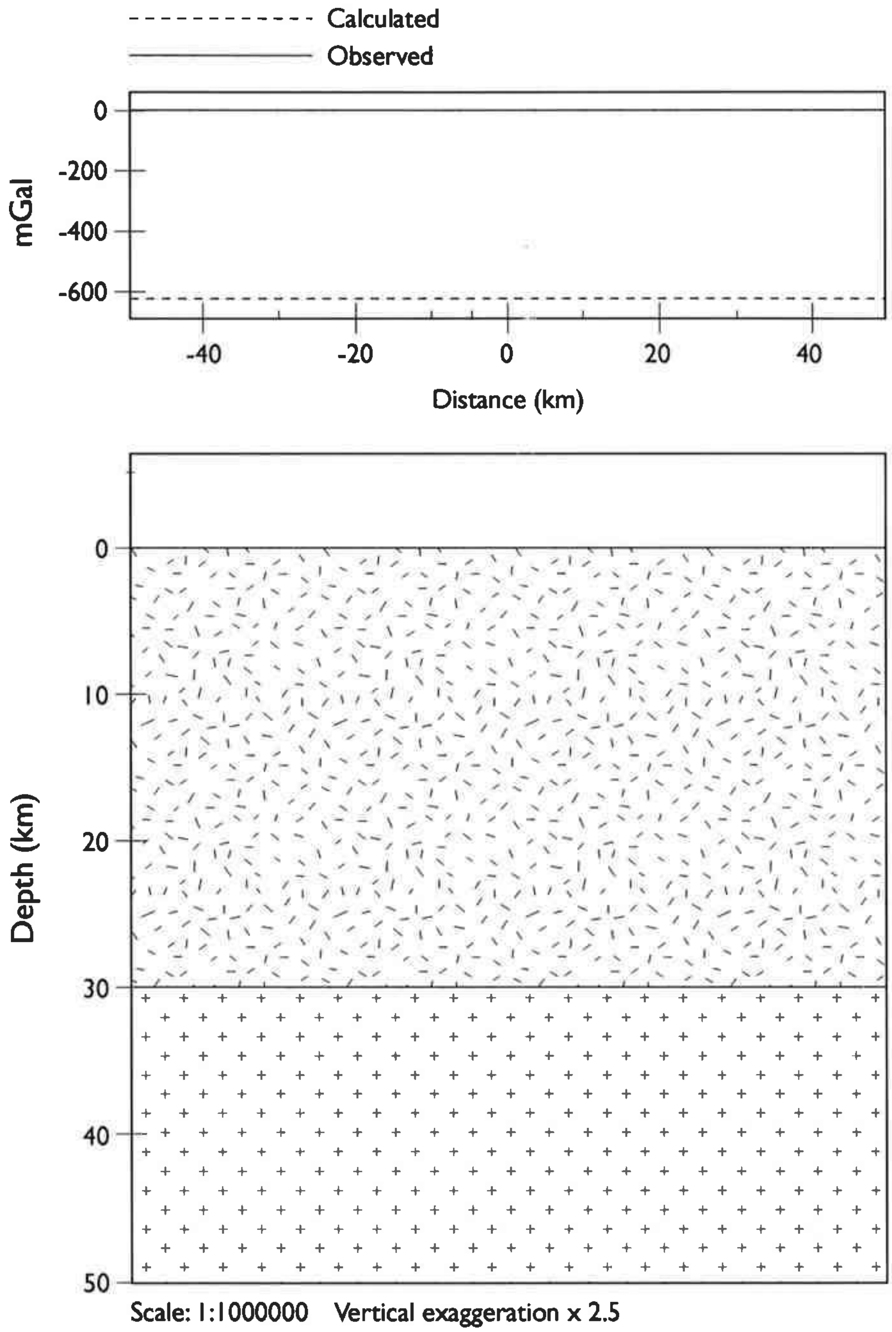

Fig. 3: Reference model for the gravity modelling consisting of 30 km thick continental crust of density 2.8 Mg/m^3 below which is mantle of density 3.3 Mg/m^3. The prisms extend 10 000 km in both directions to left and right and in both directions at right angles to the section shown. This 'reference' model generates a 'reference' anomaly of -628 milligals which was added to all the observed gravity anomalies prior to modelling them. Thus all modelling was done with respect to an assumption that a slab of continental crust 30 km thick and extending horizontally 20 000 km in all directions is in isostatic equilibrium with the mantle.

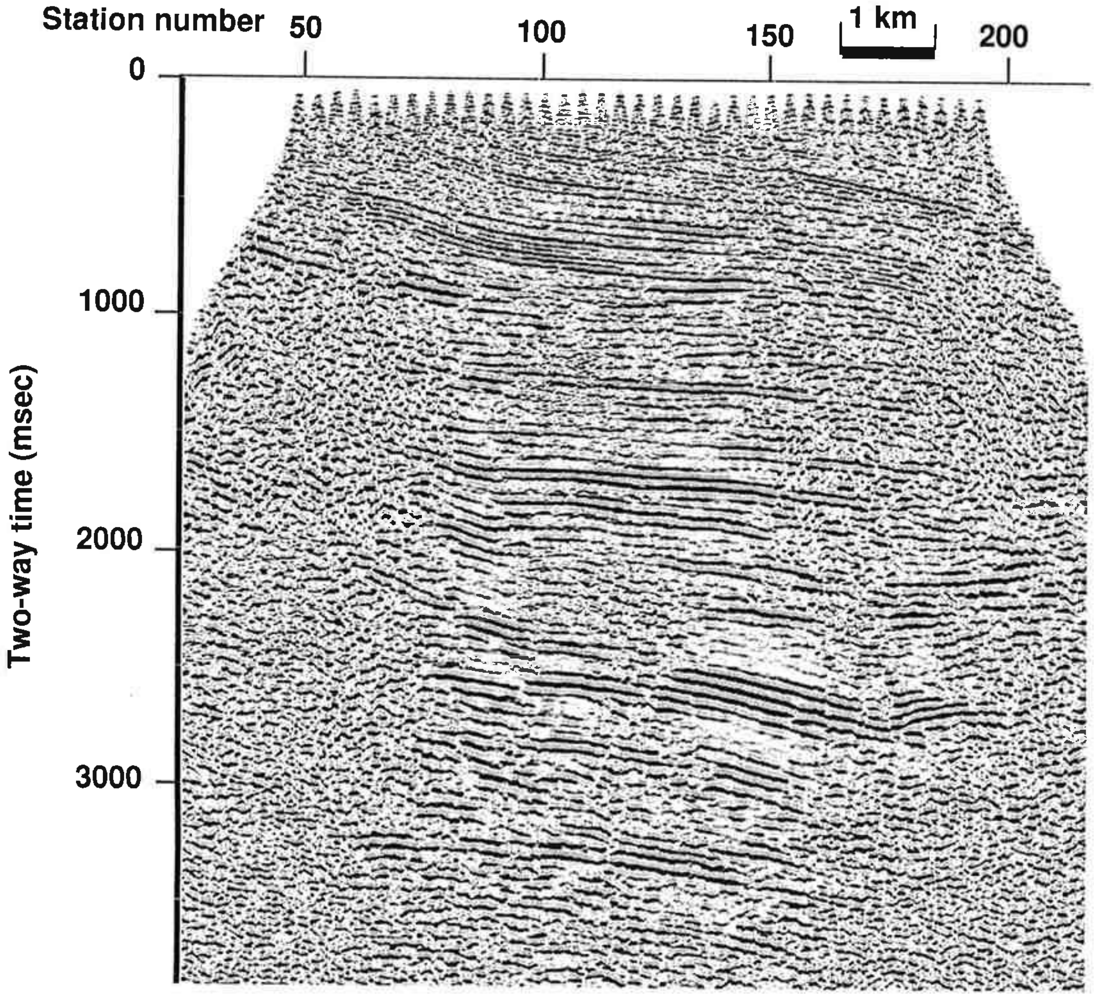

Fig. 4: Onshore seismic line GGU/NU94-01 acquired by GGU in 1994 along part of the south coast of Nuussuaq. See text for discussion.

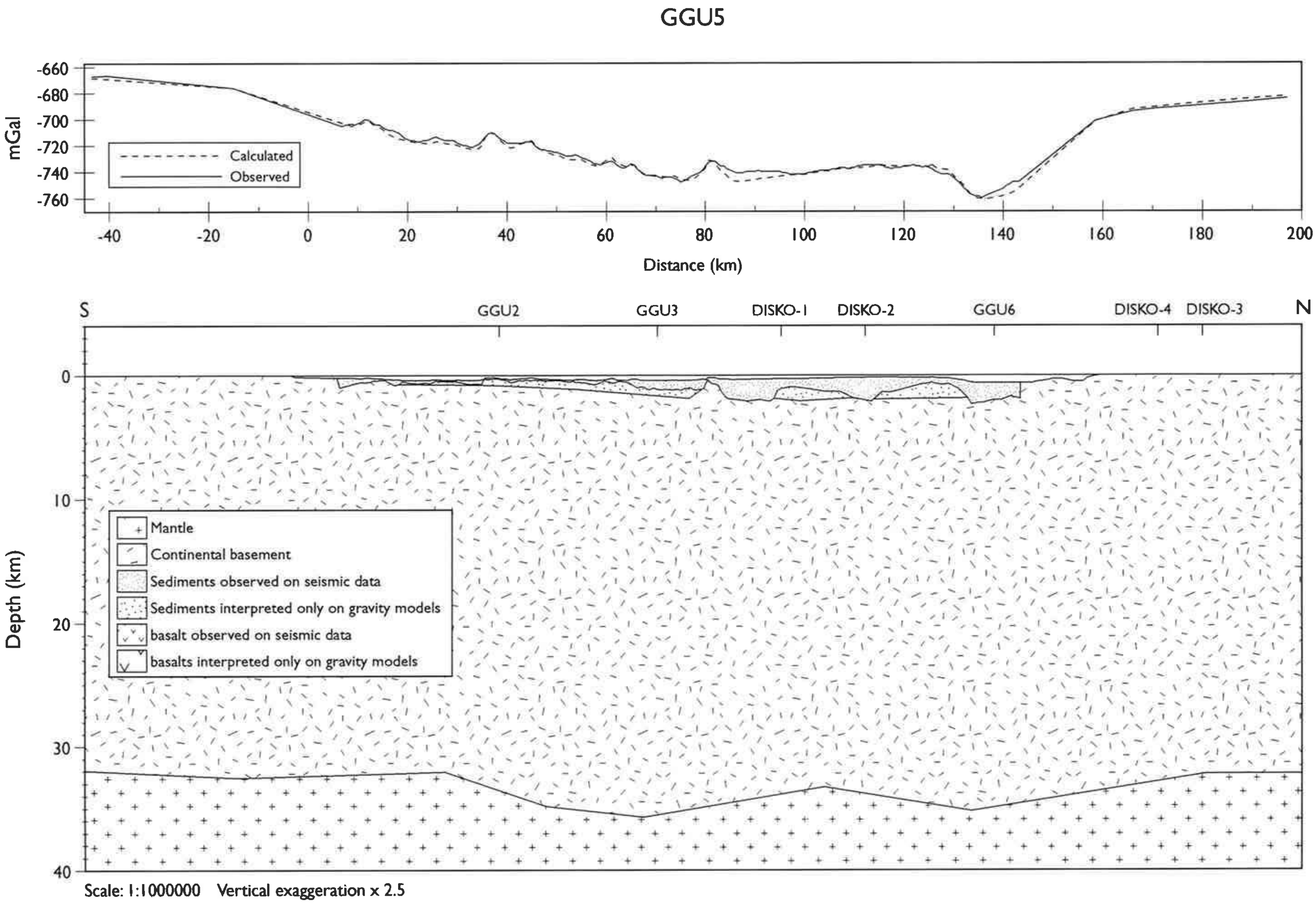

Fig.5a Gravity profile GGU5

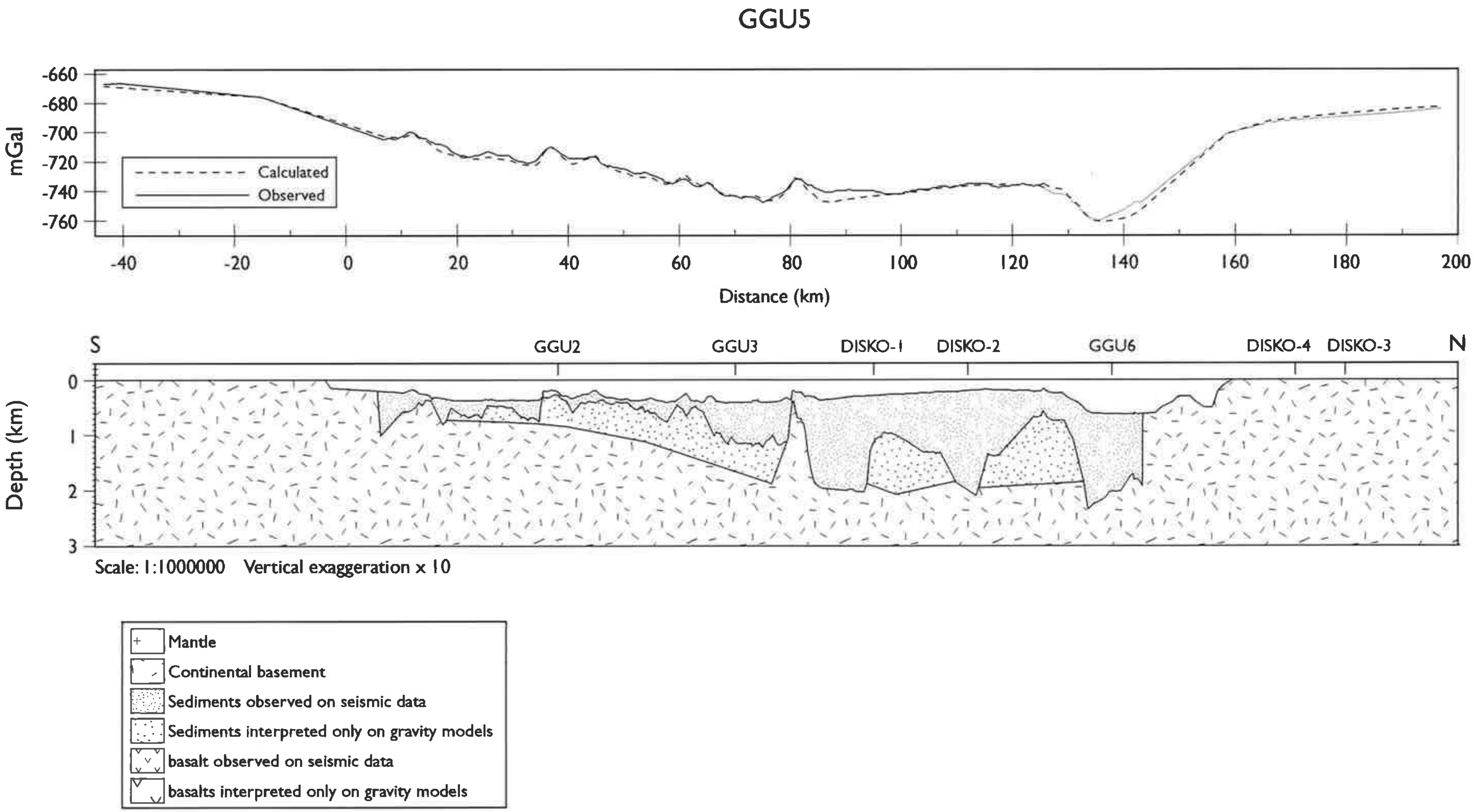

Fig.5b Gravity profile GGU5

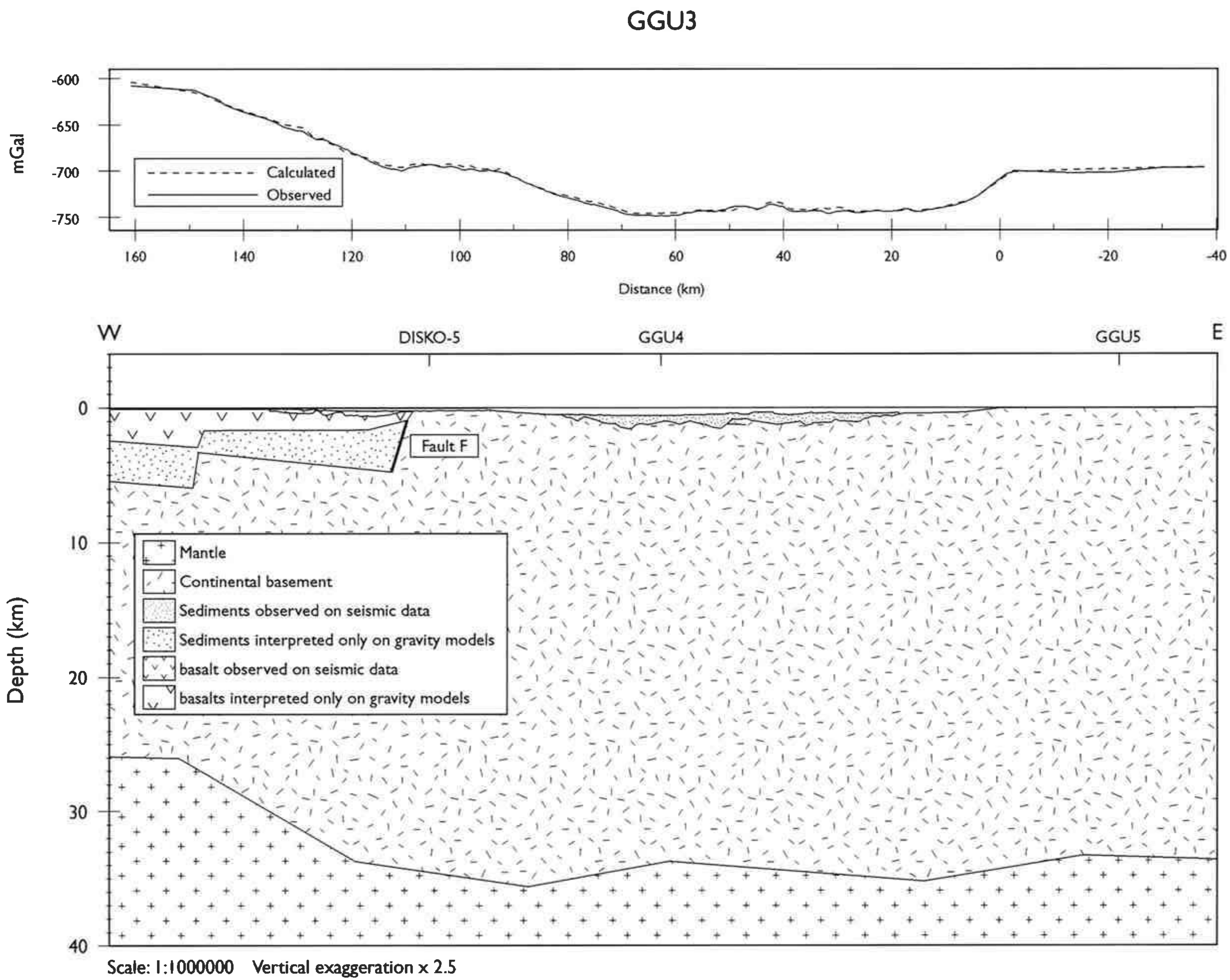

Fig.6a Gravity profile GGU3

GGU3

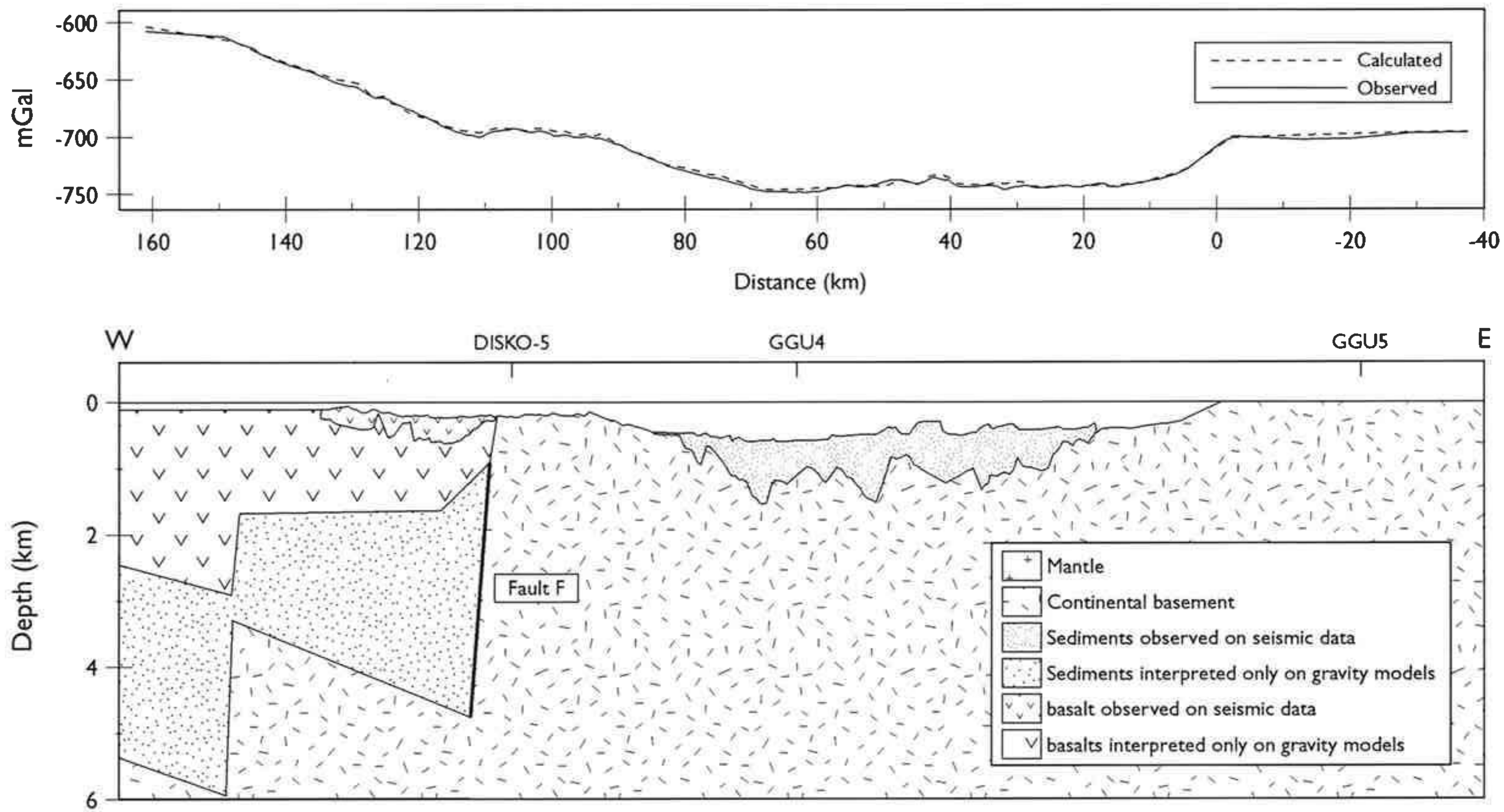

Scale: 1:1000000 Vertical exaggeration x 10

Fig.6b Gravity profile GGU3

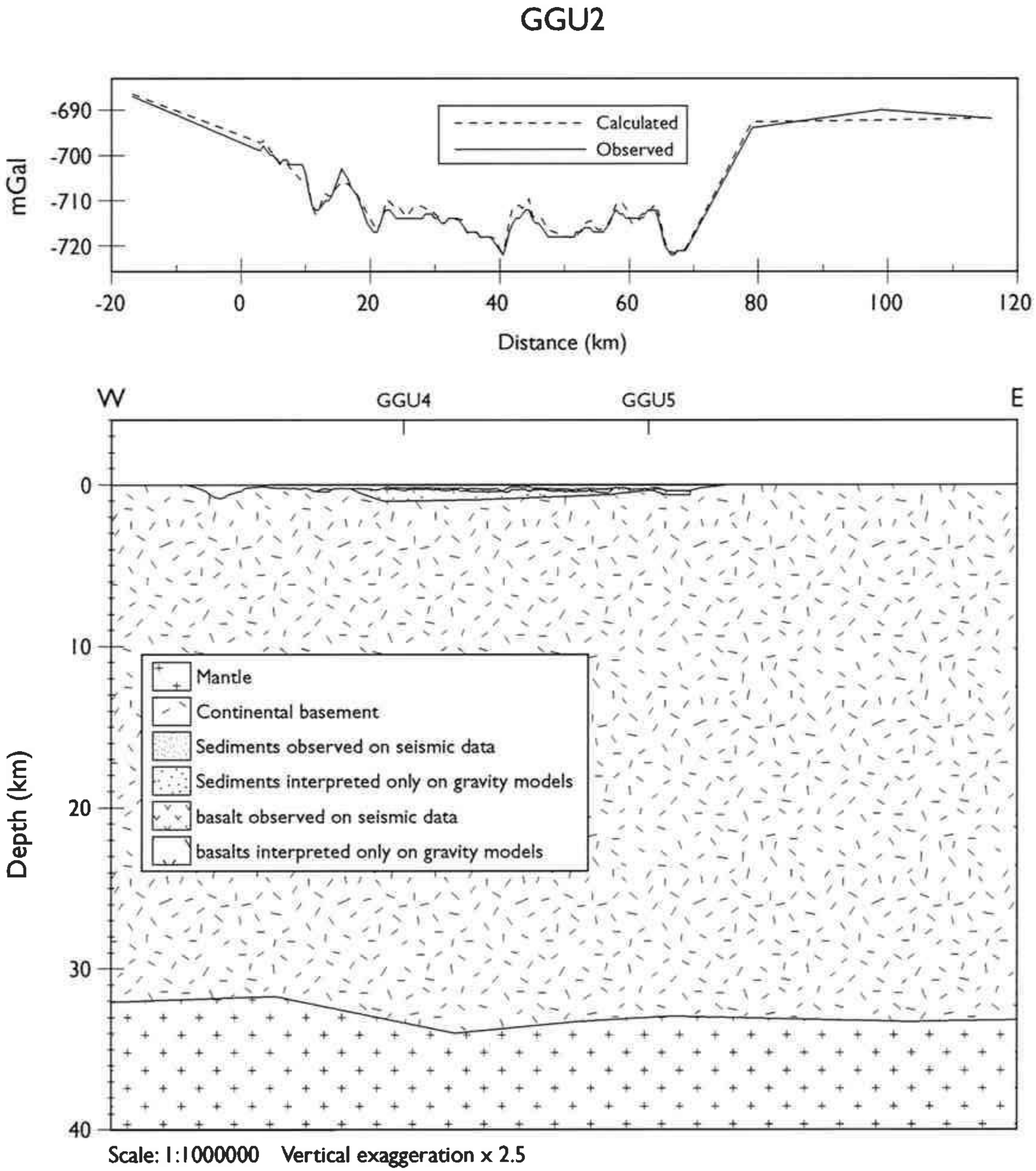

Fig.7a Gravity profile GGU2

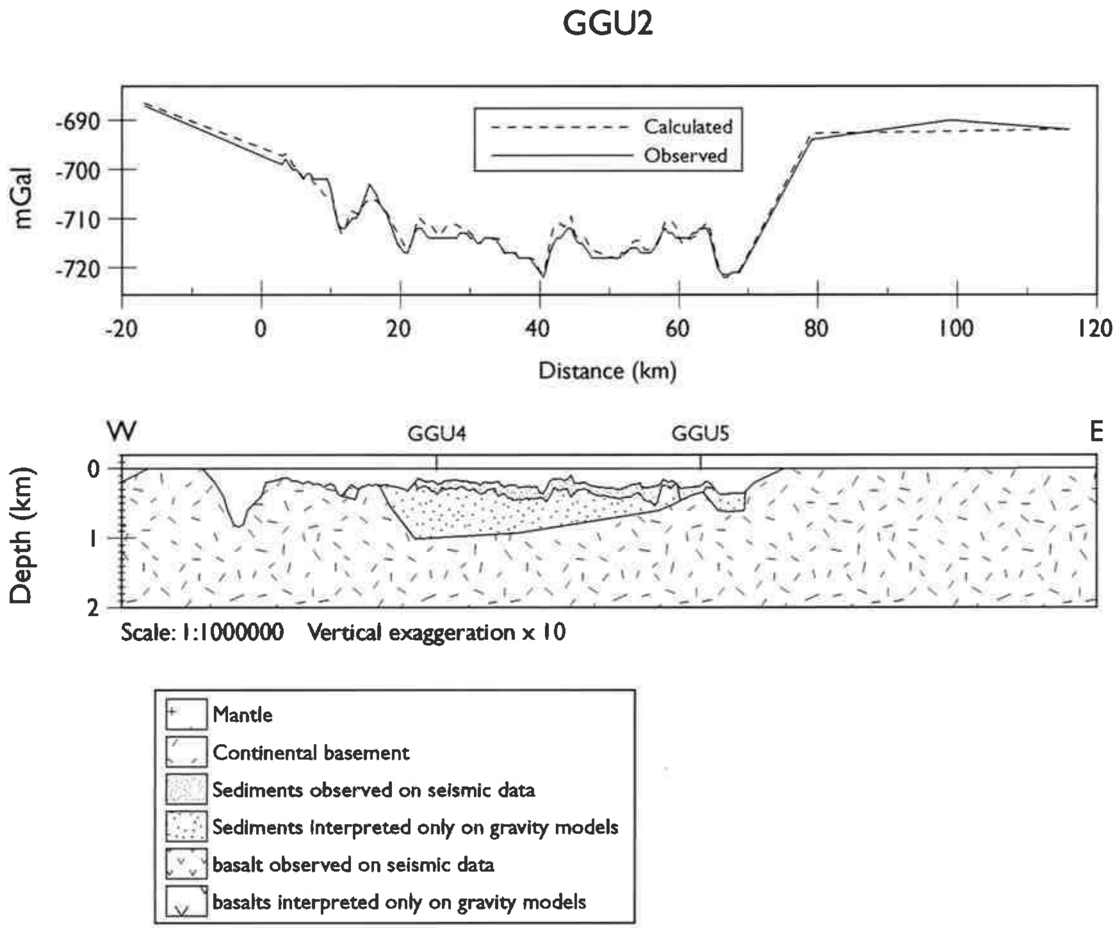

Fig.7b Gravity profile GGU2

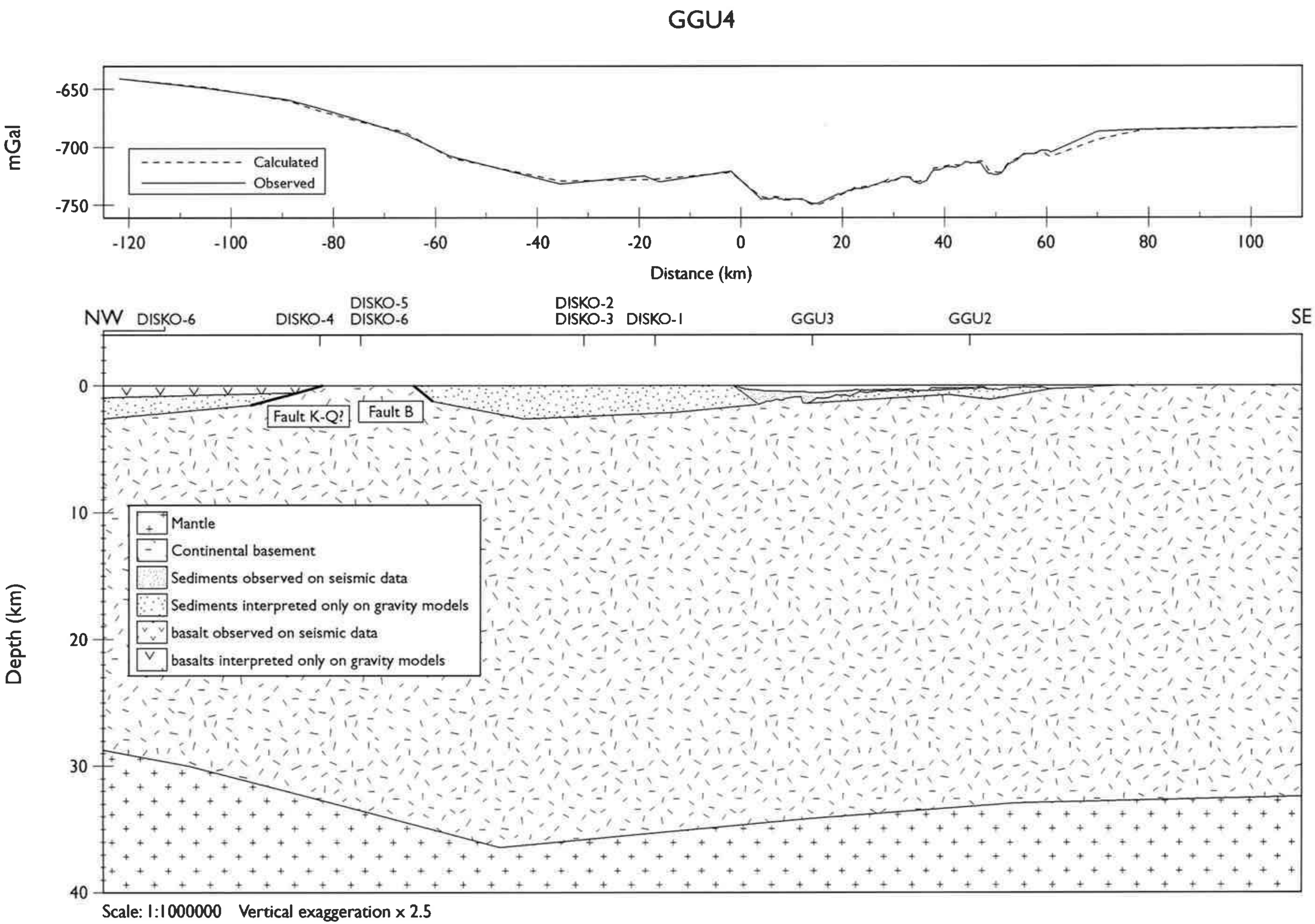

Fig.8a Gravity profile GGU4

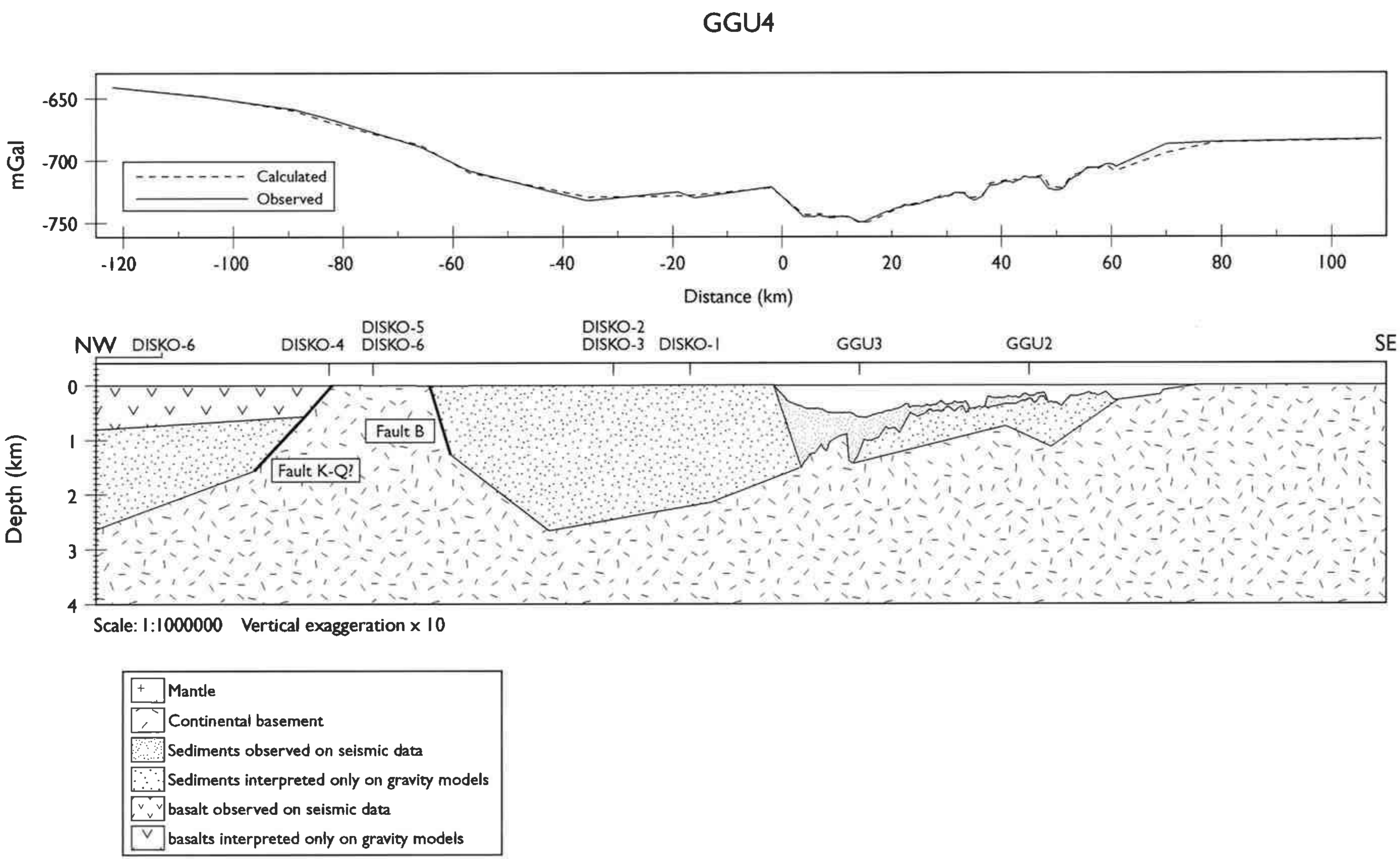

Fig.8b Gravity profile GGU4

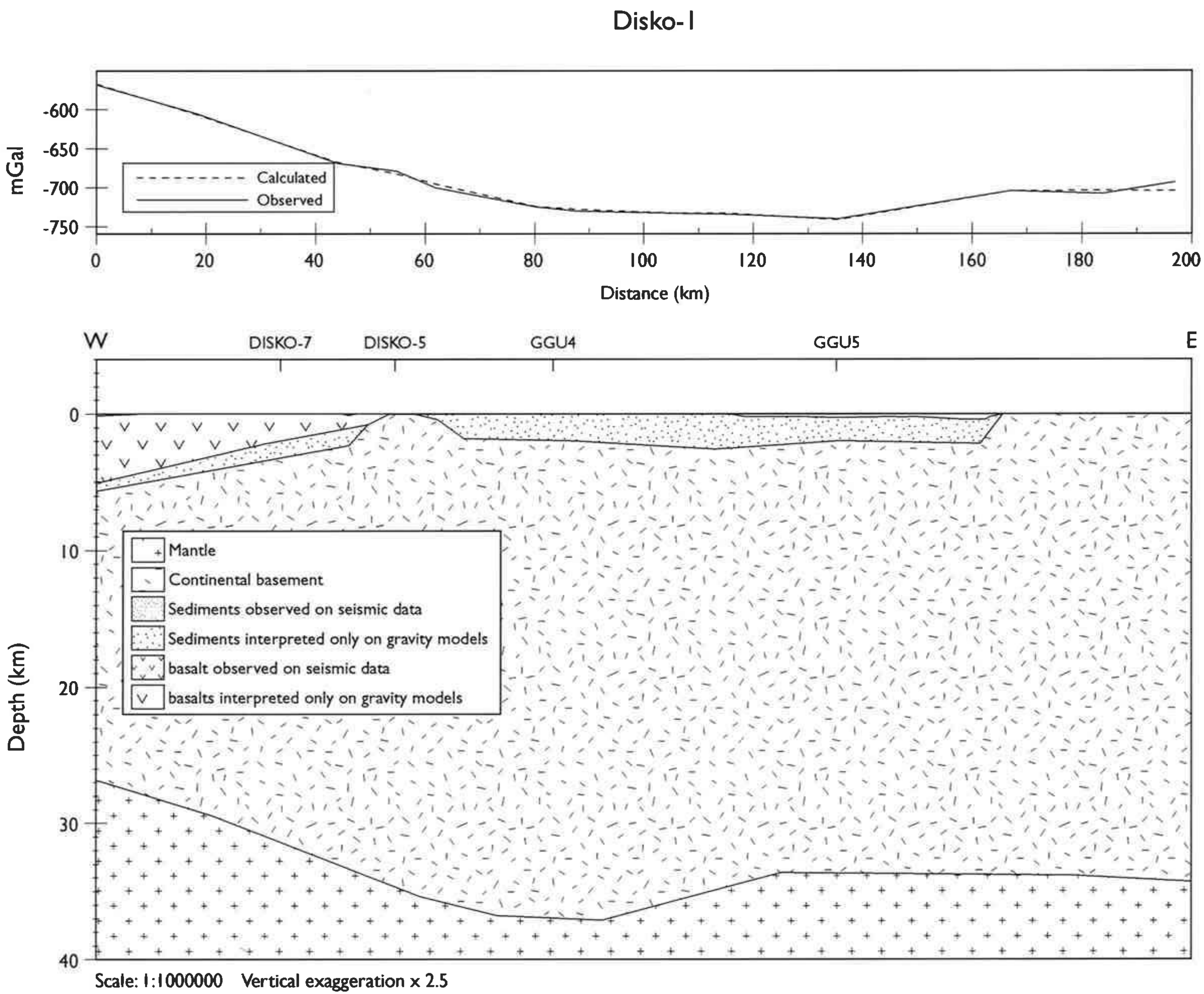

Fig.9a Gravity profile Disko-1

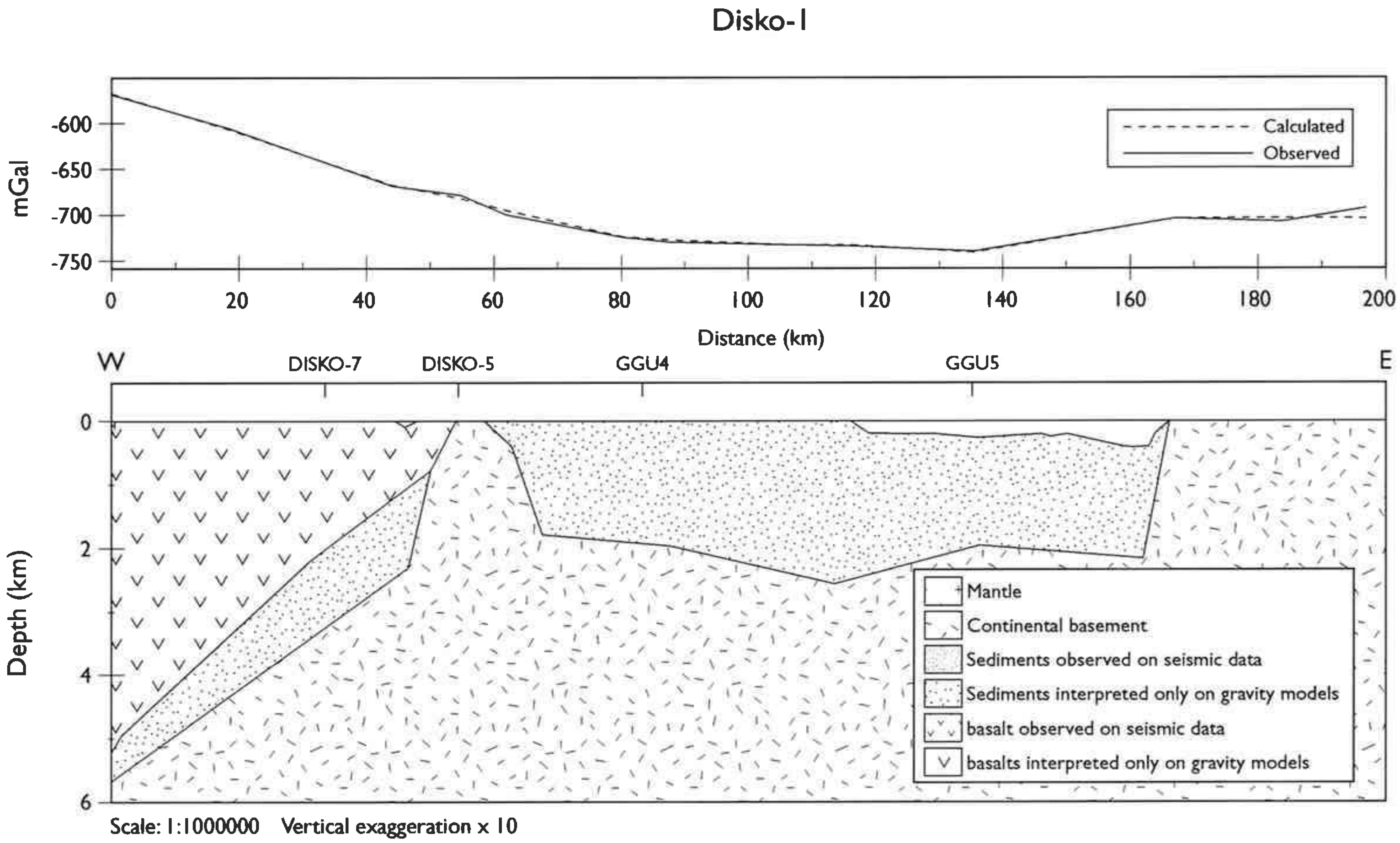

Fig.9b Gravity profile Disko-1

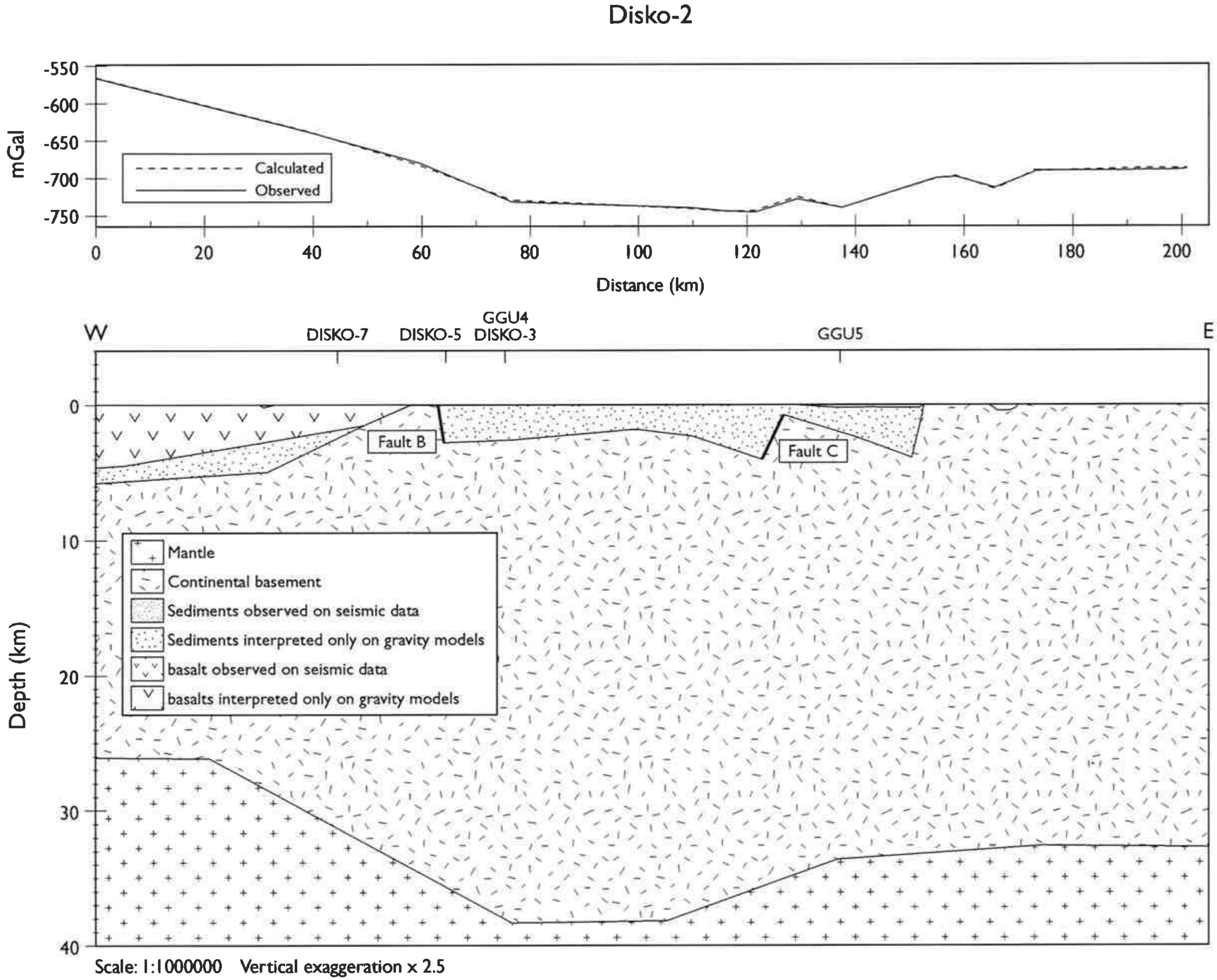

Fig.10a Gravity profile Disko-2

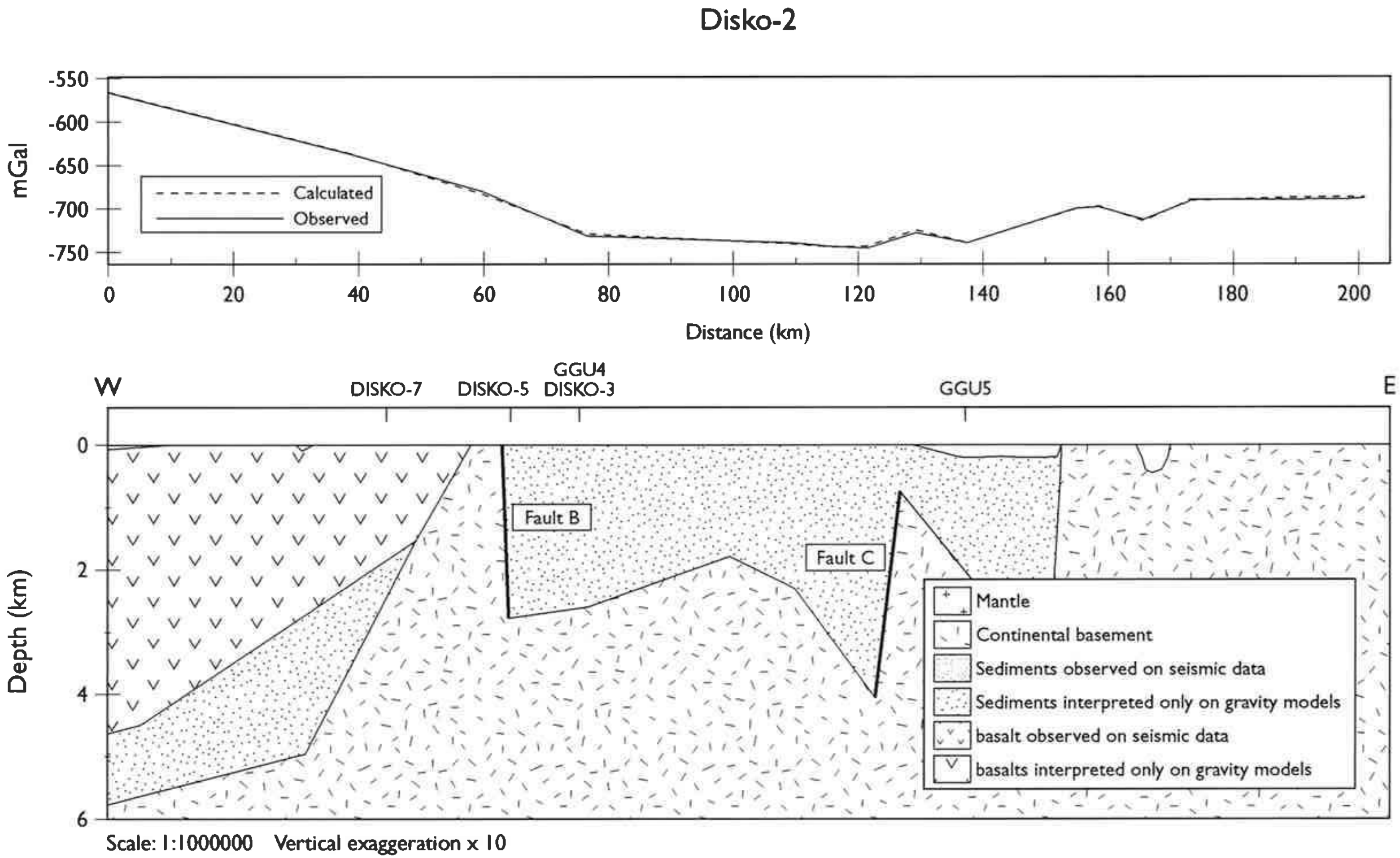

Fig.10b Gravity profile Disko-2

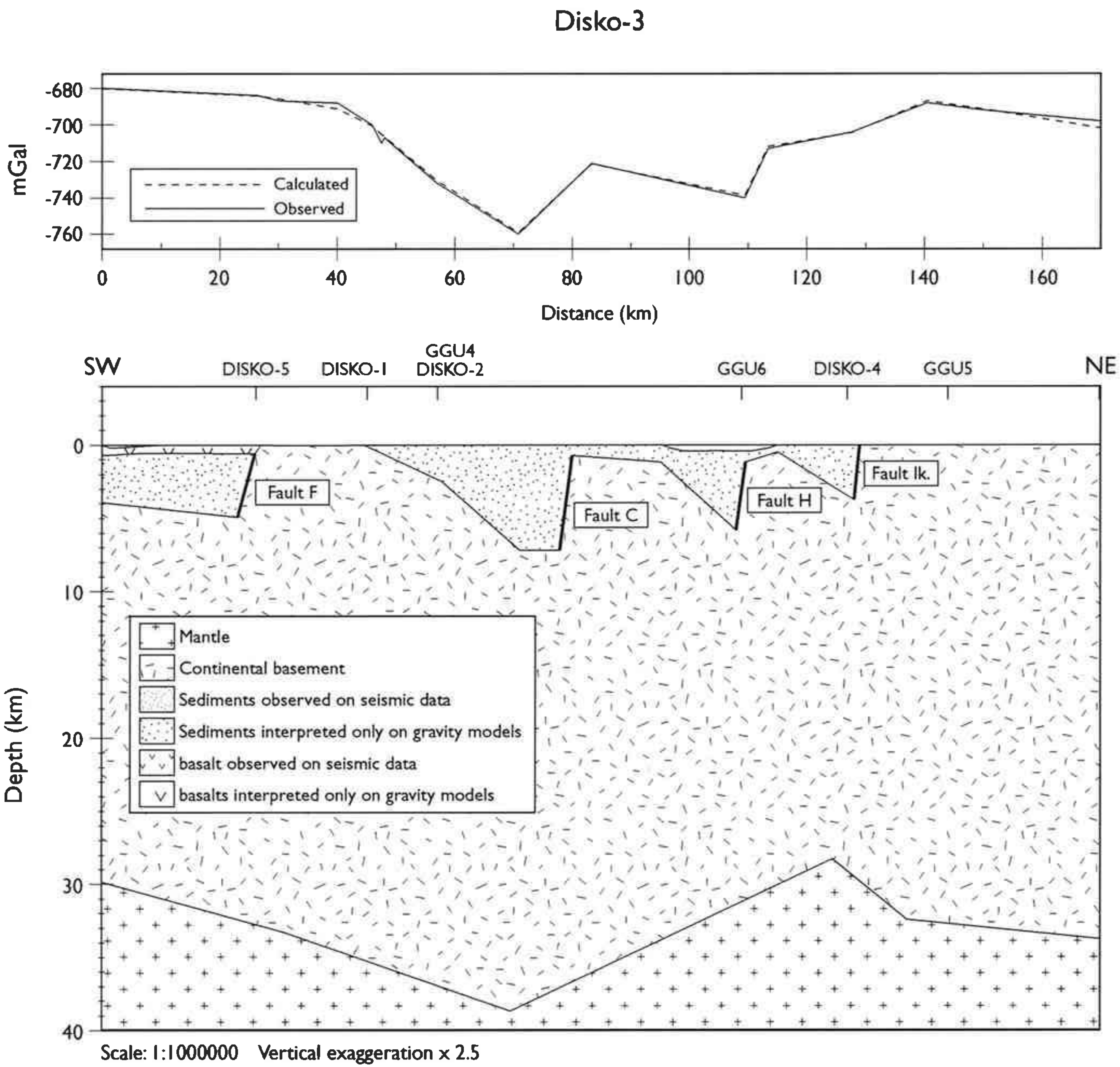

Fig.11a Gravity profile Disko-3

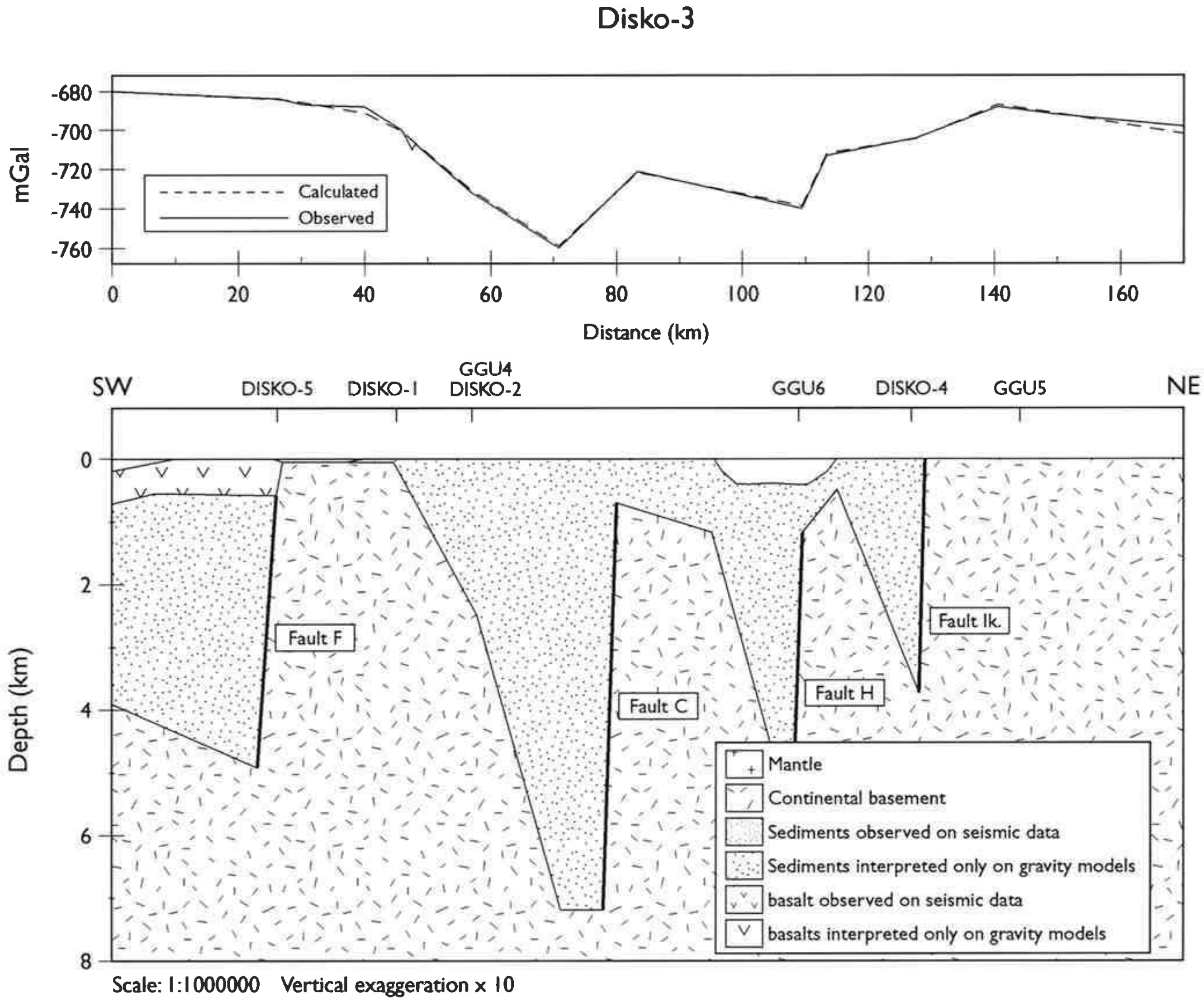

Fig.11b Gravity profile Disko-3

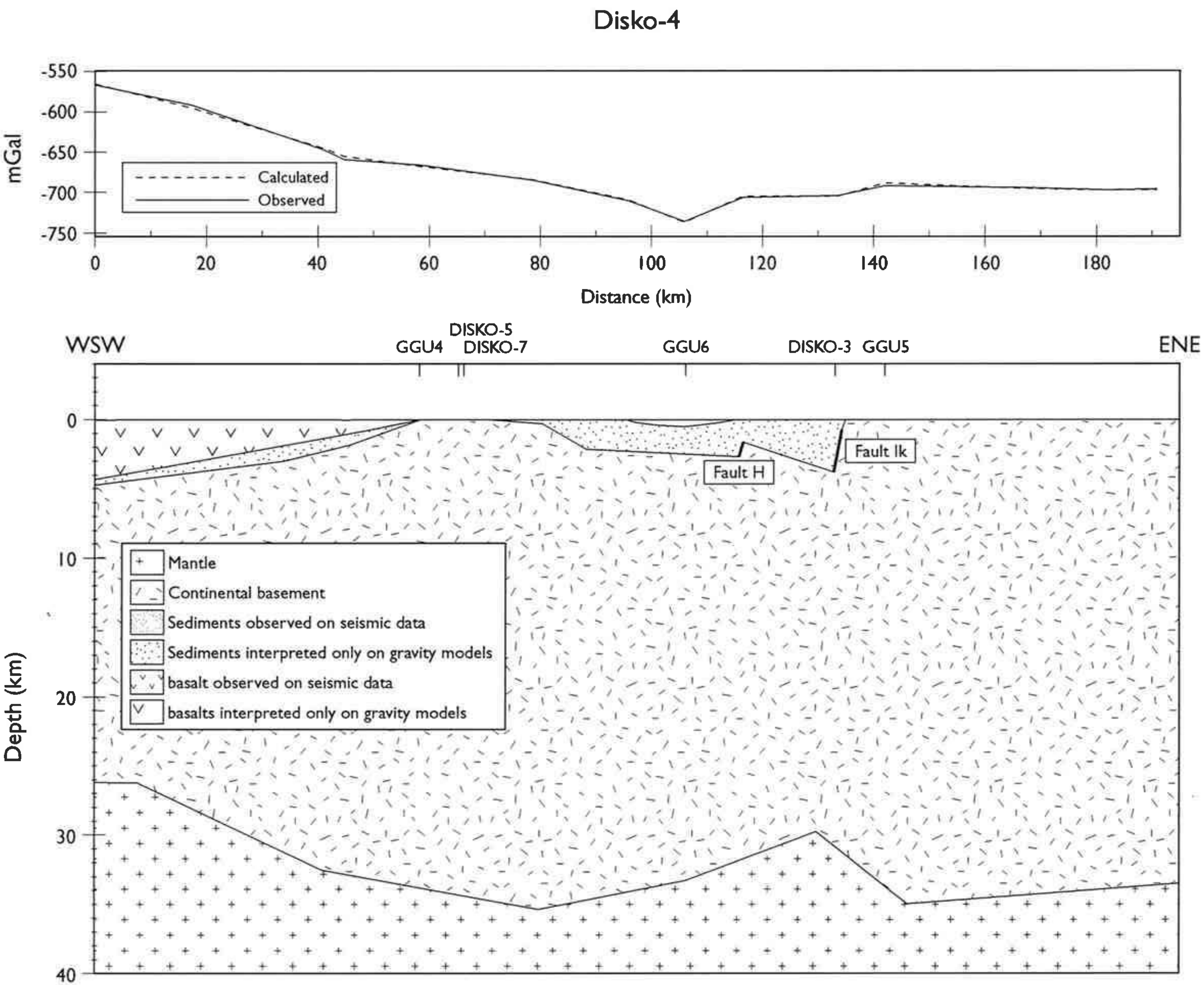

Scale: 1:1000000 Vertical exaggeration x 2.5

Fig.12a Gravity profile Disko-4

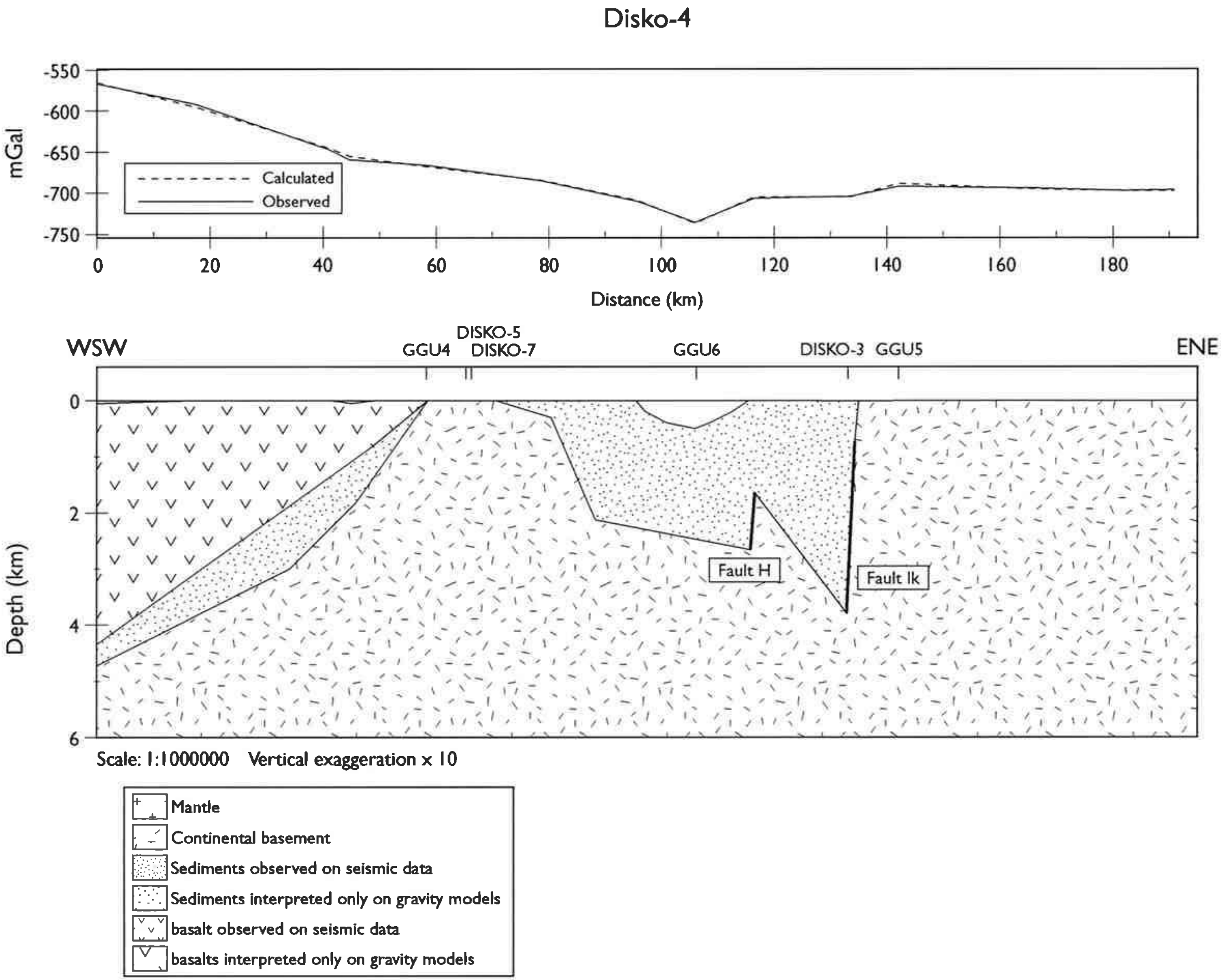

Fig. 12b Gravity profile Disko-4

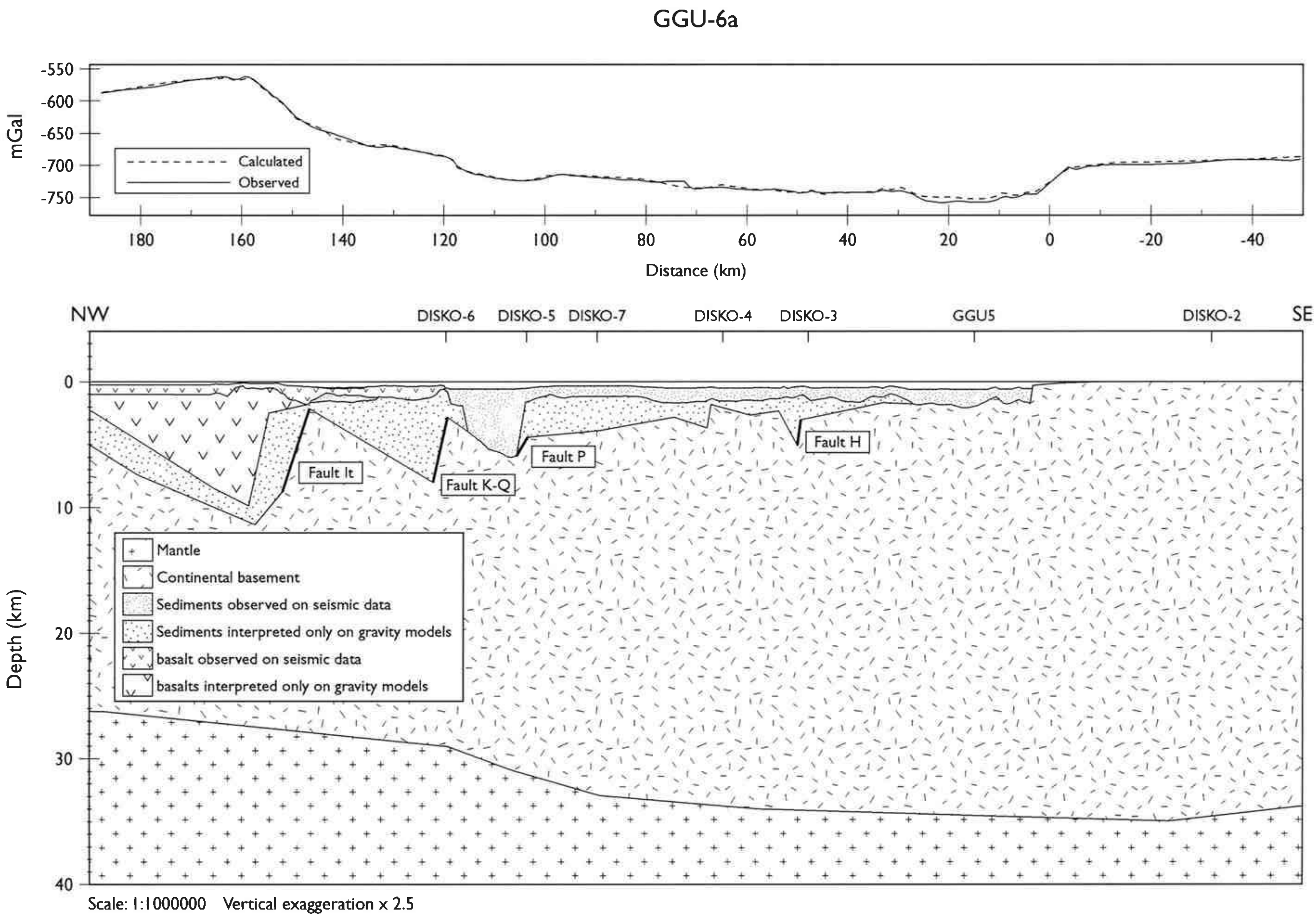

Fig.13a Gravity profile GGU6a

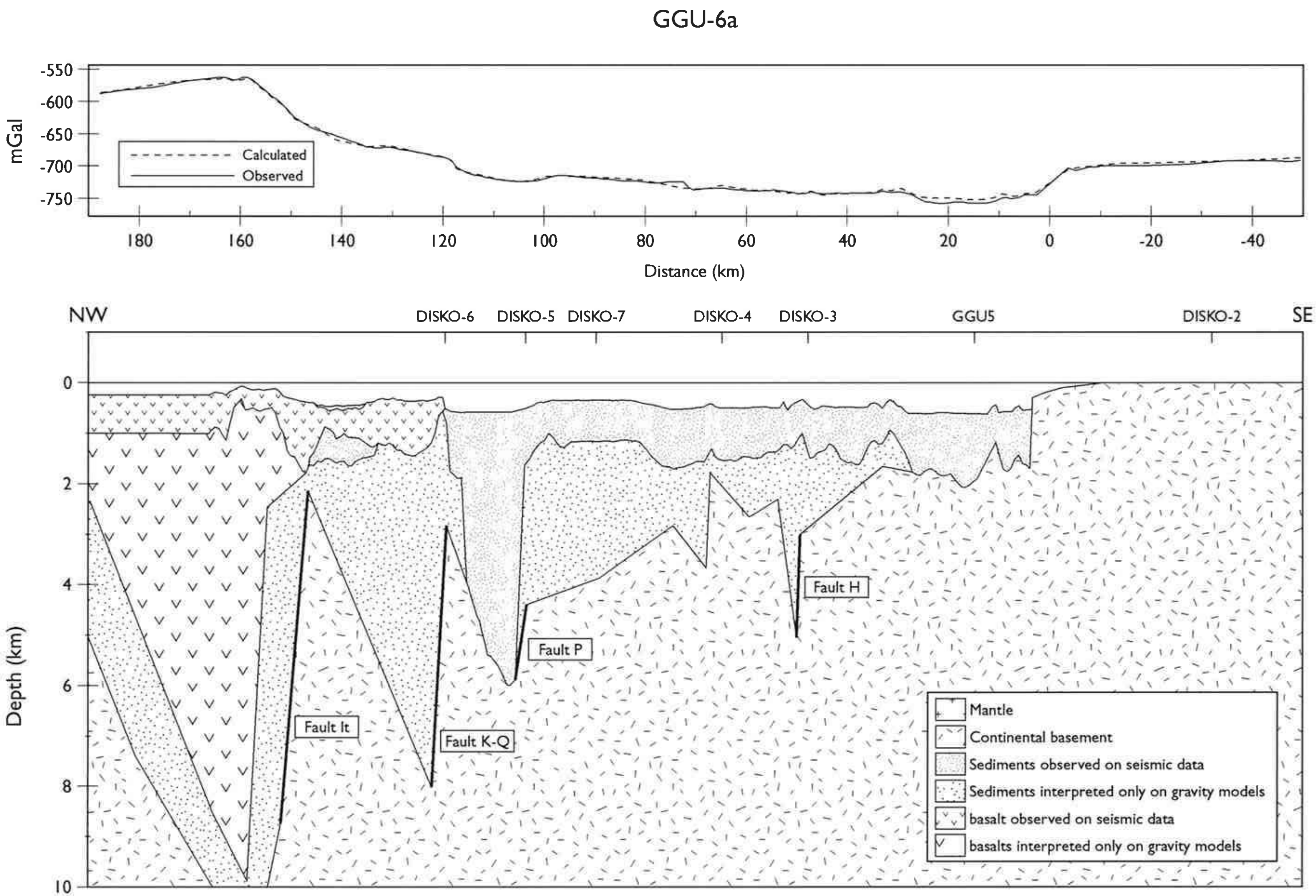

Scale: 1:1000000 Vertical exaggeration x 10

Fig.13b Gravity profile GGU6a

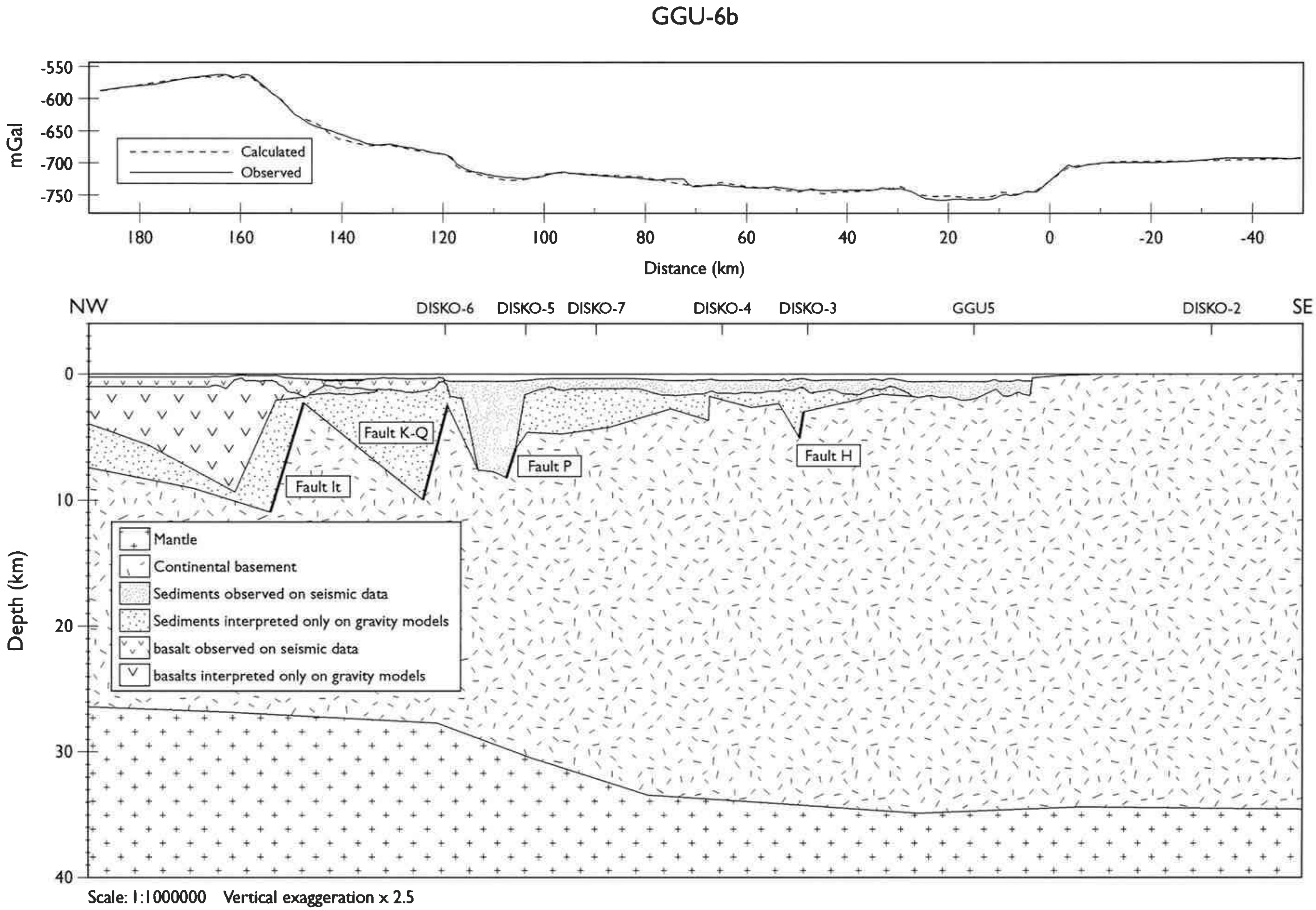

Fig.13c Gravity profile GGU6b

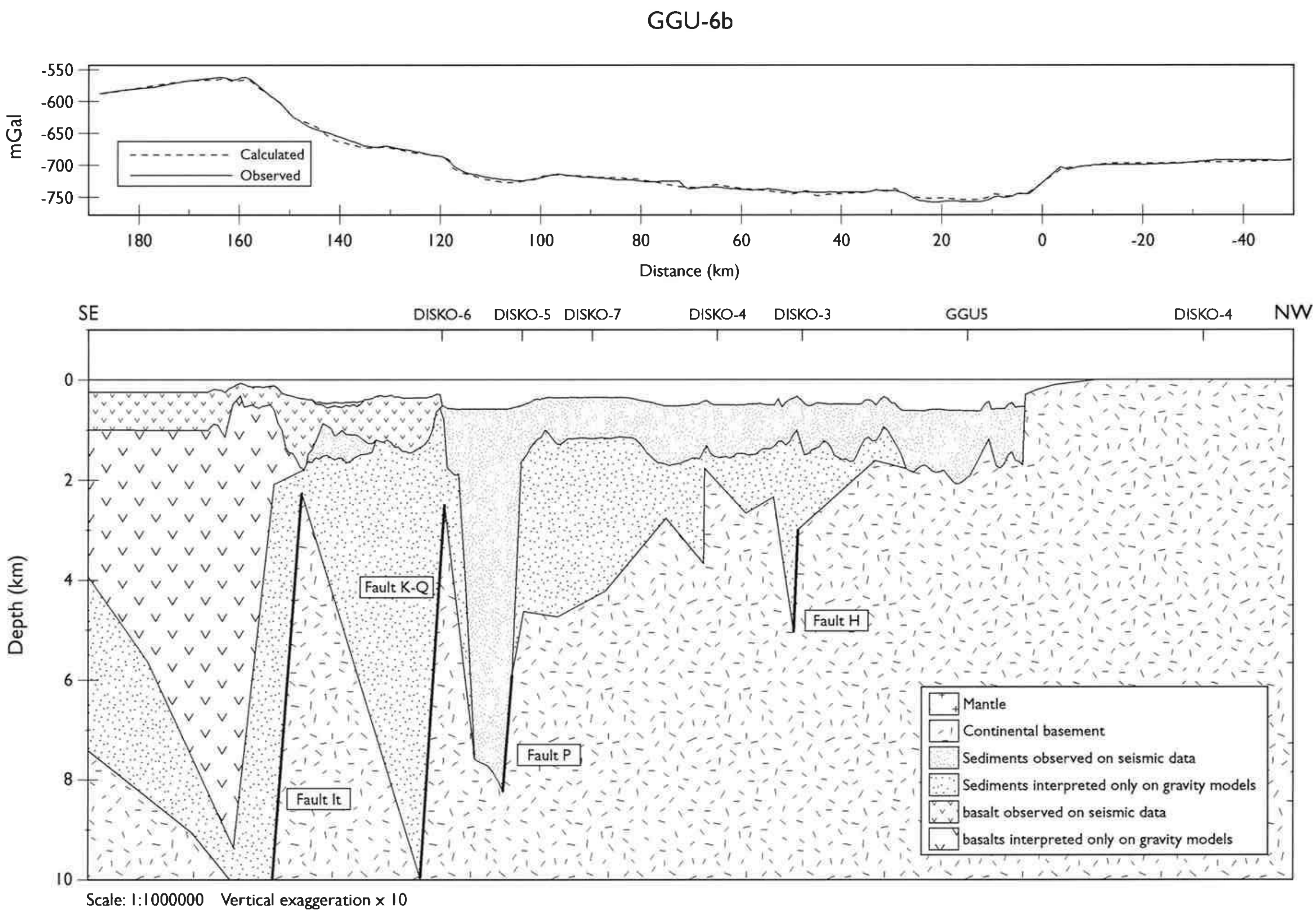

Fig.13d Gravity profile GGU6b

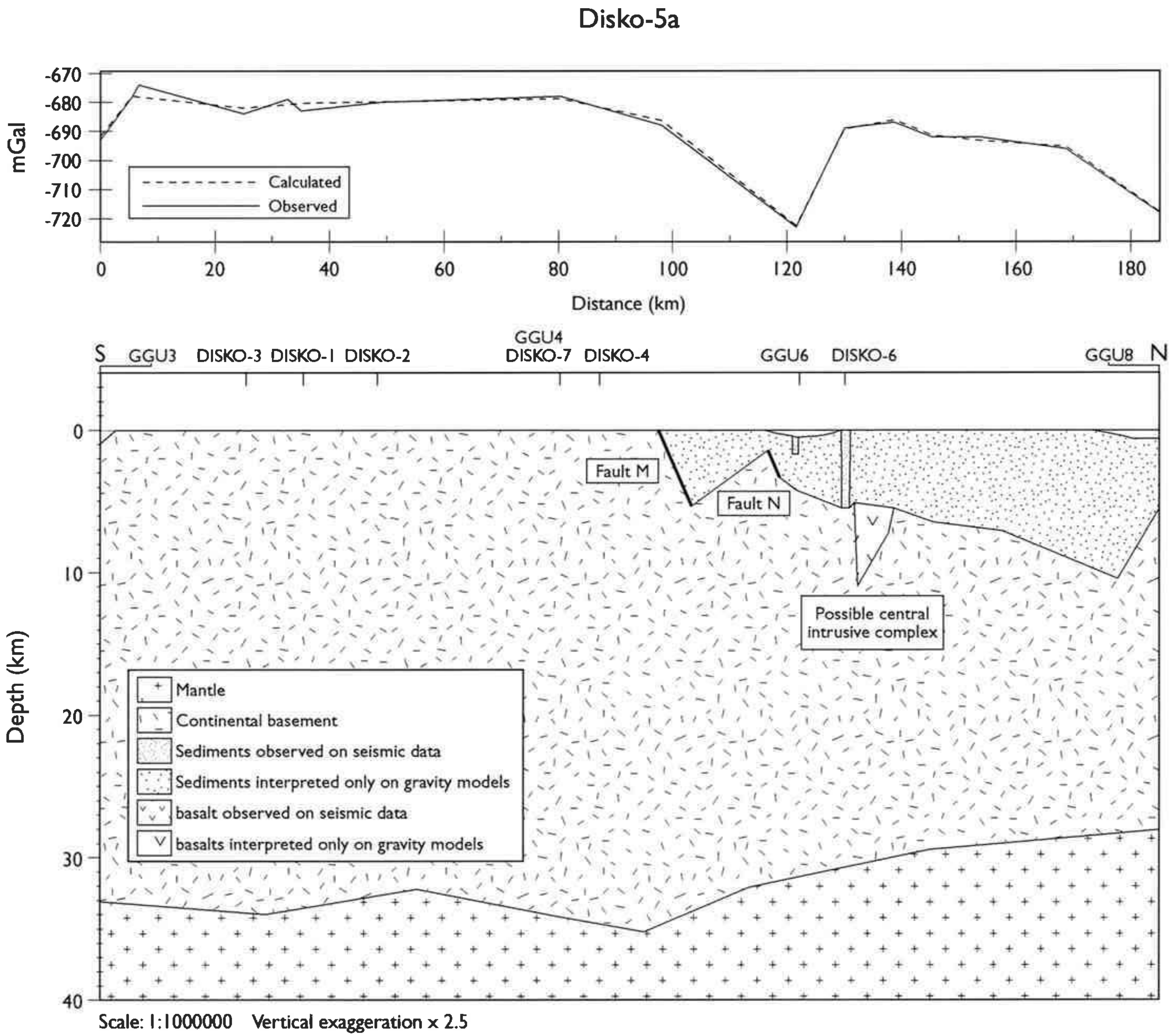

Fig.14a Gravity profile Disko-5a

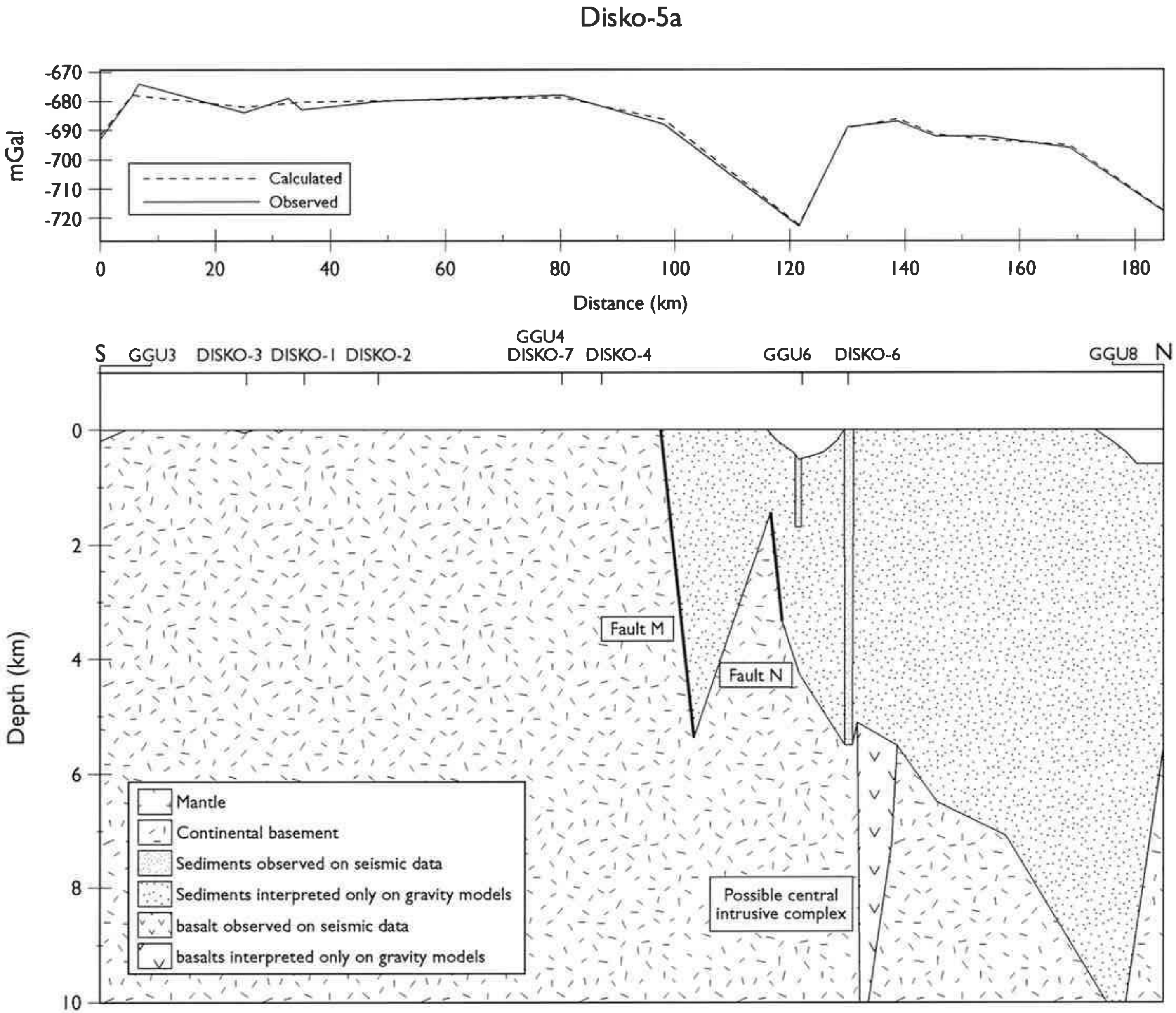

Scale: 1:1000000 Vertical exaggeration x 10

Fig.14b Gravity profile Disko-5a

Disko-5b

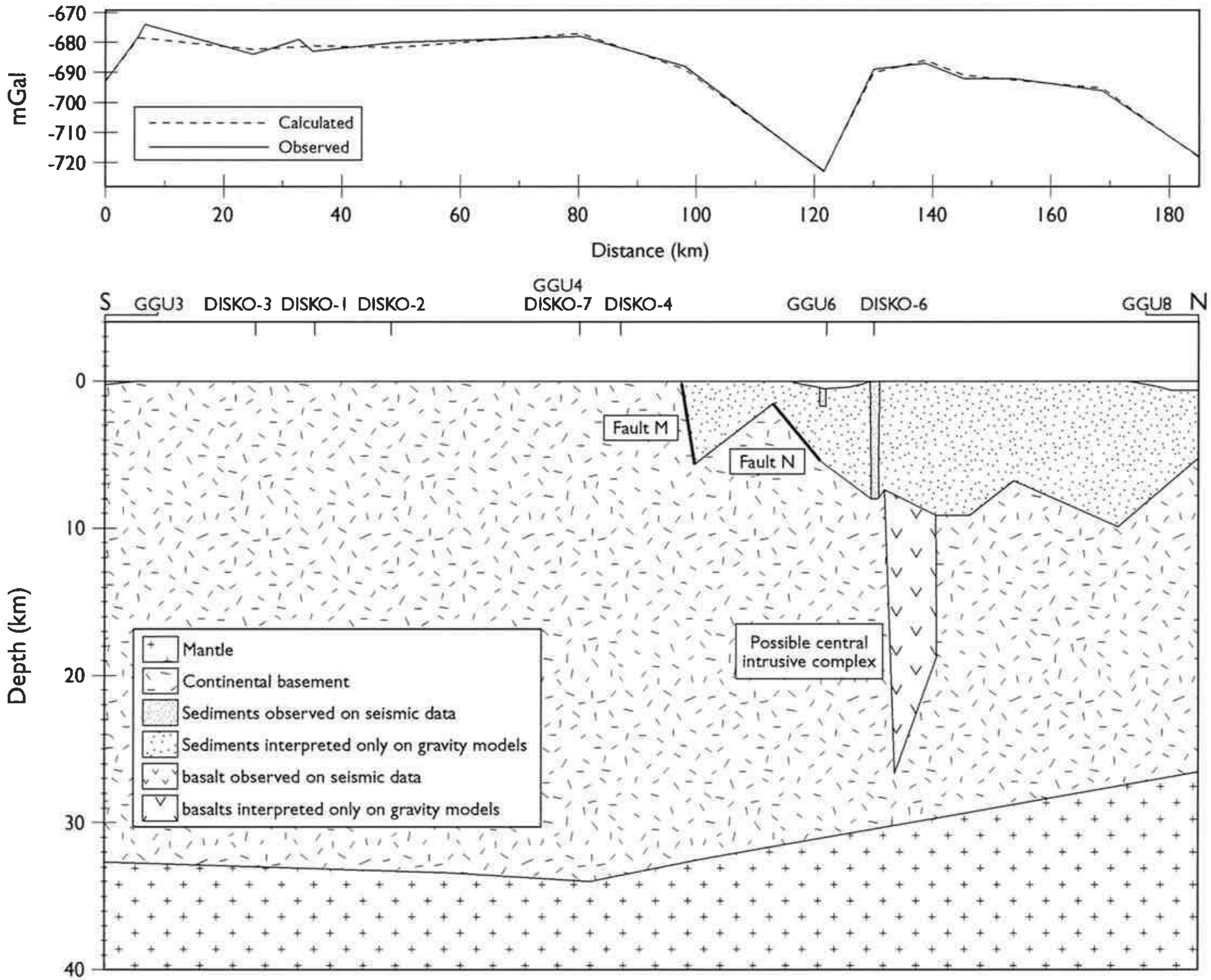

Scale: 1:1000000 Vertical exaggeration x 2.5

Fig.14c Gravity profile Disko-5b

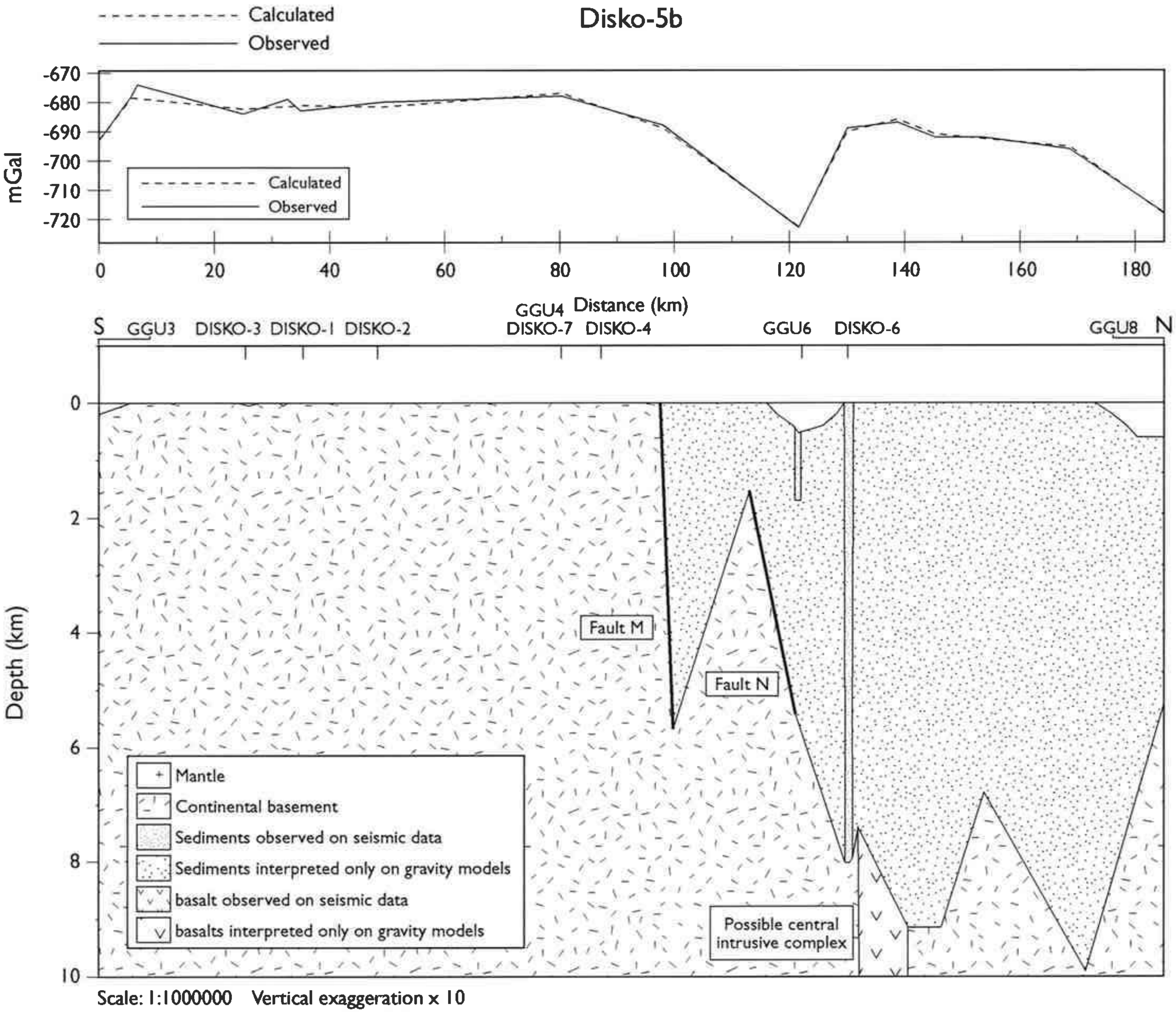

Fig.14d Gravity profile Disko-5b

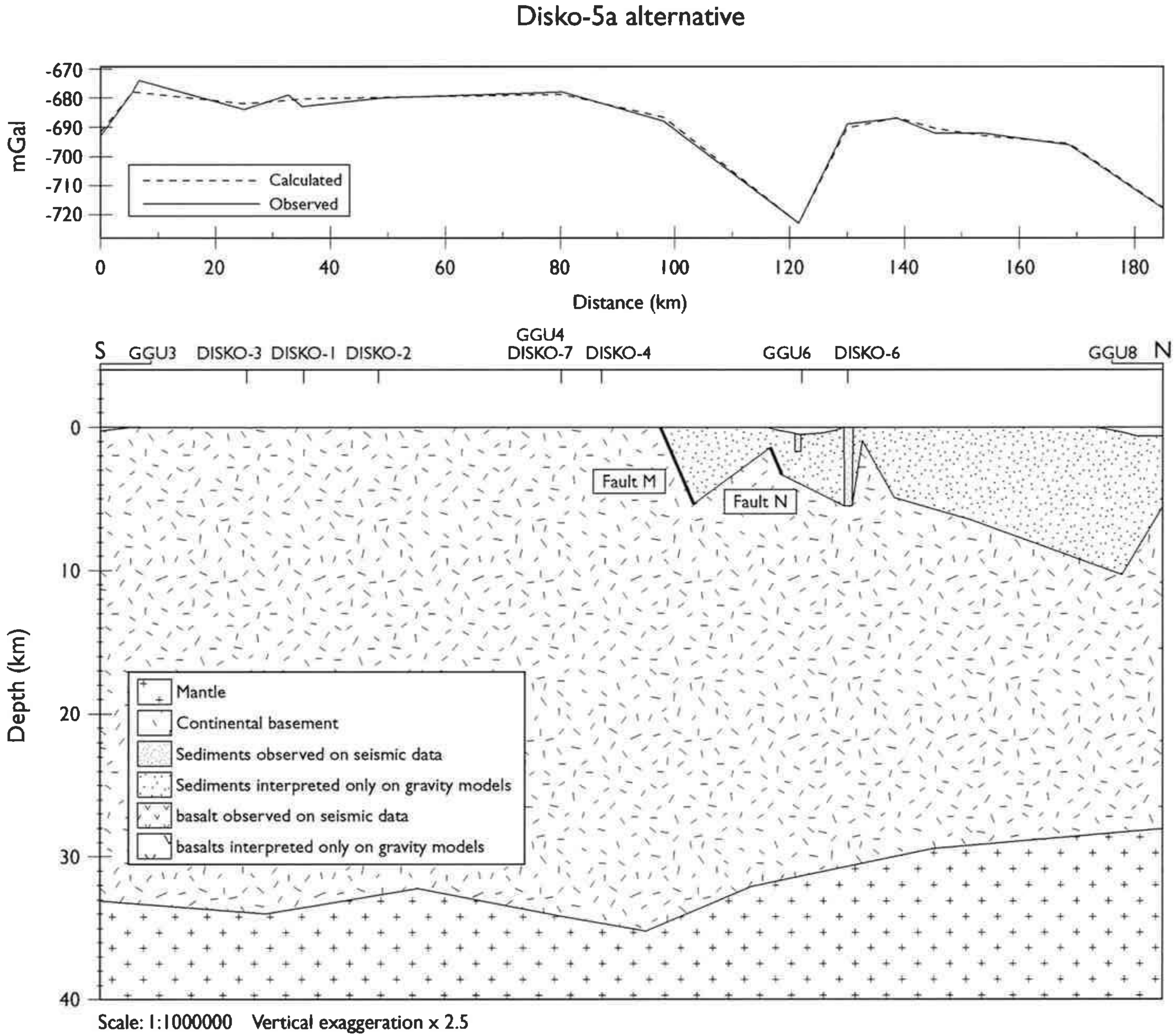

Fig.14e Gravity profile Disko-5a alternative

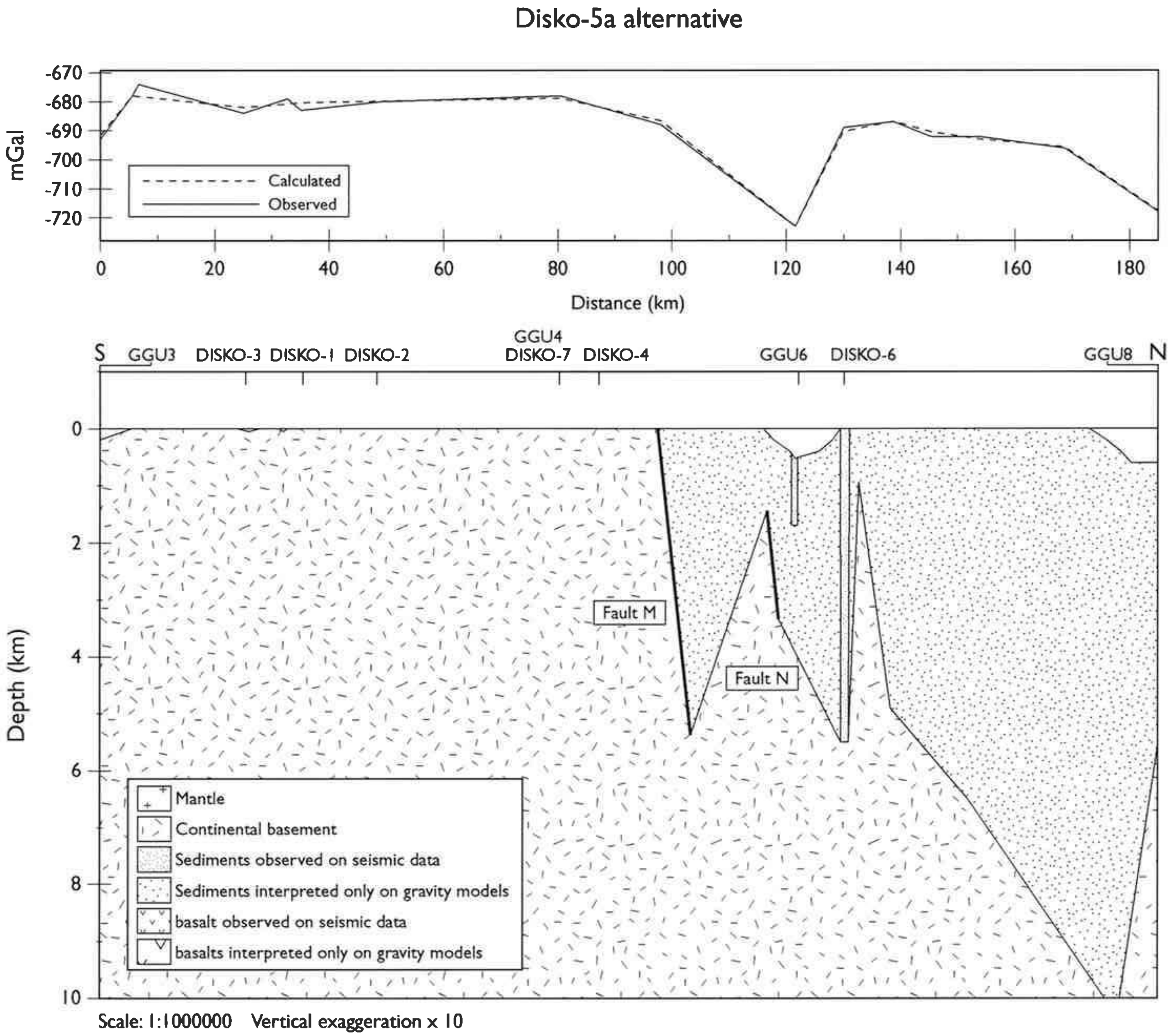

Fig.14f Gravity profile Disko-5a alternative

Disko-5b alternative

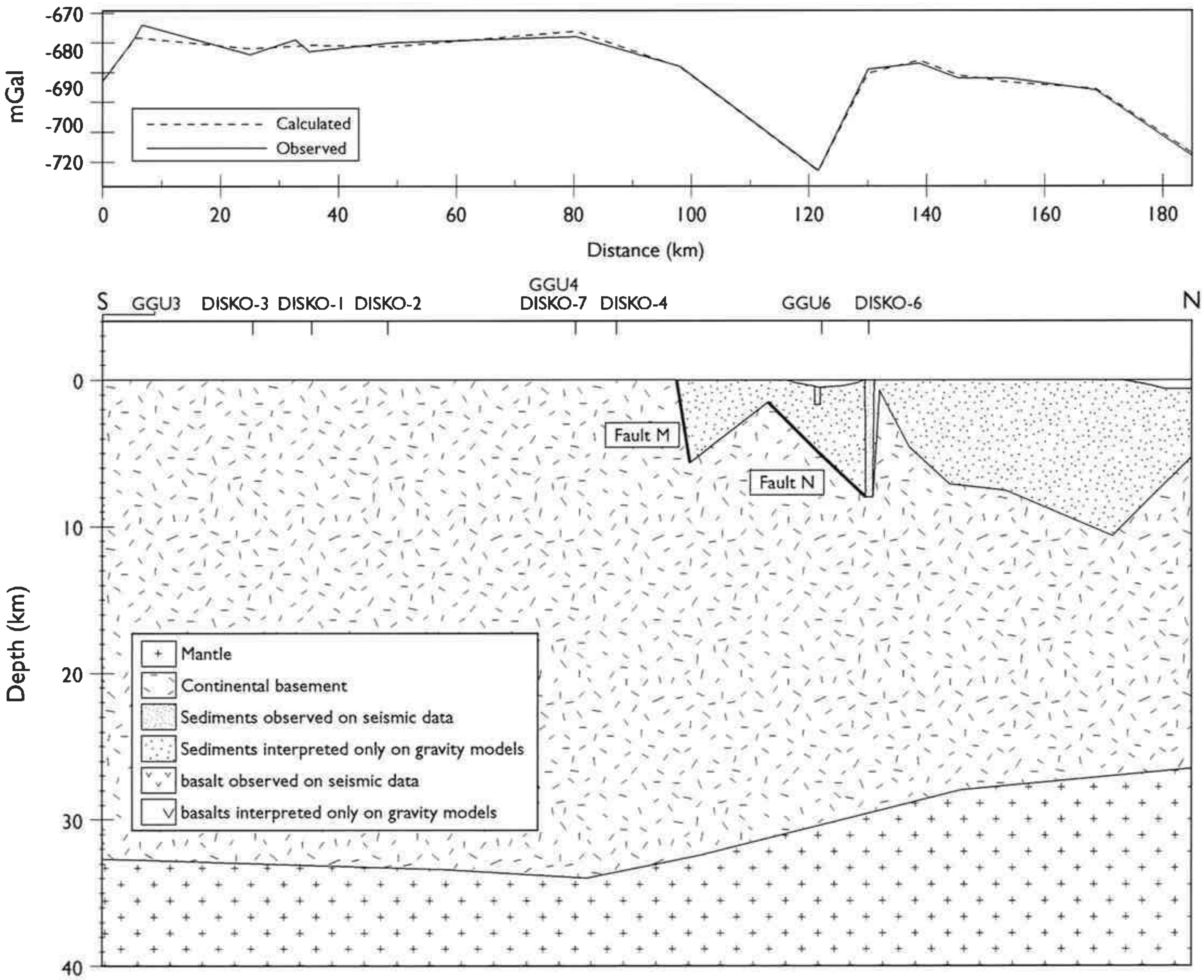

Scale: 1:1000000 Vertical exaggeration x 2.5

Fig.14g Gravity profile Disko-5b alternative

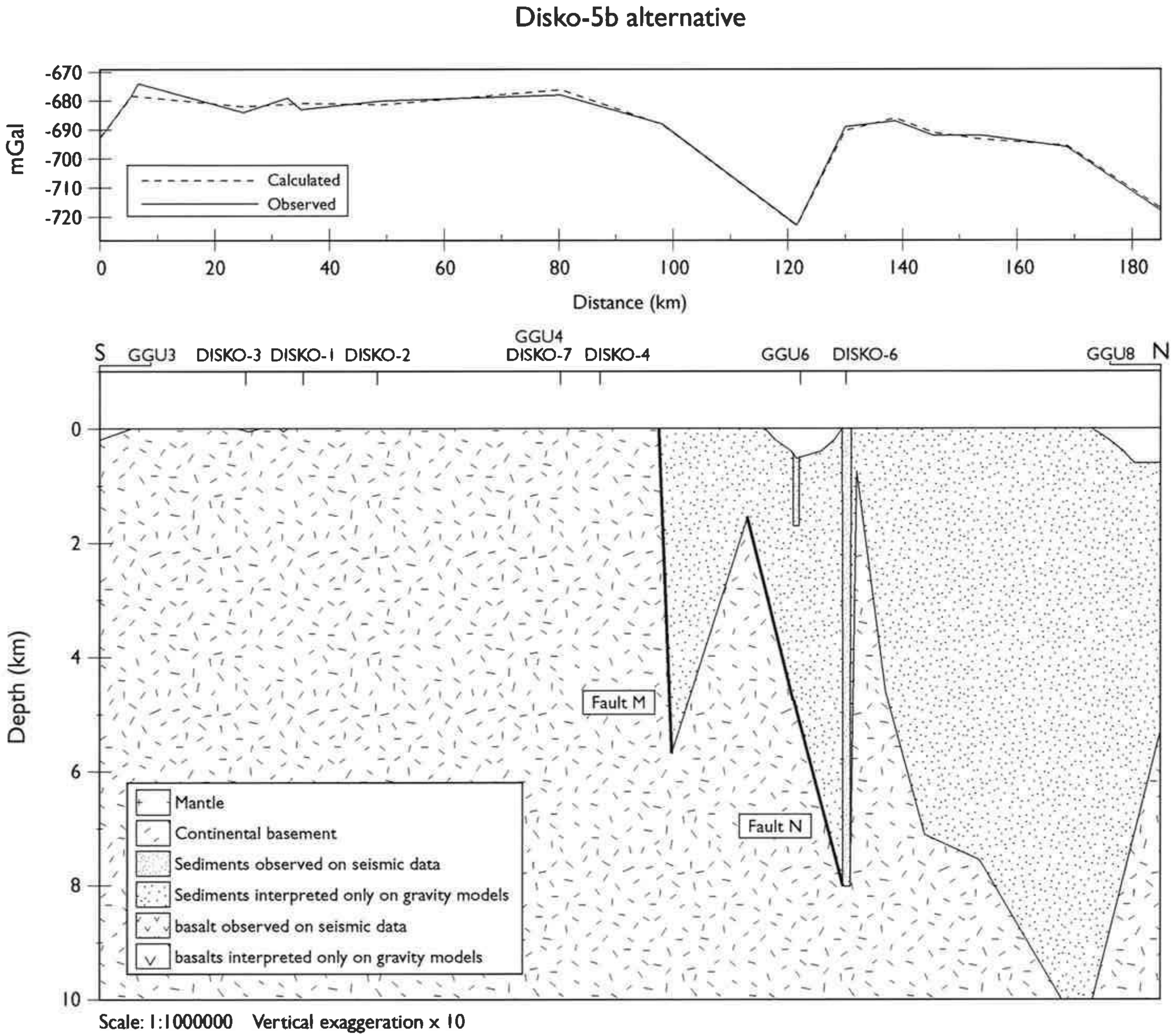

Fig. 14h Gravity profile Disko-5b alternative

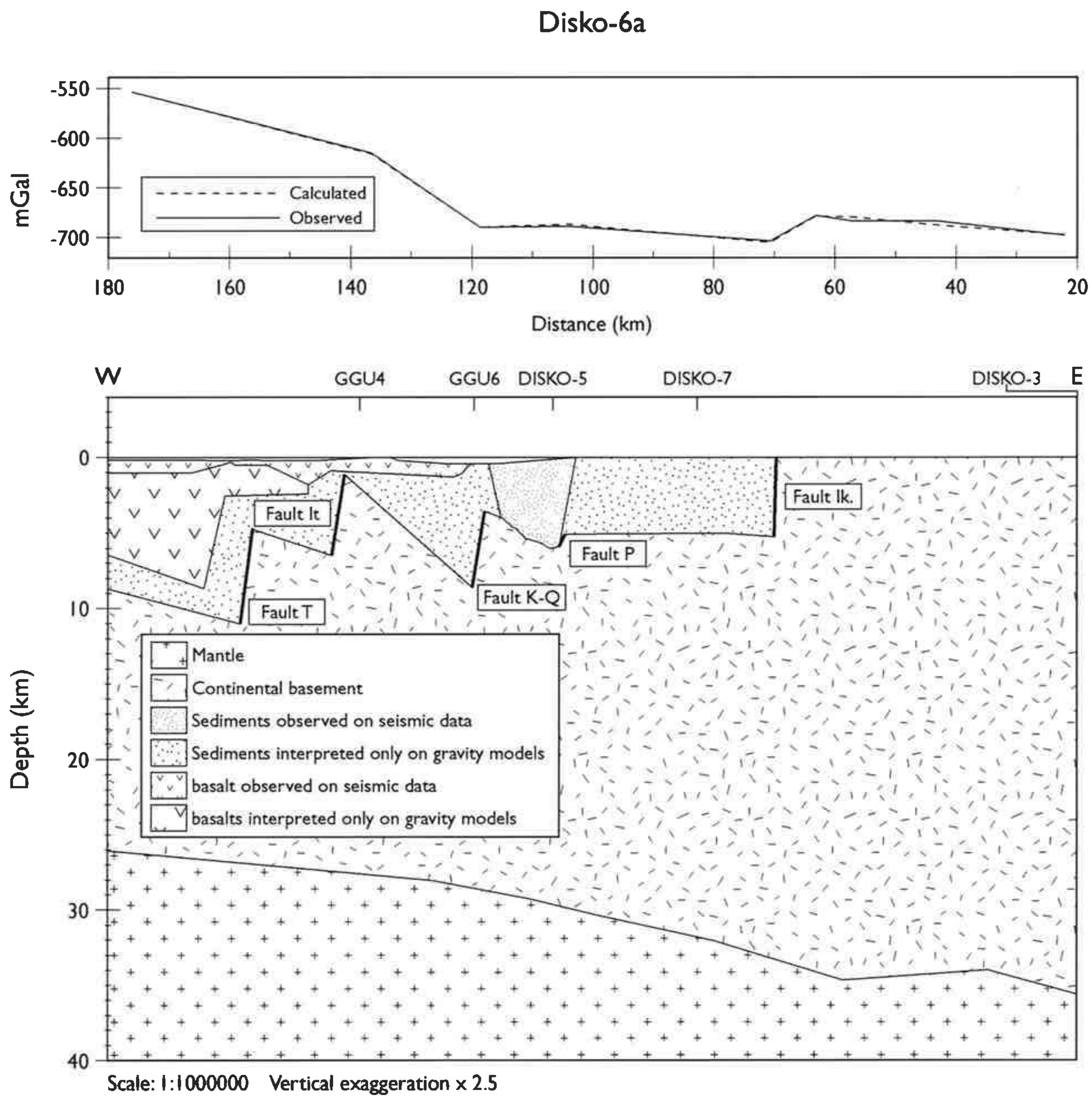

Fig.15a Gravity profile Disko-6a

Disko-6a

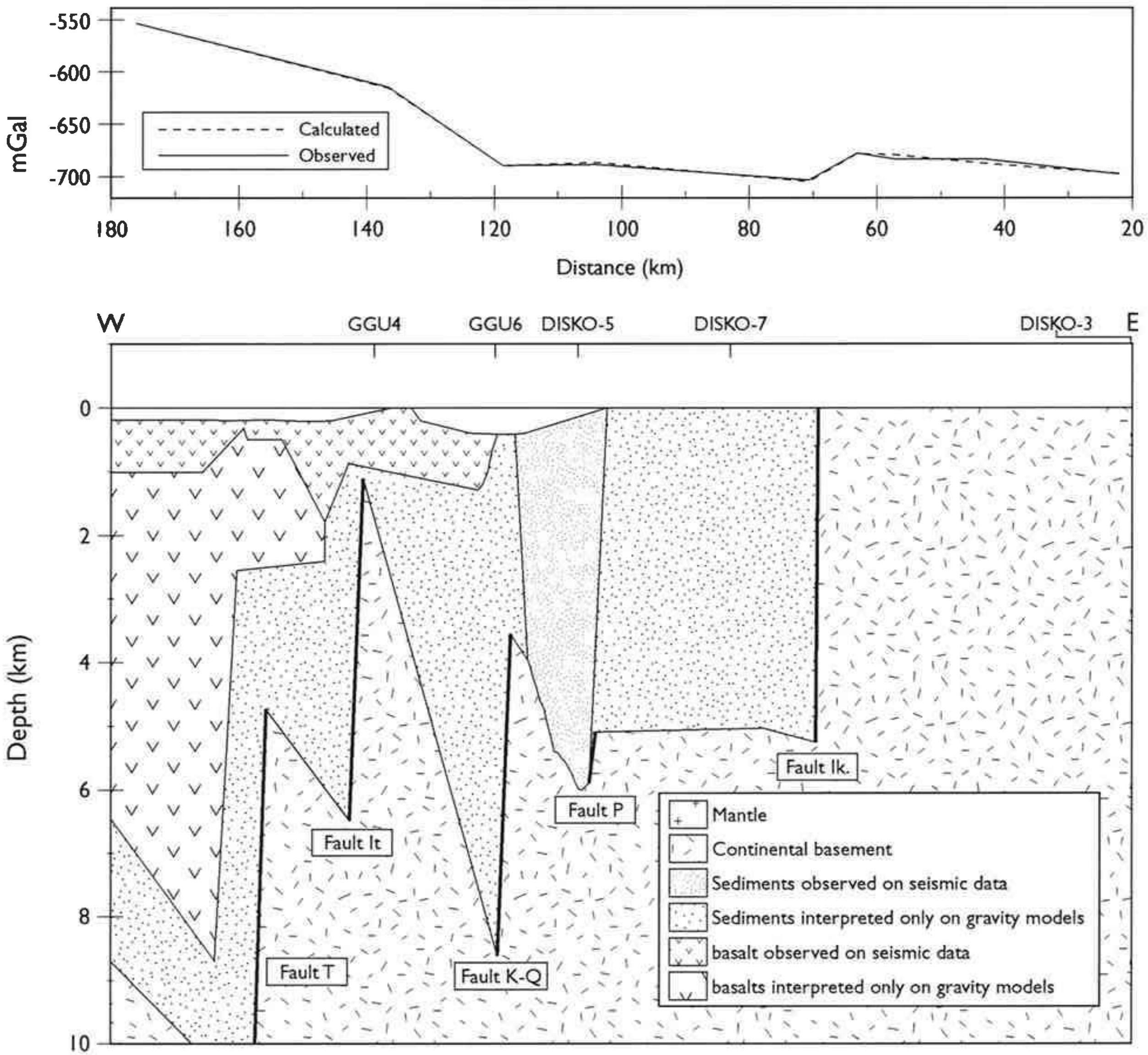

Scale: 1:1000000 Vertical exaggeration x 10

Fig.15b Gravity profile Disko-6a

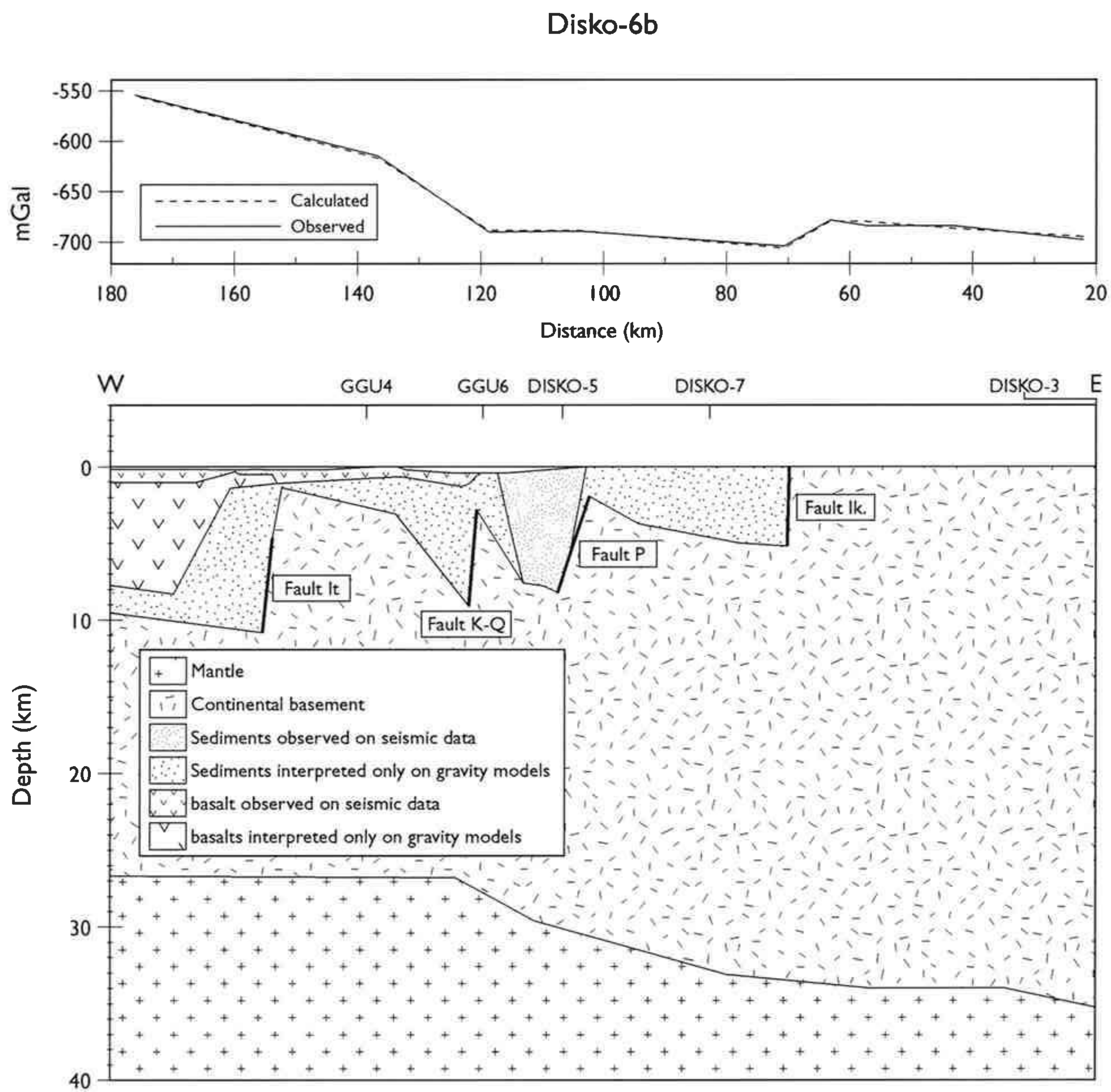

Scale: 1:1000000 Vertical exaggeration x 2.5

Fig.15c Gravity profile Disko-6b

Disko-6b

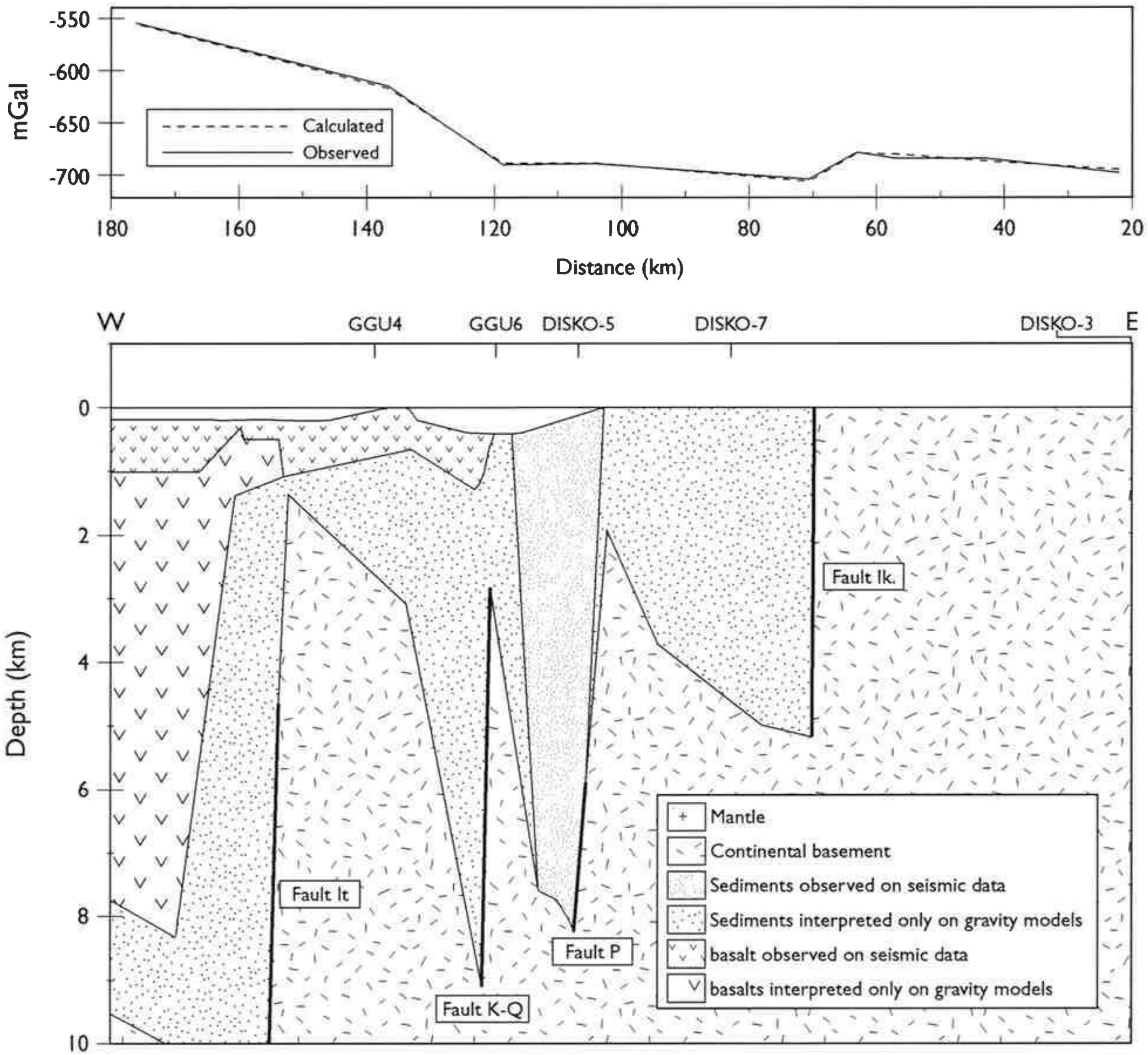

Scale: 1:1000000 Vertical exaggeration x 10

Fig.15d Gravity profile Disko-6b

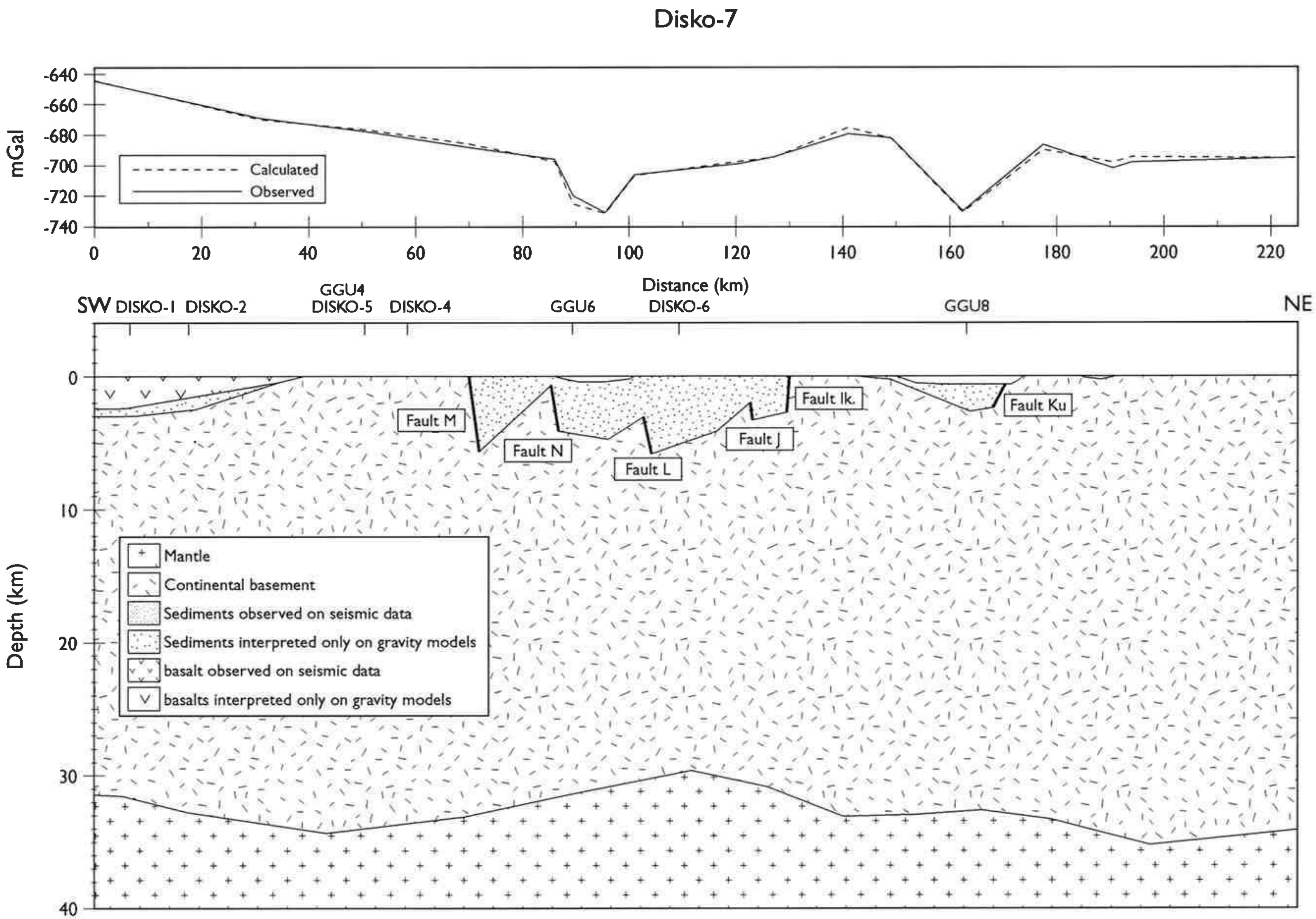

Scale: 1:1000000 Vertical exaggeration x 2.5

Fig.16a Gravity profile Disko-7

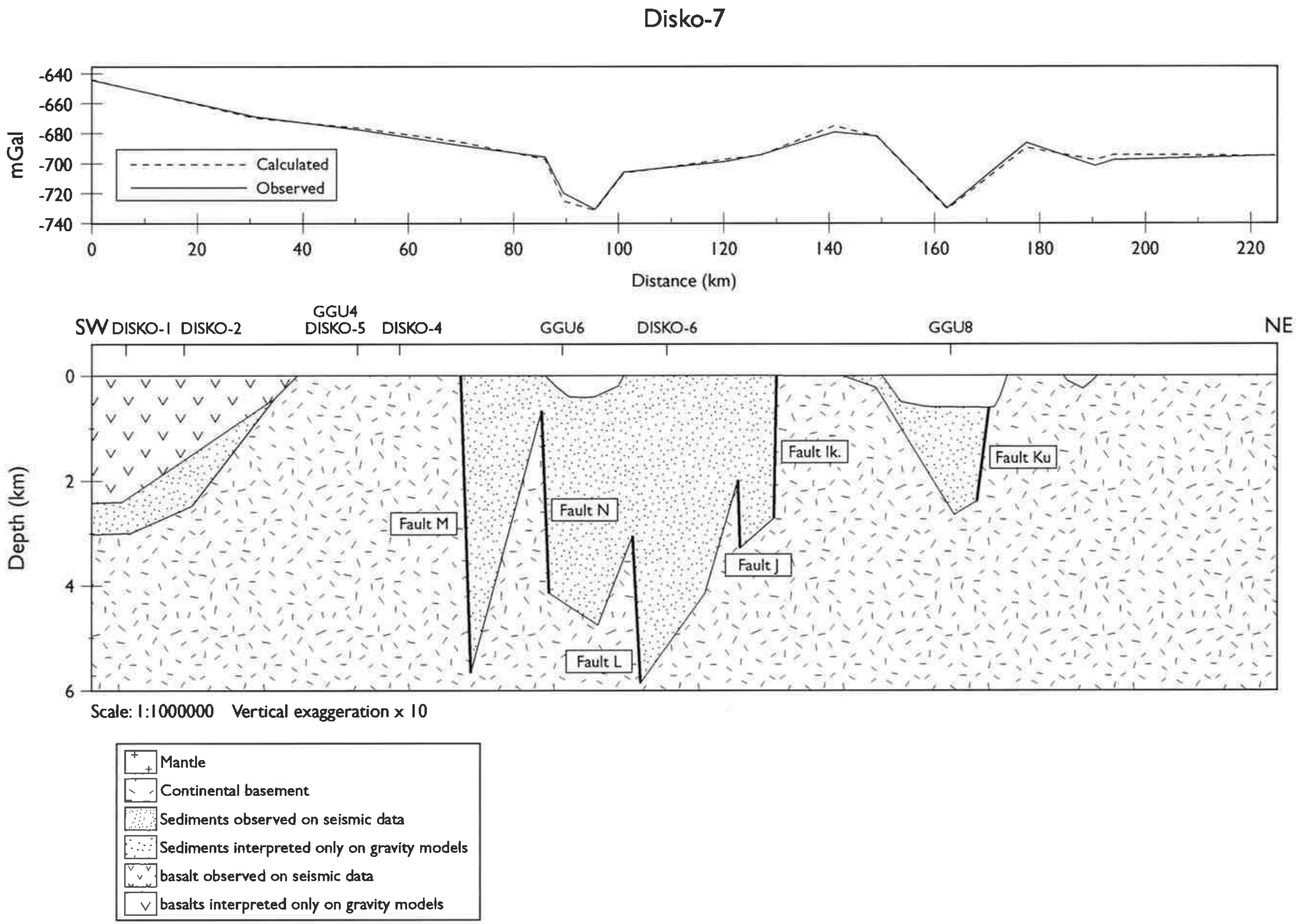

Fig.16b Gravity profile Disko-7

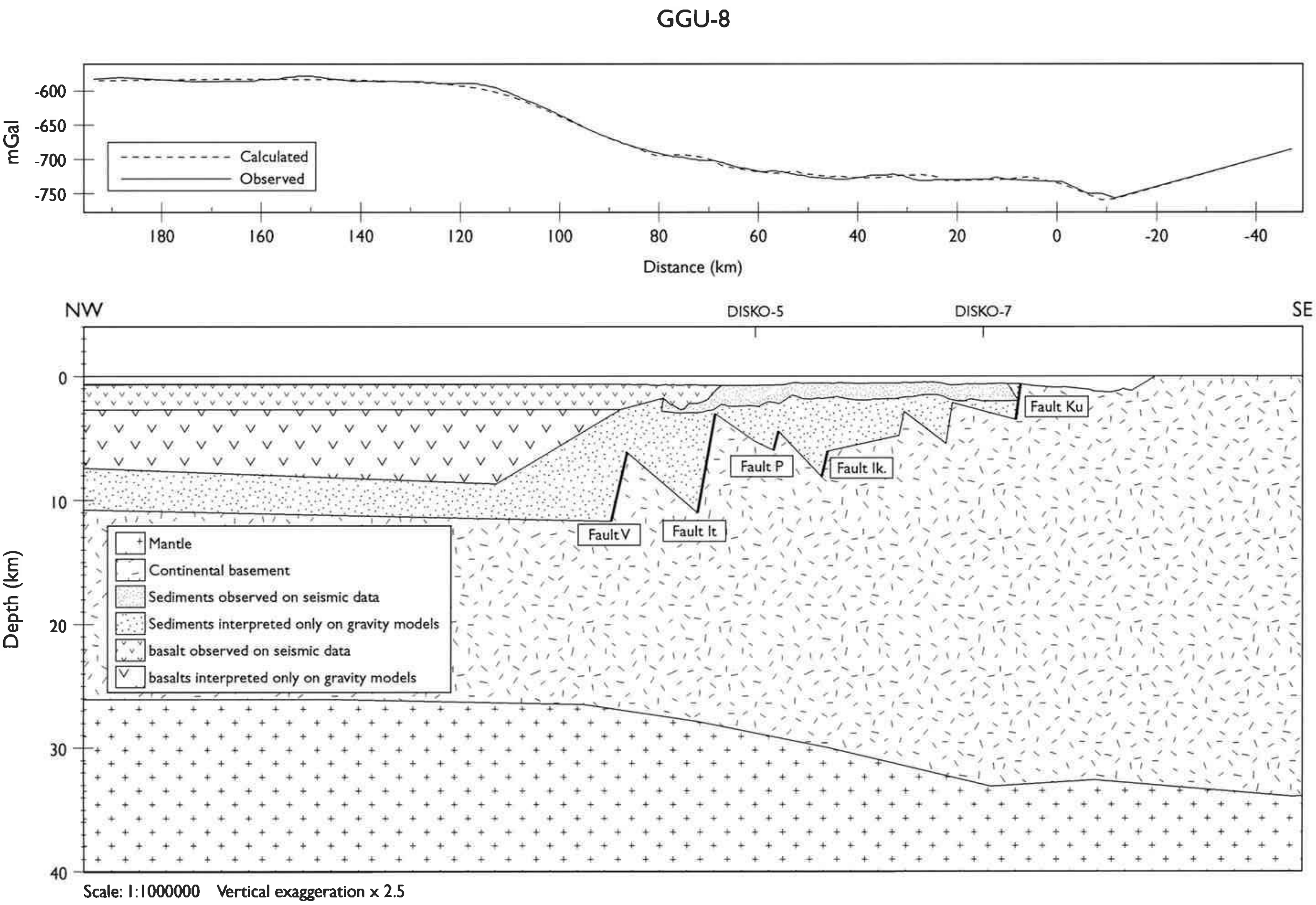

Fig.17a Gravity profile GGU8

GGU-8

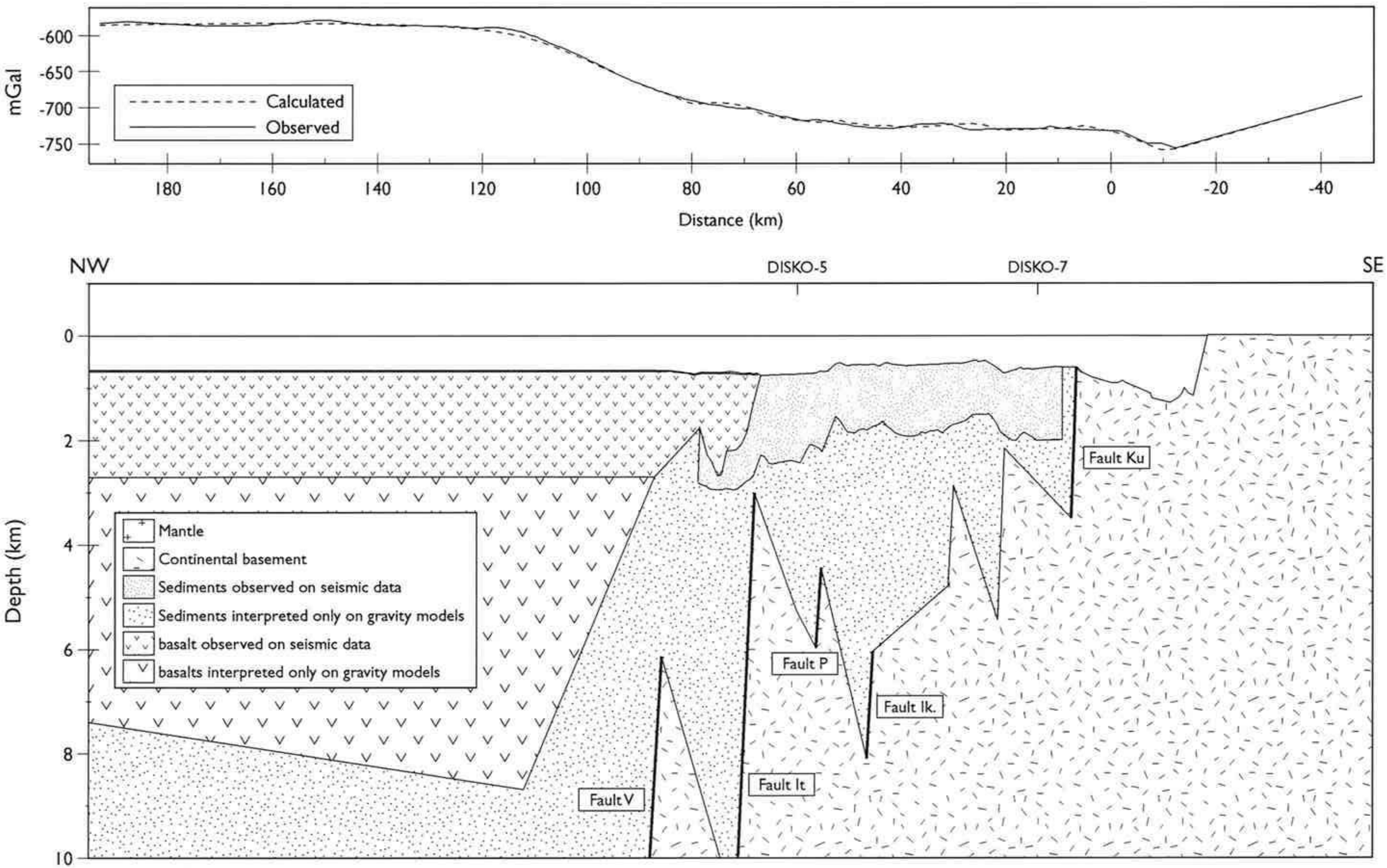

Scale: 1:1000000 Vertical exaggeration x 10

Fig.17b Gravity profile GGU8

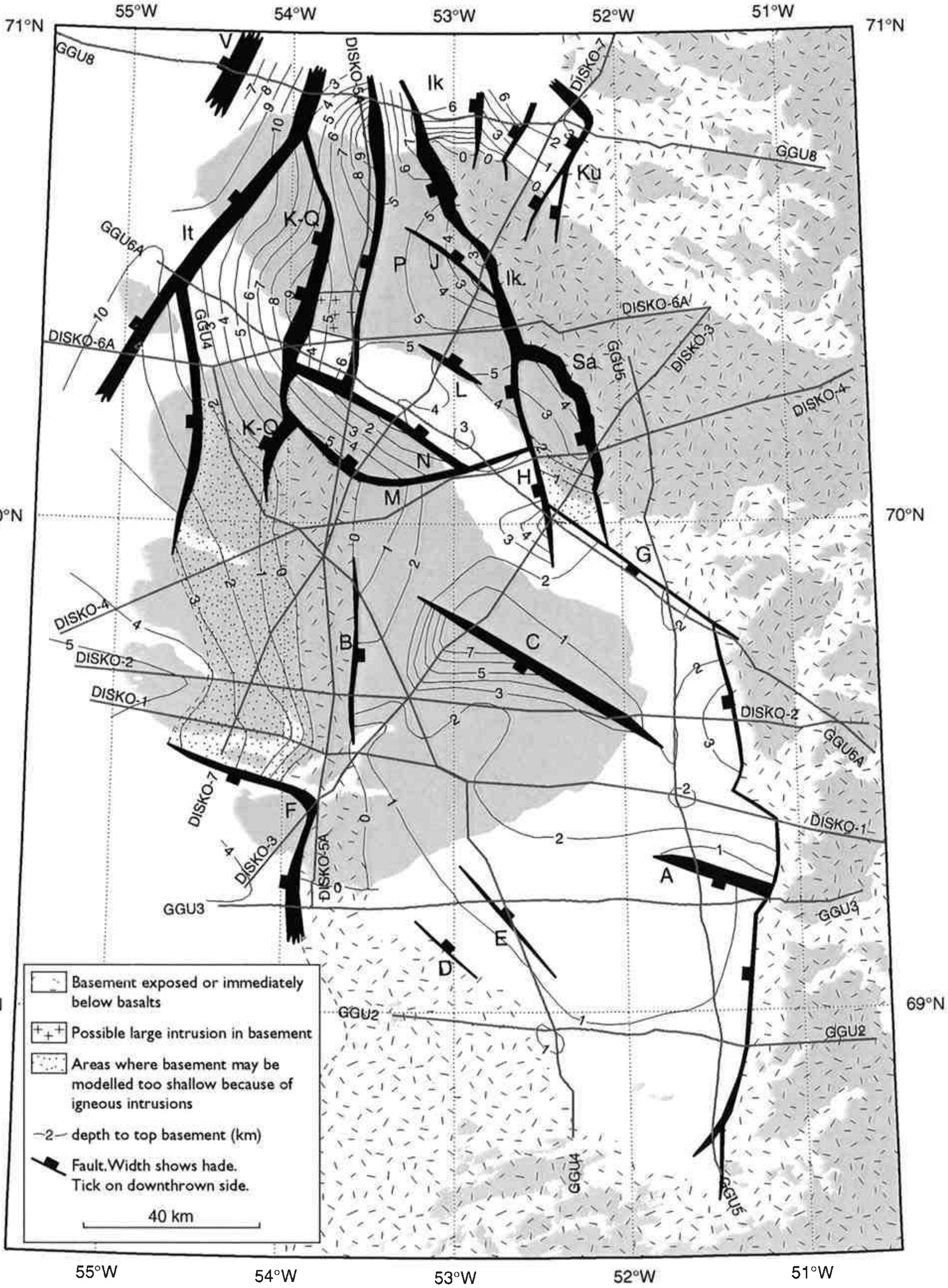

Fig. 18: Map of depths to top basement map calculated from the 'a' models

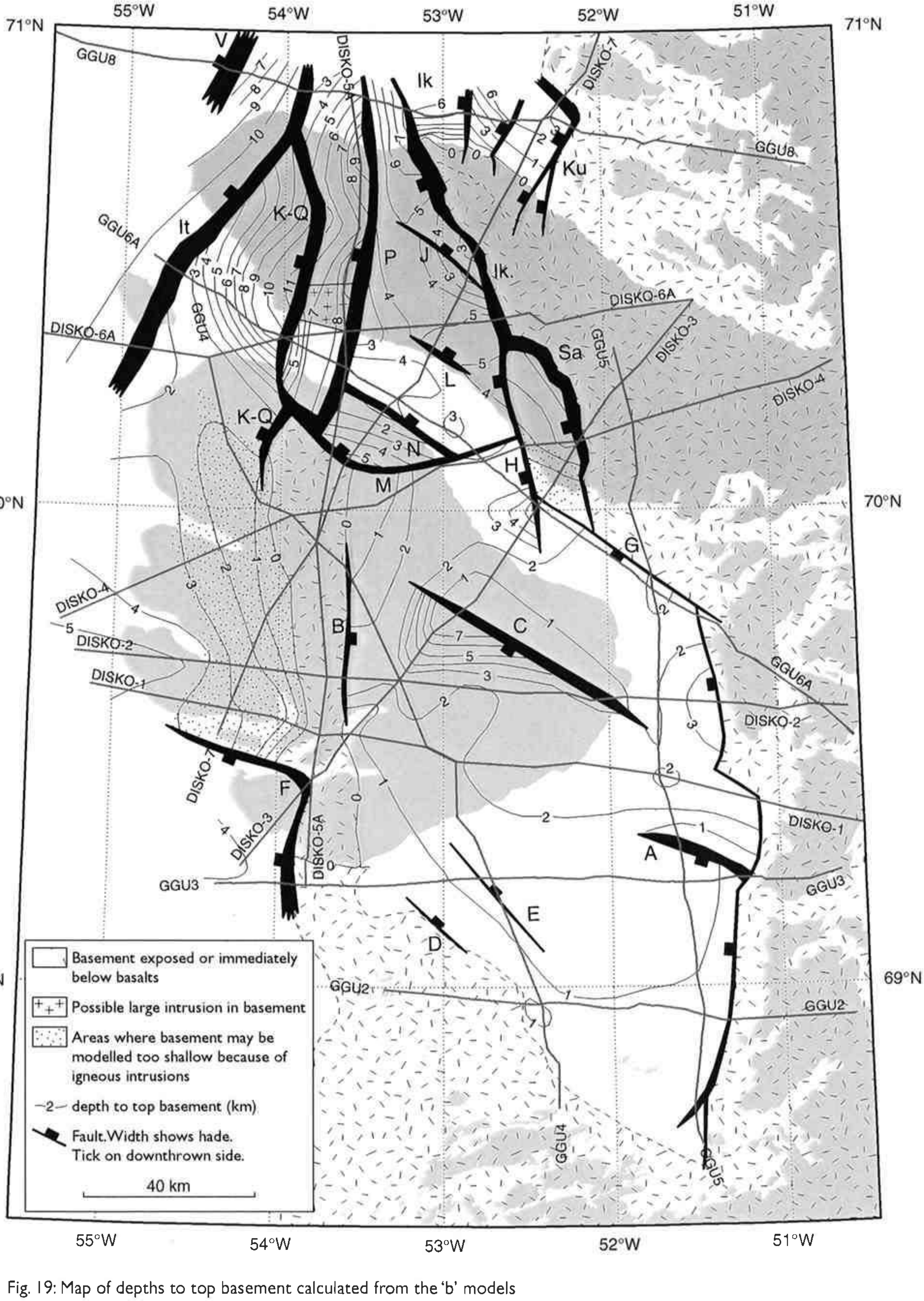

Fig. 19: Map of depths to top basement calculated from the 'b' models

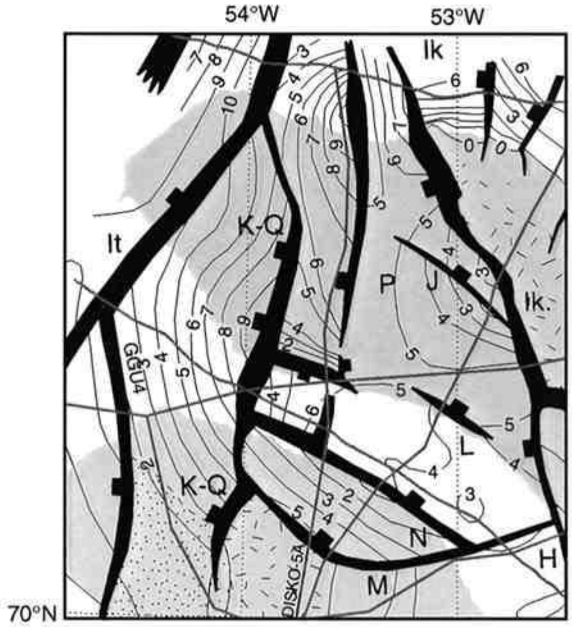

Fig. 20: Map of depths to top basement in western Vaigat and western Nuussuaq calculated from the 'a' models plus the 'alternative a' model on profile Disko-5 (see text for details).

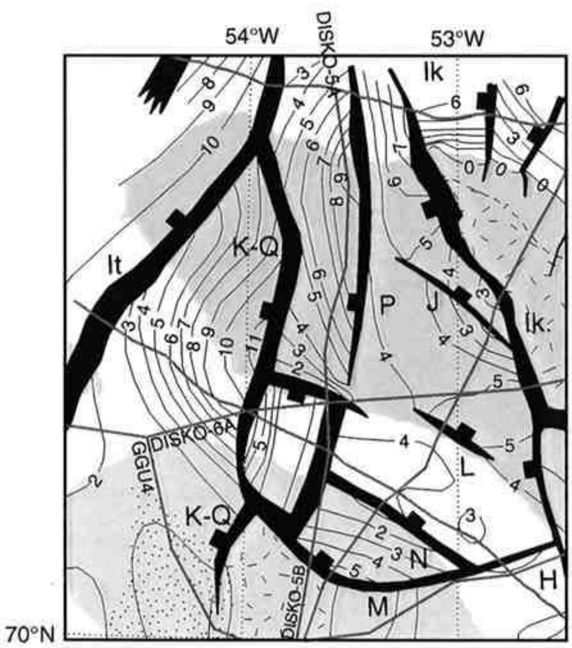

Fig. 21: Map of depths to top basement in western Vaigat and western Nuussuaq calculated from the 'b' models plus the 'alternative b' model on profile Disko-5 (see text for details).

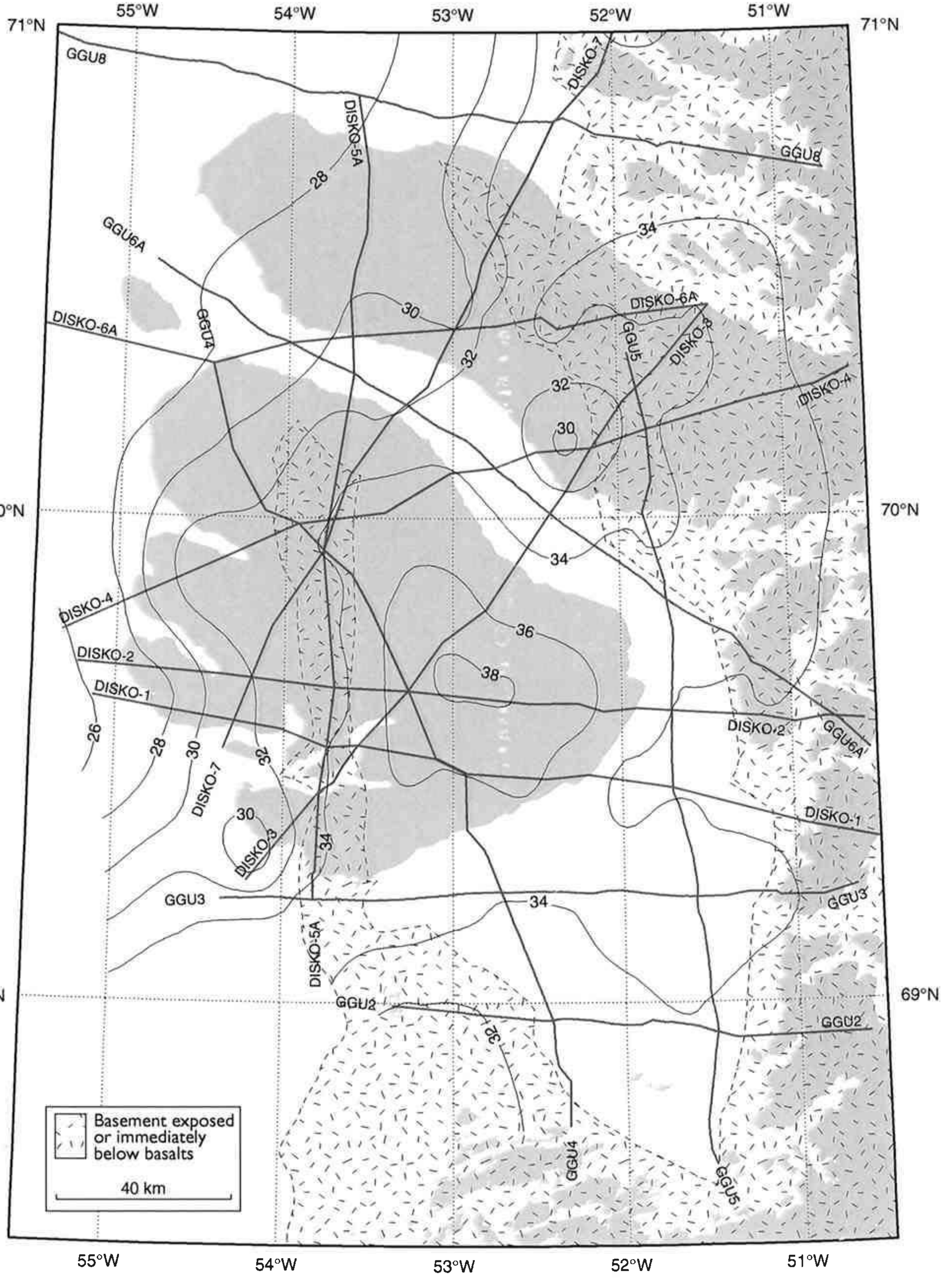

Fig 22: Map of depths to Moho calculated from the 'a' models assuming that continental crust is in isostatic equilibrium if the Moho is at 30 km depth.

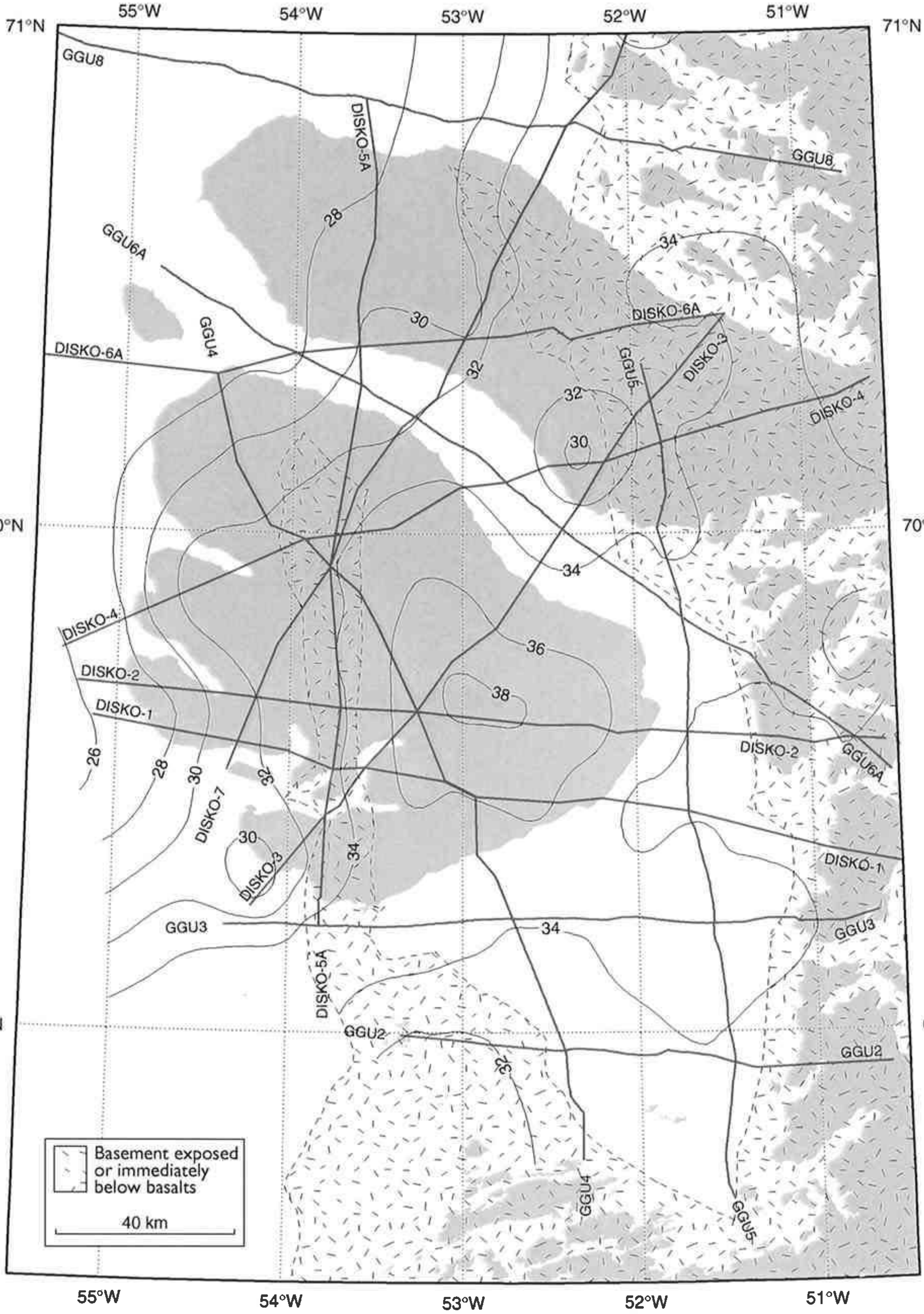

Fig 23: Map of depths to Moho calculated from the 'b' models assuming that continental crust is in isostatic equilibrium if the Moho is at 30 km depth.